# EFFECTS OF SMALL DIMENSIONAL VARIATIONS ON THE PERFORMANCE OF A TYPICAL BISTABLE FLUID AMPLIFIER

by

Charles S. Aldrich

Thesis submitted to the Graduate Faculty of the
Virginia Polytechnic Institute and State University
in partial fulfillment of the requirements for the degree of

MASTER OF SCIENCE

in

Mechanical Engineering

APPROVED:

R. A. Comparin, Chairman

H. L. Moses

W. C. Thomas

June, 1974

Blacksburg, Virginia

## ACKNOWLEDGMENTS

The author wishes to express his appreciation for the guidance and assistance given by his major professor, . Appreciation is also expressed for the assistance of the committee members and the Mechanical Engineering shop.

Thanks must also go to for his assistance in the reduction of the experimental data and preparation of some of the ink figures. is thanked for their financial support of this project.

Finally, appreciation is expressed to the author's wife for her support and encouragement which made this work possible.

TABLE OF CONTENTS

## LIST OF FIGURES

## LIST OF TABLES

## NOMENCLATURE

AR aspect ratio, b/channel depth

b nominal power nozzle width

CW width of the control port

D attachment wall offset

LN contraction length of the power nozzle

NW power nozzle width as a dimensional parameter

Pc switch pressure on the control

Po recovery pressure on the output

Ps pressure supplied to the power nozzle

Qc switch flow rate on the control

Qs flow rate supplied to the power nozzle

$R_b$ Reynolds number based on the nominal nozzle width, b

SP splitter position

WF length of the wall flat on the attachment wall

WL length of the attachment wall

VW width of the vents

Ø attachment wall angle

Subscripts

l pertaining to the left side of the model

r pertaining to the right side of the model

## INTRODUCTION

The bistable fluid amplifier, commonly called the flip-flop, is a widely used component in digital fluidic circuitry. It is usually described as a relatively simple device containing no moving parts and powered by a fluid such as air. Qualitatively, the flip-flop's operation is described simply; however, from a quantitative standpoint, the flip-flop's operation is complex.

Figure 1 shows the geometry of a typical flip-flop which is available commercially. Its operation is as follows. A confined jet issues from the power nozzle and entrains fluid from both sides of the jet. The fluid entrainment creates a low pressure region on the sides of the jet. Due to instability, one side will become dominant; and, the jet will deflect toward and attach to one of the attachment walls. The low pressure region between the attached jet and the wall is known as the separation bubble. The fluid jet proceeds down the attachment wall, across the vent and into the corresponding output leg.

In the switching process, a control flow is introduced through the control port into the separation bubble causing a rise in the bubble pressure and a corresponding increase in the bubble size. The actual switching mechanism can be one of several types depending upon the geometry. The most common mode of switching is known as the terminated wall switch. Here, the size of the bubble increases driving the attachment point of the jet down the wall until it is literally driven off the end of the attachment wall. At this point, entrainment from the opposite side causes the jet to deflect toward and attach to the opposite wall. A second type of switch (known as opposite wall switching) occurs when

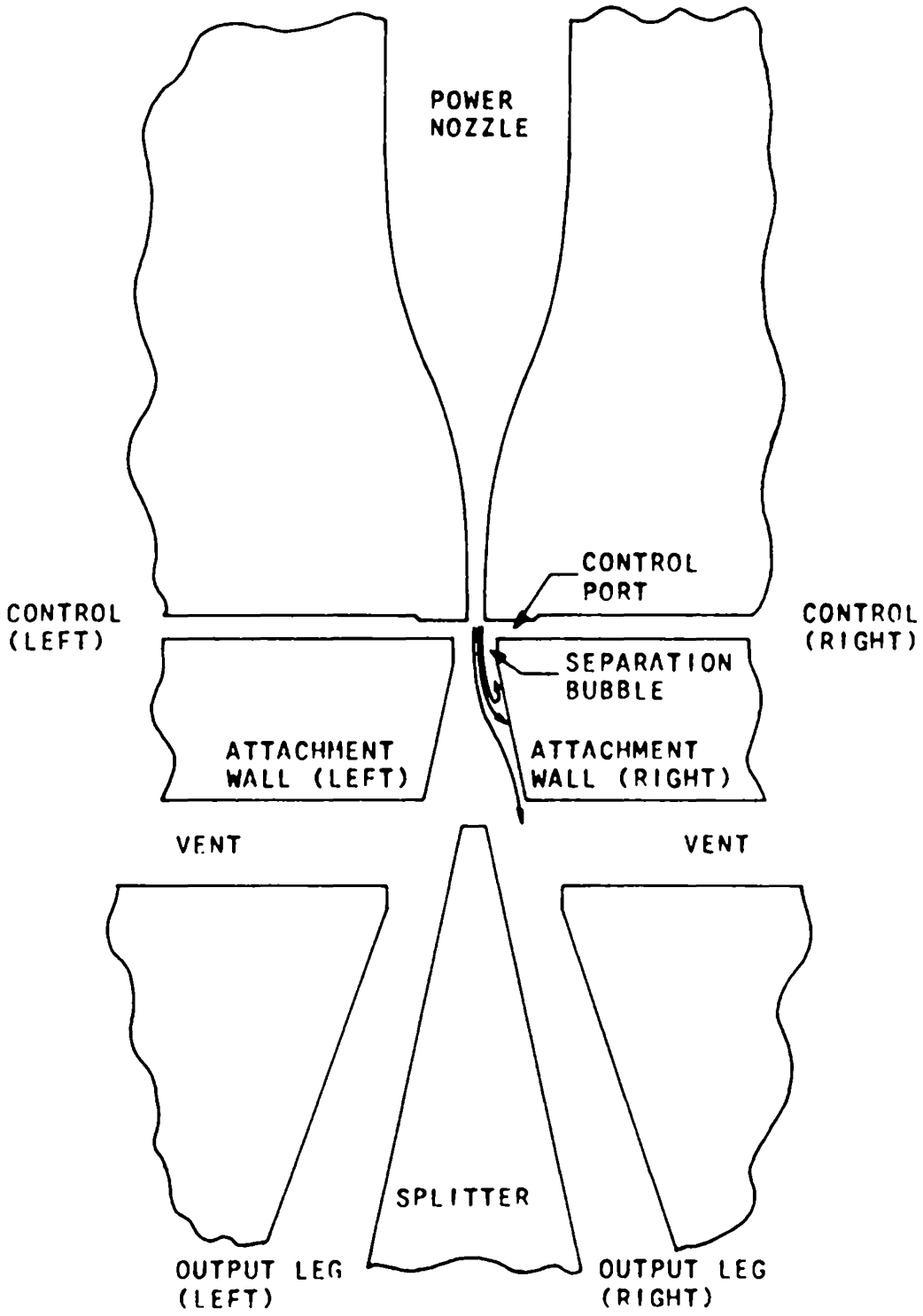


FIGURE 1. BISTABLE FLUID AMPLIFIER GEOMETRY

the attachment walls are in relatively close proximity. Here, the increase in separation bubble size causes the jet to contact and form a separation bubble on the opposite wall before the terminated wall switch occurs. The separation bubble on the opposite wall then pulls the jet to that wall. The third switching mode (seldom encountered) occurs when the splitter is placed near the attachment region. In this mode of switching, the jet is driven into the splitter; and, the presence of the splitter deflects the jet into the opposite wall.

For a more detailed look at the qualitative aspects of the attachment and switching, the reader is referred to Foster and Parker (1) and Warren (2).

Before examining the flip-flop's operation quantitatively, it is convenient to pause here and explain just what are the dimensional and fluid parameters of the flip-flop. Figure 2 shows the dimensional parameters of the power nozzle and attachment region. The power nozzle shape is defined in terms of the length, LN, over which the convergence occurs. The power nozzle width, b, is an important parameter in the sense that it is used to nondimensionalize the other parameters. The width of the port through which the control flow enters the separation bubble is known as the control width, CW. Called offset or setback, the dimension, D, indicates the position of the attachment wall relative to the end of the power nozzle. Other dimensions of the attachment wall include the wall length, WL, and wall angle, $\emptyset$. In recent years the parameter WF, wall flat, has been included in some manufactured devices. The splitter position is specified by SP and the size of the vents is called the vent width, VW. Finally, the depth of this device is specified in terms of

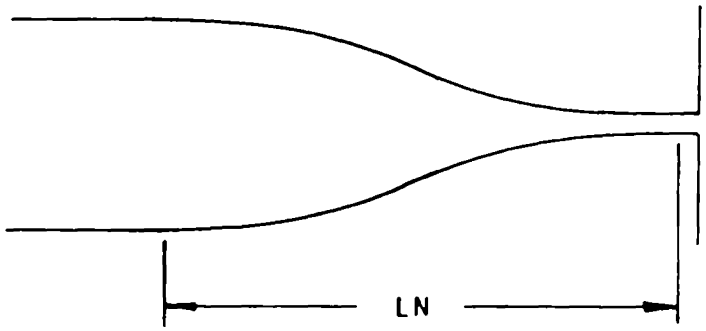


A. POWER NOZZLE

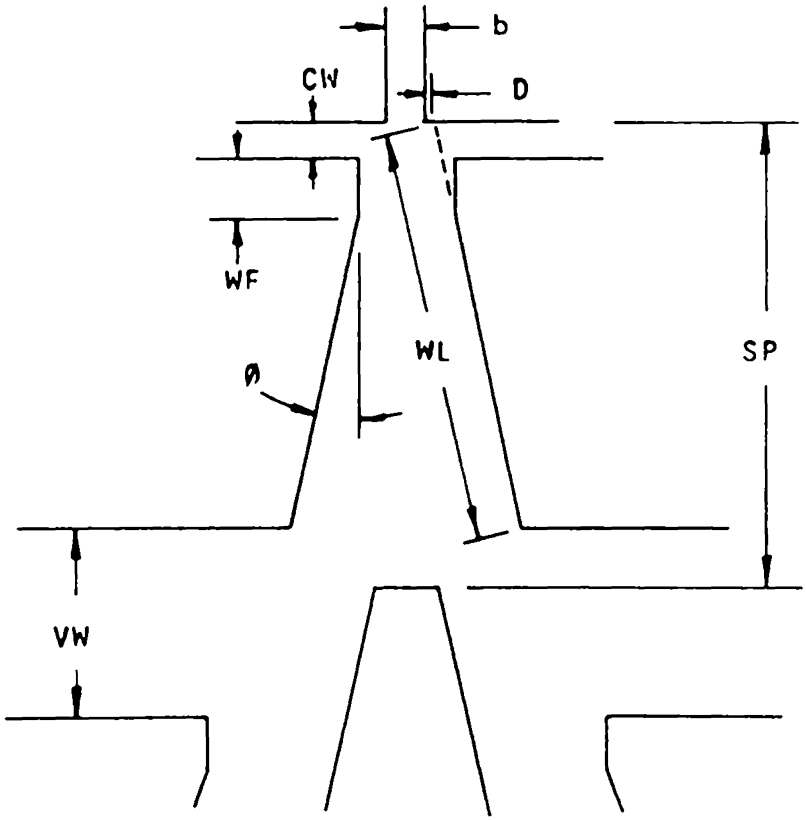


B. ATTACHMENT REGION

FIGURE 2. DIMENSIONAL PARAMETERS OF THE BISTABLE FLUID AMPLIFIER

the aspect ratio, AR, which is the ratio of the depth of the flow passages to the nozzle width.

The fluid parameters involved in the flip-flop's operation are as follows. The gage pressure supplied to the power nozzle is called the supply pressure which is symbolized by Ps. Qs indicates the volumetric flow rate in the power nozzle (called supply flow). The gage pressure and volumetric flow rate required of the control to switch the jet to the opposite wall are called the switch pressure (Pc) and switch flow (Qc) respectively. The flow impedance placed on the output legs is defined in terms of nozzle load where one nozzle load is the equivalent impedance of a control nozzle or port. The gage pressure recovered in the output leg is called recovery pressure Po.

The flip-flop and jet attachment process have been the subject of many previous experimental and analytical investigations. Some of the earlier works on the attachment process include those done by Borque and Newman (3), Levin and Manion (4), Sher (5) and Borque (6). These dealt with the basic attachment phenomena, investigating the flow from a two-dimensional standpoint with emphasis on the attachment length. McRee and Moses (7) and McRee and Edwards (8) added to the understanding of the flip-flop's operation by investigating the effects of aspect ratio and Reynolds number on the attachment process. Contributions in the area of three-dimensional flows include works by Cone (9), Nurmohamed (10), and Wagner and Owczarek (11) who looked at the effects of the inlet geometry and power nozzle shape. Investigating the recovery portion of the flip-flop, the output legs, Moses and Comparin (12) experimentally and analytically investigated the flow and pressure recovery in the output

legs, adding to the understanding of the effects of vent width and splitter position on the output characteristics.

This list of references is by no means a complete list of research that has been conducted on the attachment process and/or the flip-flop. There are many published investigations; but, they seldom deal with more than one or two isolated dimensional or fluid parameters; and further, they cover a wide variety in shapes and sizes of devices. A good number of investigators operate their experimental devices outside the range of the typical commercial counterparts; and further, they look at gross dimensional changes. These investigations are well suited for their intended purposes (studying one or two isolated parameters); however, they give little consideration to the people who design and manufacture flip-flops. The characteristics of a parameter in an environment isolated from other parameters are not necessarily those encountered in the actual device. What is needed are investigations of the entire device that are conducted in operating ranges comparable to that of existing devices.

Only a few investigators have tried to assemble a number or all of the parameters affecting the performance of the flip-flop. Moses and McRee (13) researched the fluid parameters, switch pressure and flow, as affected by the dimensional parameters offset, wall angle, and wall length; but, the experimental model used did not include the output legs or receivers. Further, the investigation dealt with a Reynolds number (based on nozzle width) much higher than those encountered in actual flip-flops. Goto and Drzewiecki (14) have put together a sophisticated analytical model solving 61 equations simultaneously. The model contains some empiricism but does cover a good portion of the dimension parameters.

Additional experimental data to check the validity of this mathematical model would be invaluable. Finally, Moses and Comparin (15) have provided a good summary of the state of the art which includes experimental data on a good number of dimensional and fluid parameters.

From the designer's and manufacturer's standpoint, the last three references cited (13, 14, 15) have assisted in the gross design of flip-flops but have been of little assistance in refining the designs. Narrowing the field of vision from this gross design, it was the purpose of this investigation to study the effects of offset, wall length, control width, nozzle width, wall flat, and power nozzle shape on the switch pressure, switch flow, and recovery pressure of the flip-flop. These dimensional parameters were investigated for their effects of relatively small variations from the current geometric configuration used in a typical commercial amplifier. Exceptions to this were the power nozzle shape, in which case the shapes studied were those recommended by Nurmohamed (10), and wall flat for which no published investigations were found. Further, the investigation was carried out with typical operating conditions imposed on the amplifier. The Reynolds number (based on nozzle width) was varied over a range of 2000 to 6000. This corresponds to the actual amplifier's operating range. Two output loadings of blocked and one nozzle load were studied. Finally, the entire investigation was carried out in a manner which closely simulated the actual flip-flop's operation.

## DESCRIPTION OF APPARATUS

The geometric configuration of the power nozzle and attachment region for a typical flip-flop is shown in Fig. 3. The dimensions are shown in terms of the nominal nozzle width b. It should be noted here that the nozzle width is given two symbols, b and NW. The nominal nozzle width is indicated by b and is used as the characteristic dimension of the flip-flop. NW is used in the investigation of the effects of nozzle width variance. The dimensional parameters are shown in symbolic form as defined previously where nominally D is 0.2b, CW is 1.0b, WL is 10.86b, WF is 1.55b, NW is 1.0b, LN is 27.0b, and the depth of the flow passages is 2b. Now in the actual device b is 0.01 in.; so, it is obviously impractical to build an experimental model of actual size to study small dimensional changes. For this reason, the experimental model constructed was 10 times actual size thus making b equal to 0.1 in.

The model, constructed in three layers, consisted of a 1/2-in. aluminum base plate, 0.2-in.-thick Plexiglas pieces machined to form the flow passages, and a 1/4-in.-thick Plexiglas cover plate. The 0.2-in.-thick Plexiglas pieces were secured to the base plate with recessed machine screws. The confirguration is shown in Fig. 4. Enough clearance was used in the securing screws to allow at least $\pm$ 20% change in the dimensions studied. Dimensional changes in power nozzle shape, wall length, and wall flat were accomplished by fabricating replaceable pieces secured with recessed machine screws. Where recesses and gaps occurred in the flow passages, modeling clay was used to fill these places.

The assembled model (base plate, flow passages, and cover plate)

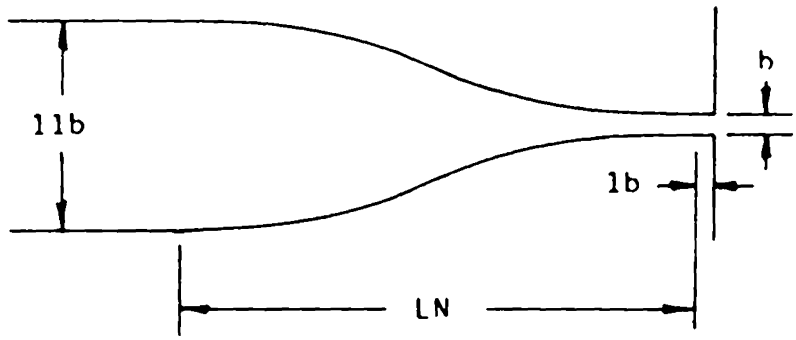


A. POWER NOZZLE

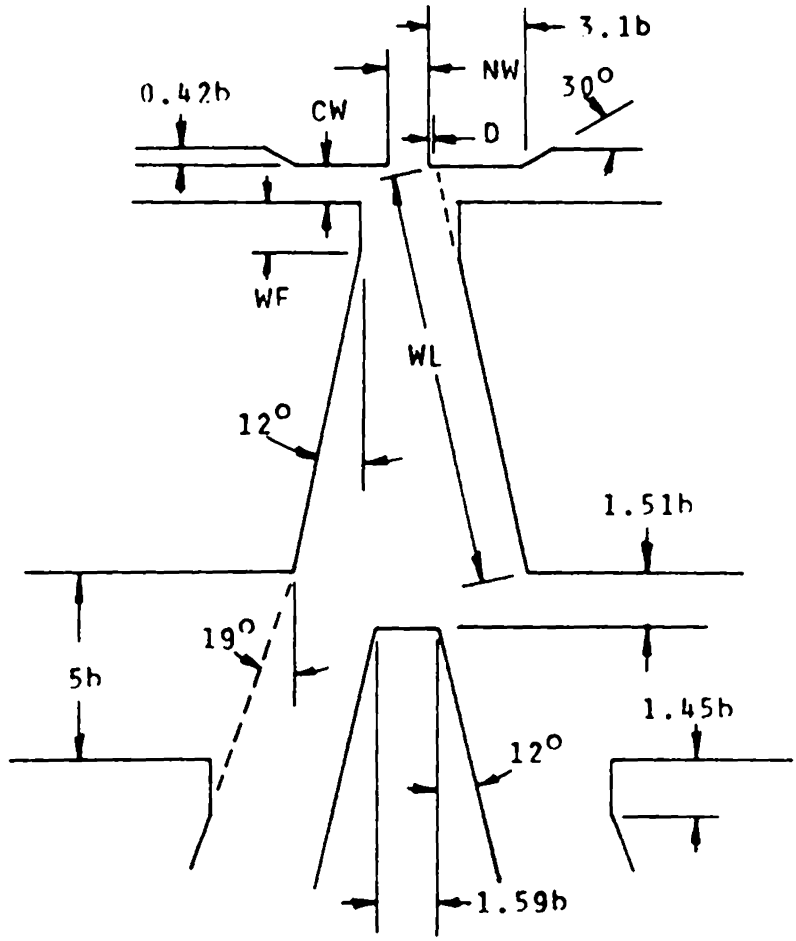


B. ATTACHMENT REGION

FIGURE 3. GEOMETRY OF A TYPICAL AMPLIFIER

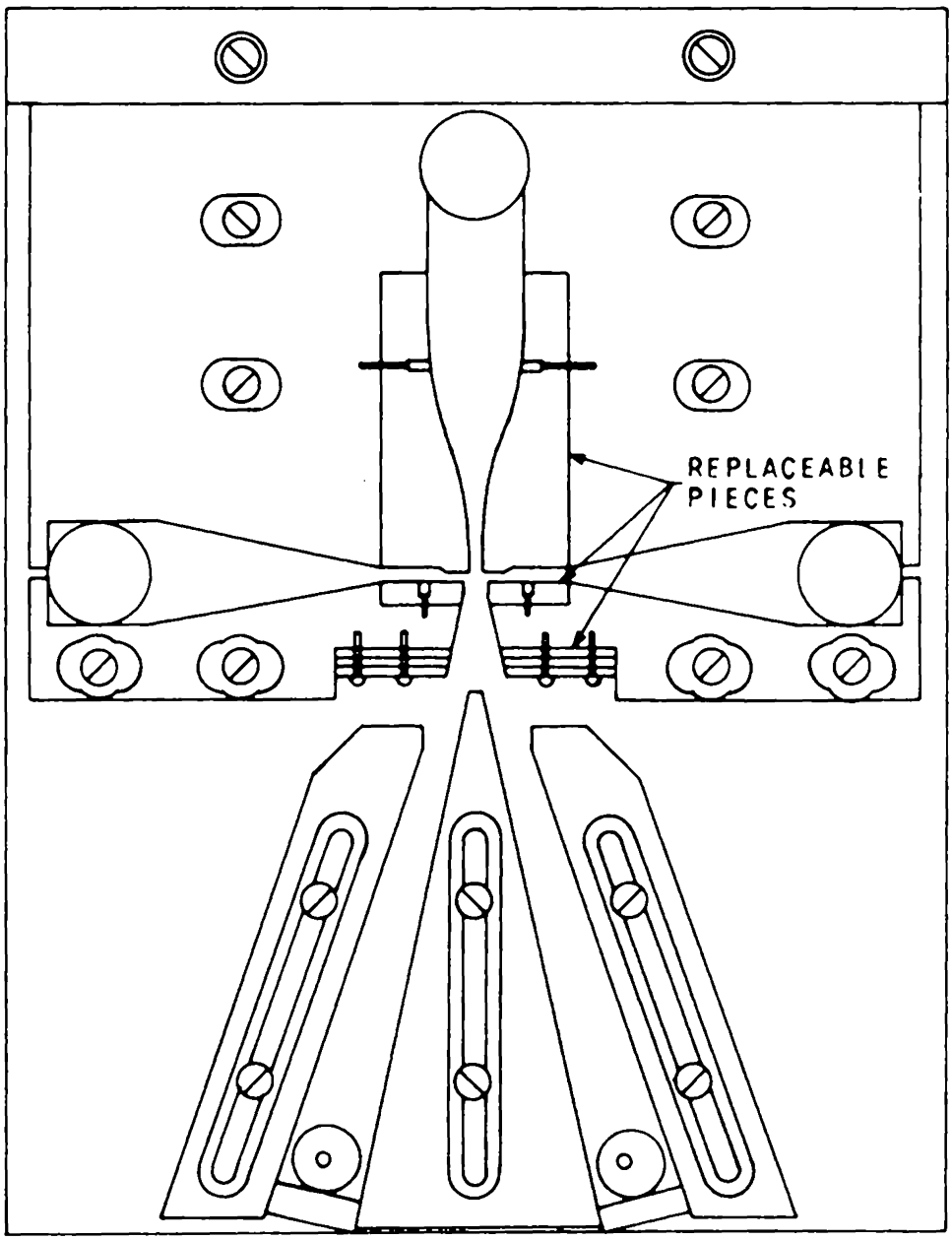


FIGURE 4. EXPERIMENTAL MODEL CONFIGURATION

was placed in a clamping structure designed to assure sealing of the passages as well as provide quick access to the model to perform dimensional changes. This structure, shown in Fig. 5, consisted of a 2-in. aluminum base plate and a door-like structure of steel bars. Twenty-one screws in the door structure sandwiched the model to the base plate of this clamping structure. The door structure was hinged on one side and secured in the closed position with four bolts on the opposite side. Flow passages to the power nozzle and controls, and from the outputs were conveniently located in the base plates of the clamping structure and model. The base plate of the clamping structure was also a convenient place to locate the static pressure taps for the supply, controls, and outputs as well as a place for the output load orifices.

As pointed out by Cone (9) and Wagner and Owczarek (11), inlet geometry can introduce secondary flows to the power nozzle and influence flip-flop performance. For this reason, care must be used in the design of the inlet geometry to the power nozzle. In this experimental apparatus the supply flow entered a 4-in.-long, $12^{o}$ included angle, diffuser. The diffuser, fabricated of Plexiglas, mated with the 1.2-in.-diameter passage carrying the flow to the power nozzle. To further assure uniform flow here, a screen fabricated of 1/4-in.-thick Plexiglas, perforated with 1/32-in. holes, was placed at the end of the diffuser. The supply pressure tap (a 1/64-in.-diameter hole in the side of the clamp base) was located 1 1/2 in. above this screen. Similar pressure taps were located in the passages for the control and output flows.

The passages to the controls do not need to be as elaborate as the supply. Pipe couplings were used to interface the 3/8-in. plastic control

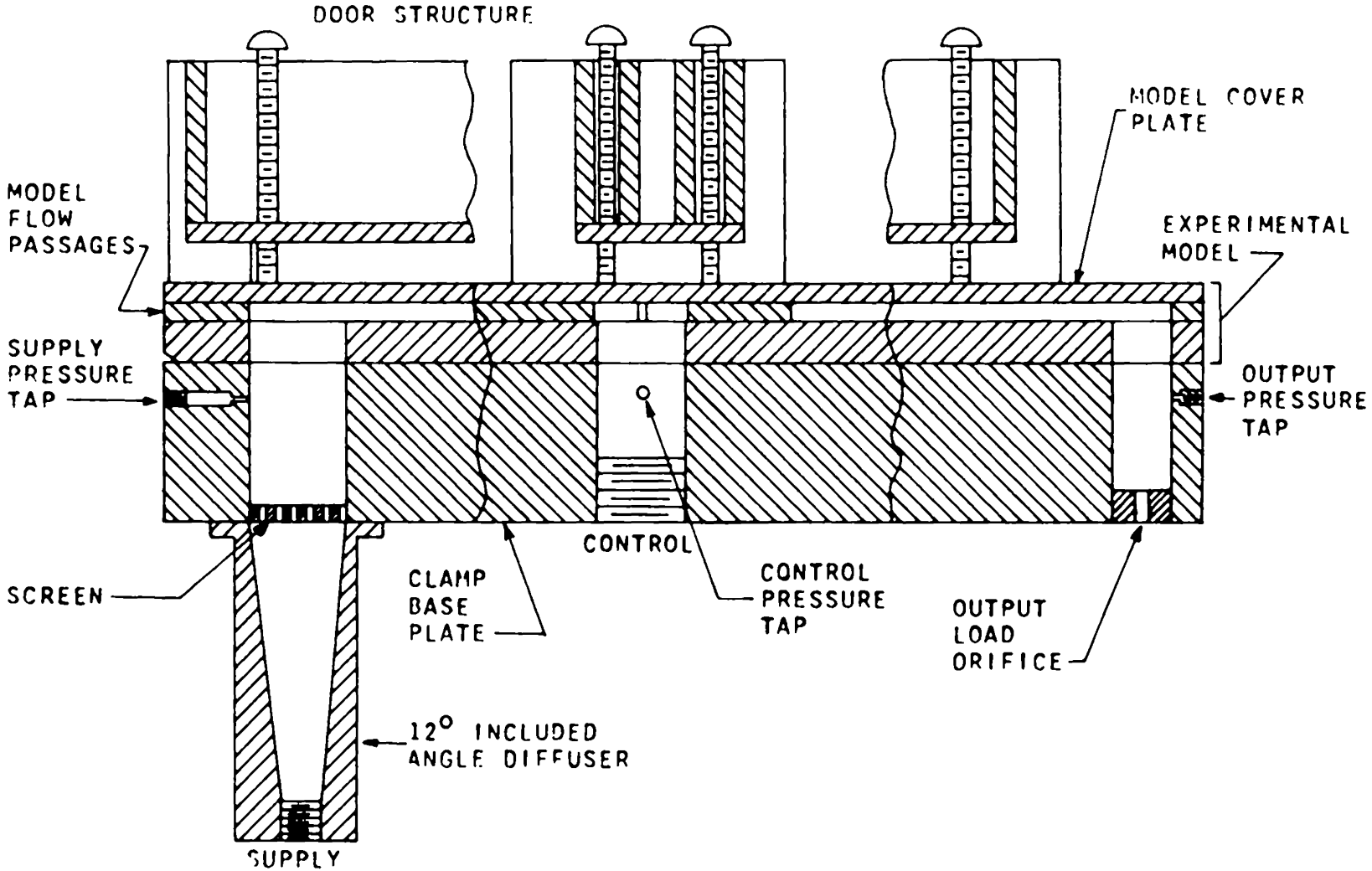


FIGURE 5. CROSS SECTION OF THE MODEL FIXTURE

tubing to the 1-in. diameter control passages in the clamp base. The control pressure taps were located 1 3/4 in. from the bottom of the clamp base plate.

The output pressure taps were also located 1 3/4 in. from the bottom of the clamp base plate. The 3/4-in.-diameter output passages were convenient places to locate output loadings. The output load impedance of 1 nozzle load (impedance of a control nozzle) was simulated by placing an orifice in the bottom of each output passage. The area of the orifice was computed by multiplying the area of a control port by the ratio of discharge coefficients of a nozzle to an orifice. The coefficient of discharge for the control nozzle or port was assumed to be 0.98 and 0.6 for the orifice; so that, for this apparatus, the area of the orifice was 0.033 sq in. The orifices (3/8-in.-thick brass plugs with a 0.204-in.-diameter hole) were fitted into the output passages. To simulate the blocked output load, it was a simple matter to place a piece of tape over the orifices.

The performance measurement system is shown in Fig. 6. Shop air at 100 psi was supplied through 3/8-in. plastic tubing to two regulators in parallel. The supply flow regulator (a Norgren 0-60 psig pressure regulator) dropped the line pressure to 20 psig and fed it to a needle valve. The needle valve was used for control of the air flow to the power nozzle. Exiting the valve, the supply flow passed through a Brooks rotameter, size no. R-8M-25-5, for measurement of volume flow rate and then passed on to the diffuser and power nozzle. All connections for this path were done with 3/8-in. plastic tubing. The control flow pressure regulator (a Fairchild Hiller, Model no. 10, 0-10 psig) dropped the

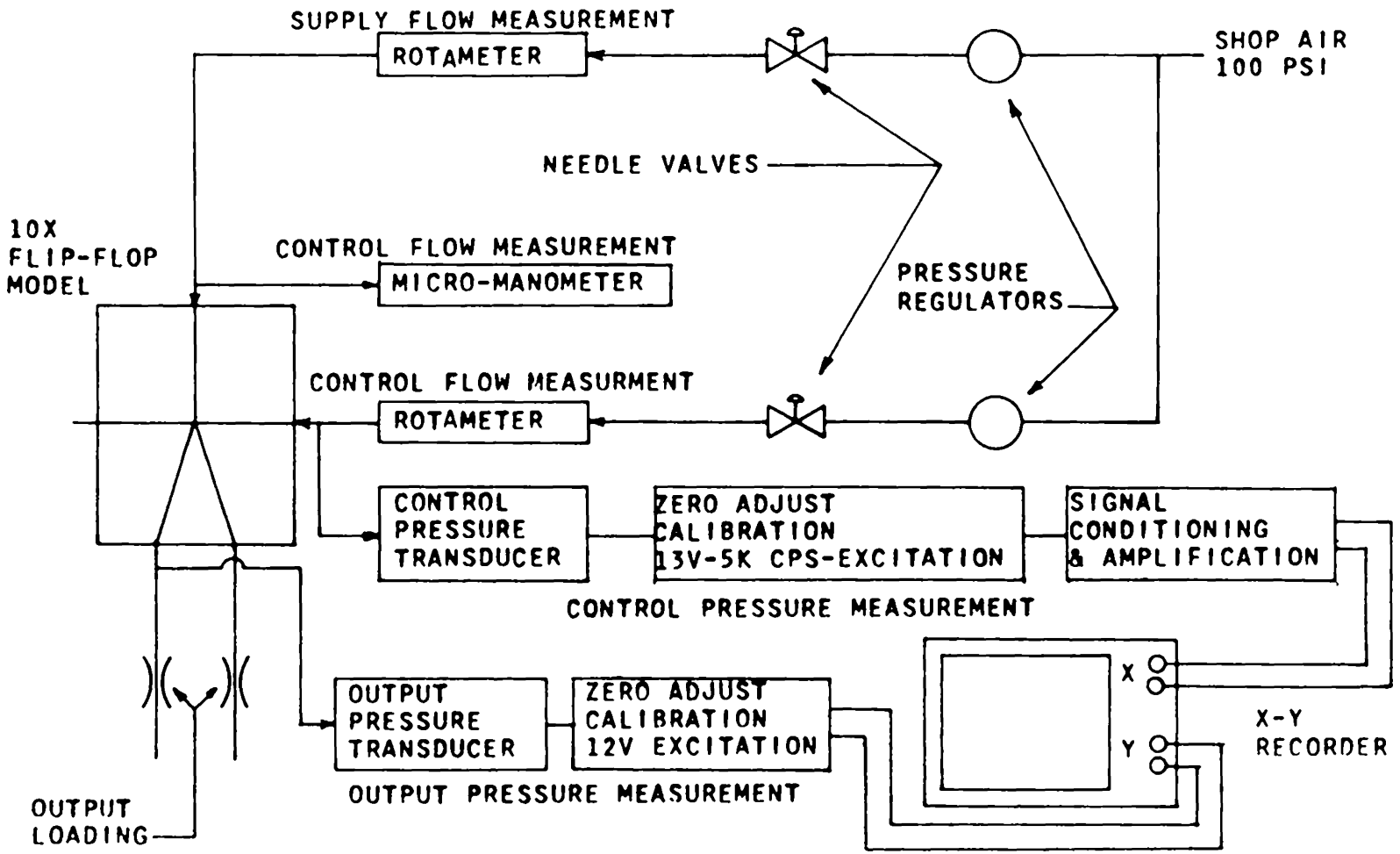


FIGURE 6. PERFORMANCE MEASUREMENT SYSTEM

line pressure to 6 psig. The flow was then fed to a needle valve for control and then on to a rotameter (a Lab-Crest Div. F. S. P. Co. catalog no. 448-308 with a glass float). Exiting the rotameter, the flow passed to the control passage of the model. All connections in this path were also made with 3/8-in. plastic tubing.

The measurement of supply pressure was done with a micro-manometer manufactured by E. Vernon Hill, 0-5 in. $H_2O$. The measurement of switch pressure was not as simple as that for the supply. To accomplish this measurement, a system was devised where the control pressure was recorded on the x axis of an x - y recorder; and, the output pressure was recorded on the y axis. The system provided an accurate means of measuring the switch pressure.

The control pressure tap was connected with 1/4-in. plastic tubing to a Pace, Model P109D, variable reluctance differential pressure transducer with a range of $\pm$ 1 in. $H_2O$. The excitation voltage for this transducer (13 volts at 5000 cps) was supplied by a Sanborn Transducer Converter, Model 592-300. Balancing and calibration circuitry were constructed for this transducer. The output signal of the transducer was demodulated by the Sanborn Transducer Converter; but, it was found necessary to further filter this signal and then amplify it before passing it to the x - y recorder. A low pass filter was constructed; and, the signal amplification was done by a Hewlett Packard, Model 2470A, d-c amplifier. The x - y recorder used was a F. L. Moseley, Model 135 recorder.

The output pressure tap was connected to a Statham, Model PM5TC $\pm$ 0.3-350, range $\pm$ 0.3 psi, strain gage differential pressure transducer

with 1/4-in. plastic tubing. This transducer was supplied with an excitation of 12V d-c. Balancing and calibration circuitry were also constructed for this transducer. The signal from the transducer needed no further conditioning and was fed directly to the y axis of the x - y recorder.

To complete this section, a photograph of the entire experimental apparatus is shown in Fig. 7.

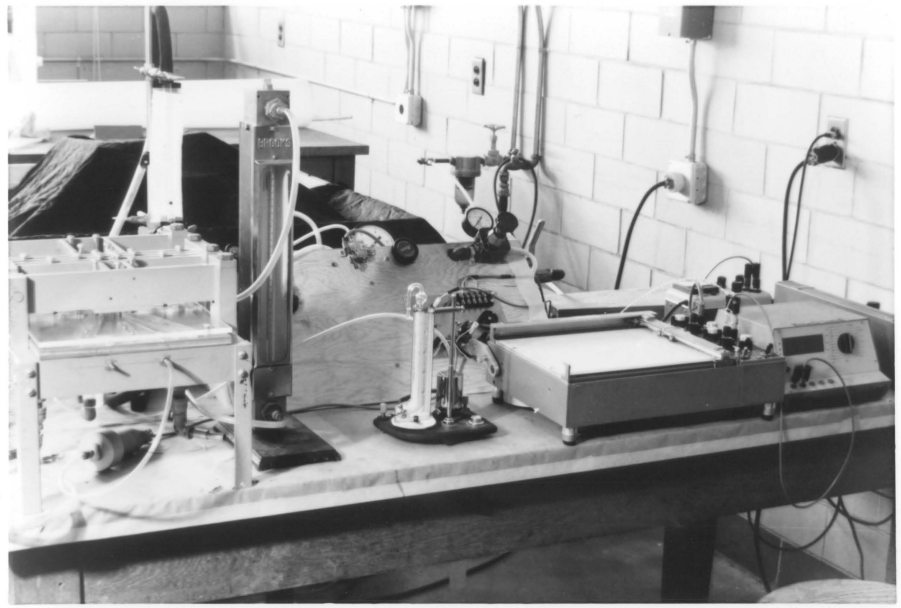

FIGURE 7. EXPERIMENTAL APPARATUS

## PROCEDURE

The first step in preparation for the operation of the facility was to calibrate the various measuring equipment. It was especially important to assure that the outputs of the two pressure transducers were linear.

With all control and output pressure measurement equipment connected as shown in Fig. 6, the equipment was allowed a two hour warm-up period; and, each transducer was calibrated and checked for linearity using a micro-manometer as a reference. The control pressure transducer's linearity was checked over the range 0-1 in. $H_2O$ gage; the calibration signal was found equivalent to 0.287 in. $H_2O$. The output pressure transducer's linearity was checked over the range 0-1.5 in. $H_2O$ gage; and, the calibration signal was found equivalent to 0.682 in. $H_2O$.

The two rotameters were calibrated with a Brooks, Model 1057, Vol-U-Meter. For each rotameter, a flow was set and a stop watch was used to measure the time required to pass a particular volume of air. The control flow rotameter was calibrated over the range 0.04-0.4 cfm; and, the supply flow rotameter was calibrated over the range 0.1-1 cfm.

In the operation of the facility, the model's dimensional parameters were set using feeler gages, a four-inch dial caliper and a jig constructed to set the receiver of the model. The feeler gages were stacked together and placed in the flow passages. The Plexiglas pieces forming the flow passages were then butted against the gages and secured there. This procedure allowed the setting of nozzle width, control, width, and offset to within $\pm$ 0.001 in. The dimensional parameters of power nozzle shape, wall flat, and wall length were varied by replacing

the respective Plexiglas parts. The accuracy of these dimensional parameters was, therefore, limited to that of the technique of fabricating the replaceable parts. The accuracy of these dimensions was held within $\pm$ 0.001 in. The jig was fashioned out of 1/4-in. Plexiglas and was placed in the vent and output passages. This jig allowed the positioning of the receivers to within $\pm$ 0.002 in. The caliper was used to assure that the correct dimension had been set.

The dimensional parameters studied were varied one at a time holding all other dimensions shown in Fig. 3 to their nominal values. This procedure of holding other dimensions constant was done so that the effects of a particular dimensional parameter were nearly isolated. To give an example of what is meant by nearly isolated, when the offset, D, was increased, the dimensions LN, CW, NW, and WF were held to their nominal values. Further, the vent width and splitter position were held constant; but in this example, the width of the output legs had to be increased. The point made here is that the effects of a particular parameter could not be totally isolated.

The values of the parameters for which performance data were taken are presented in Table 1. The underlined values in this table indicate the nominal dimensions.

With the model set in a particular geometric configuration, it was mounted in the clamping structure; and, the following performance data were acquired. First of all, output or recovery pressure (Po) was recorded on each of the outputs (left and right), for both one nozzle and blocked output loadings, and for Reynolds numbers (based on nominal nozzle width b) of 1950, 2900, 3900, 4850 and 5800. It should be noted here

Table 1

Dimensions Investigated

Offset (D):

| | | | | |
|---|---|---|---|---|
| D/b = 0.4 | D/b = 0.3 | D/b = 0.2 | D/b = 0.1 | D/b = 0.0 |

Wall Length (WL):

| | | | | |
|---|---|---|---|---|
| WL/b = 12.84 | WL/b = 11.84 | WL/b = 10.86 | WL/b = 9.83 | WL/b = 8.81 |

Control Width (CW):

| | | | | |
|---|---|---|---|---|
| CW/b = 1.2 | CW/b = 1.1 | CW/b = 1.0 | CW/b = 0.9 | CW/b = 0.8 |

Power Nozzle Width (NW):

| | | | | |
|---|---|---|---|---|
| NW/b = 1.2 | NW/b = 1.1 | NW/b = 1.0 | NW/b = 0.9 | NW/b = 0.8 |

Wall Flat (WF):

| | | |
|---|---|---|
| WF/b = 0.0 | WF/b = 1.55 | WF/b = 2.52 |

Power Nozzle Shape (LN):

| | | |
|---|---|---|
| LN/b = 27.0 | LN/b = 15.0* | LN/b = 10.0* |

*These dimensions are those as recommended by Nurmohamed (10).

that these Reynolds numbers were calculated from the supply pressure. This was done by assuming that the velocity of the supply flow at the pressure tap was essentially zero and that the static pressure at the nozzle exit was atmospheric. This, along with the assumption of incompressible flow, allows the use of Bernoulli's equation to compute the velocity at the exit of the power nozzle and thus computation of the Reynolds numbers. The Reynolds numbers cited above correspond to supply pressures of 0.359, 0.807, 1.434, 2.242, and 3.227 in. $H_2O$ respectively. All 20 recovery pressures recorded were taken with the controls to the flip-flop open to the atmosphere. The next step in the data acquisition procedure was to record switch pressure, Pc, and switch flow rate, Qc. In order to later nondimensionalize Qc, the supply flow rate, Qs, was also recorded. The switch pressures and flows were recorded for each of the two controls, for each of the two output loads, and for each of the above cited Reynolds numbers. Further, these switch data were repeated four to six times so that a mean value could be computed. It should be noted here that the inactive control was open to the atmosphere during this portion of the procedure. This is true in the actual device.

The actual mechanics of operating the faciltiy were as follows. Before any data were taken, the instrumentation was allowed a two hour warm-up period. After this, calibration and scaling of the x - y recorder were performed. The supply pressure (and thus Reynolds number) was adjusted with the needle valve on the supply line. This pressure was set within $\pm$ 0.005 in. $H_2O$. During the acquisition of switching data, the flip-flop's behavior was such that an increase in control pressure caused a rise in supply pressure so that the supply pressure was set to

give a desired value when the switch actually occurred. The supply flow rate was also recorded at this point. The switching process was done by slowly opening the needle valve on the control line causing a rise in control pressure and flow. The switch pressure was recorded on the x - y recorder and the switch flow rate was read from the rotameter. The device was then reset; and, the process was repeated.

To handle these large amounts of data, a digital computer was used to manipulate the data. Recovery pressures were nondimensionalized by dividing by the supply pressure. The same was done with the switch pressures. The nondimensional values were averaged to produce a mean switch pressure for each configuration, for each Reynolds number, for each output loading, and for each side. The switch flow rates were nondimensionalized with the supply flow and averaged in the same manner as the switch pressures.

## RESULTS

This section presents the results obtained during this investigation. Contained herein are six tables (2 through 7). Each table presents all of the experimental data obtained for the particular dimensional parameter. Following each table are six figures in which typical cases from the tables are plotted.

To be more specific, the contents of this section are as follows. Table 2 contains the offset results and Fig. 8 through 13 show typical cases for this dimensional parameter. Table 3 presents the wall length results and Fig. 14 through 19 show the typical characteristics of this parameter. Table 4 presents the control width results and associated with this parameter are Fig. 20 through 25. Table 5 contains the power nozzle width results and Fig. 26 through 31 show the typical characteristics of this parameter. Table 6 presents the results of wall flat and associated with it are Fig. 32 through 37. Finally, Table 7 contains the results of power nozzle shape and Fig. 38 through 43 show the typical cases for this parameter.

Each table is divided into two major sections. The first section presents the results for a 1 nozzle loading on the outputs. The second section presents results for blocked outputs. Underlined dimensions in the table indicate that the data are for the nominally dimensioned device. Each switch pressure and flow presented in the tables is a mean value of at least 4 observations of the switch point. In the averaging process caution must be used so that relevant information is not destroyed. Where unusual behavior was noted in the operation, notes are placed in the tables where the behavior occurred; and, at the bottom of the tables is a

description of that behavior. These notes became the key to justifying the curves and characteristics that were fitted to the data points. A detailed explanation of the manner in which these curves were drawn is contained in the next section. Notes placed on the curves in the figures correspond to notes in the tables. The six figures following each table show the effects of the dimensional parameter on the switch pressure, switch flow, and recovery pressure for both output loadings. The typical cases shown in the figures are for Reynolds numbers of 1950, 3900, and 5800.

As a final item to note, the data for the nominally dimensioned device in Tables 6 and 7 were simply reprinted from Table 5. After having established repeatability of this nominal data in Tables 2 through 5, it was deemed unnecessary to completely retest the nominal device.

Table 2. Offset Results

1 nozzle load:

| D/b | $R_b$ | $Pc_r/Ps$ | $Pc_l/Ps$ | $Qc_r/Qs$ | $Qc_l/Qs$ | $Po_r/Ps$ | $Po_l/Ps$ |
|---|---|---|---|---|---|---|---|
| 0.0 | 1950 | .045 | .047 | .144 | .150 | .209 | .209 |
| | 2900 | .132 | .144 | .248 | .256 | .229 | .229 |
| | 3900 | .147 | .164 | .265 | .273 | .251 | .248 |
| | 4850 | .154 | .171 | .270 | .280 | .259 | .257 |
| | 5800 | .155 | .150 | .266 | .260 | .265 | .263 |
| 0.1 | 1950 | .025 | .028 | .145 | .156 | .195 | .195 |
| | 2900 | .110 | note a | .252 | note a | .223 | .223 |
| | 3900 | note b | .167 | note b | .308 | .244 | .237 |
| | 4850 | .148 | .161 | .285 | .298 | .252 | .250 |
| | 5800 | .135 | .133 | .270 | .269 | .257 | .257 |
| 0.2 | 1950 | .025 | .033 | .144 | .163 | .209 | .209 |
| | 2900 | note c | .132 | note c | .274 | .217 | .217 |
| | 3900 | .128 | .137 | .280 | .286 | .234 | .234 |
| | 4850 | .149 | .132 | .298 | .283 | .241 | .243 |
| | 5800 | .131 | .119 | .276 | .270 | .246 | .249 |
| 0.3 | 1950 | .026 | .026 | .155 | .160 | .195 | .195 |
| | 2900 | .071 | note d | .231 | note d | .217 | .204 |
| | 3900 | .116 | .124 | .278 | .286 | .230 | .220 |
| | 4850 | .131 | .122 | .290 | .285 | .234 | .232 |
| | 5800 | .119 | .120 | .282 | .292 | .238 | .235 |
| 0.4 | 1950 | .015 | .022 | .136 | .151 | .195 | .181 |
| | 2900 | .050 | .053 | .213 | .217 | .204 | .198 |
| | 3900 | .101 | .113 | .274 | .285 | .216 | .213 |
| | 4850 | .126 | .122 | .299 | .300 | .223 | .221 |
| | 5800 | .125 | .123 | .298 | .304 | .226 | .228 |

Notes on Table 2:

note a A large amount of scatter in the switch points was noticed which strongly indicates the coexistence of two switch points here.
$Pc_l/Ps$ 0.100 - 0.165 $Qc_l/Qs$ 0.250 - 0.290

note b Mild indications of two switch points were noted.
$Pc_r/Ps$ 0.120 - 0.142 $Qc_r/Qs$ 0.260 - 0.283

note c Indications of two switch points coexisting here were noted.
$Pc_r/Ps$ 0.083 - 0.110 $Qc_r/Qs$ 0.234 - 0.270

note d Indications of two switch points coexisting here were noted.
$Pc_l/Ps$ 0.064 - 0.100 $Qc_l/Qs$ 0.229 - 0.265

Table 2. Continued

blocked output

| D/b | $R_b$ | $Pc_r/Ps$ | $Pc_l/Ps$ | $Qc_r/Qs$ | $Qc_l/Qs$ | $Po_r/Ps$ | $Po_l/Ps$ |
|---|---|---|---|---|---|---|---|
| 0.0 | 1950 | .045 | .048 | .152 | .153 | .279 | .279 |
| | 2900 | .078 | .083 | .202 | .209 | .291 | .291 |
| | 3900 | .105 | .109 | .230 | .234 | .310 | .307 |
| | 4850 | .121 | .122 | .243 | .247 | .317 | .317 |
| | 5800 | .121 | .128 | .241 | .245 | .324 | .325 |
| 0.1 | 1950 | .039 | .040 | .158 | .163 | .251 | .251 |
| | 2900 | .067 | .086 | .212 | .225 | .285 | .285 |
| | 3900 | .091 | .101 | .240 | .247 | .303 | .300 |
| | 4850 | .107 | .121 | .257 | .266 | .308 | .310 |
| | 5800 | .112 | .121 | .255 | .261 | .315 | .319 |
| 0.2 | 1950 | .024 | .034 | .151 | .160 | .265 | .265 |
| | 2900 | .059 | .063 | .214 | .216 | .285 | .279 |
| | 3900 | .085 | .086 | .245 | .244 | .300 | .296 |
| | 4850 | .107 | .108 | .262 | .264 | .306 | .308 |
| | 5800 | .113 | .106 | .265 | .260 | .313 | .315 |
| 0.3 | 1950 | .024 | .024 | .153 | .155 | .265 | .251 |
| | 2900 | .054 | .060 | .205 | .209 | .279 | .266 |
| | 3900 | .079 | .083 | .240 | .243 | .296 | .286 |
| | 4850 | .098 | .099 | .261 | .263 | .301 | .299 |
| | 5800 | .107 | .105 | .267 | .267 | .307 | .305 |
| 0.4 | 1950 | .018 | .020 | .155 | .166 | .265 | .237 |
| | 2900 | .054 | .055 | .220 | .224 | .273 | .266 |
| | 3900 | .081 | .080 | .258 | .256 | .286 | .279 |
| | 4850 | .095 | .095 | .272 | .272 | .292 | .292 |
| | 5800 | .104 | .101 | .279 | .282 | .294 | .297 |

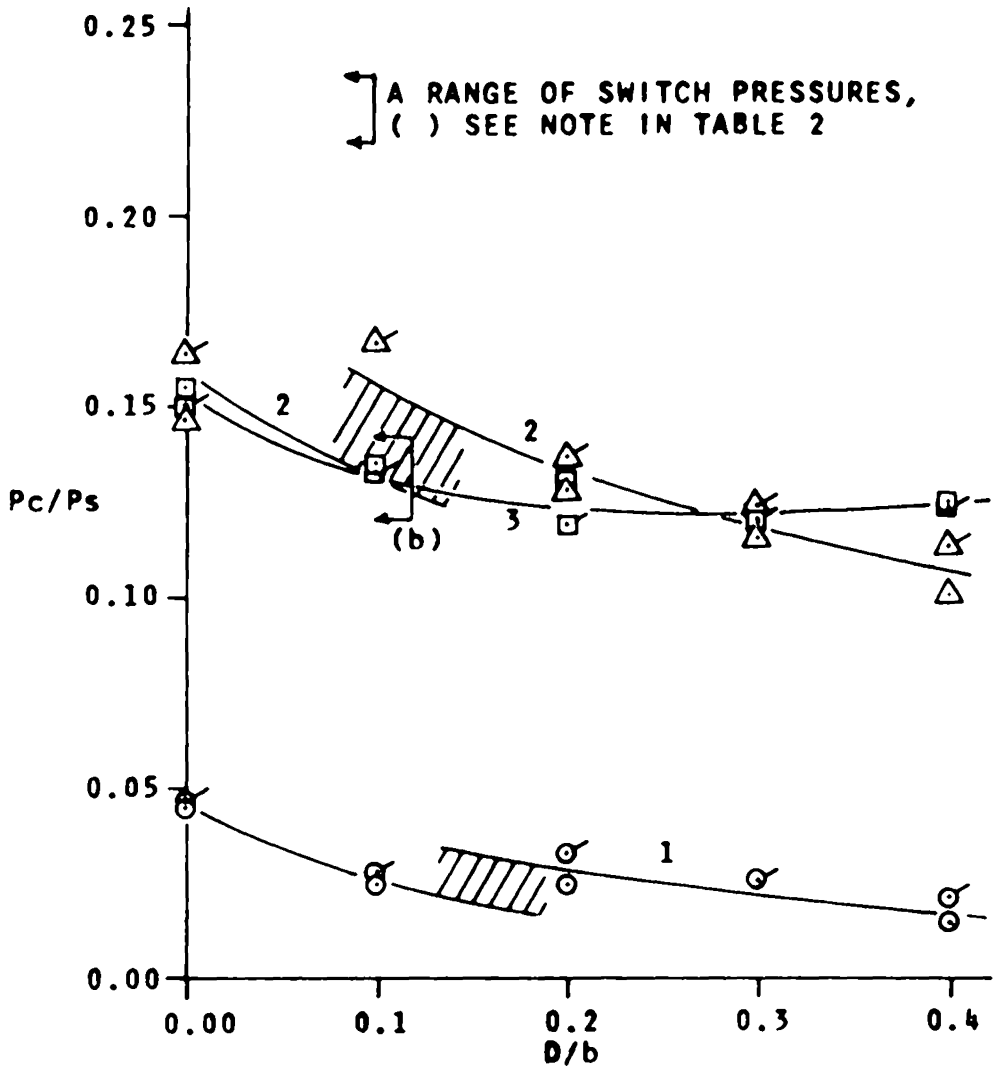


FIGURE 8. OFFSET EFFECTS ON SWITCH PRESSURE; 1 NOZZLE LOADING

LEGEND:

| REYNOLDS NO. | RIGHT SIDE | LEFT SIDE | CURVE LABEL |
|---|---|---|---|
| 1950 | ○ | ○ | 1 |
| 3900 | △ | △ | 2 |
| 5800 | □ | □ | 3 |

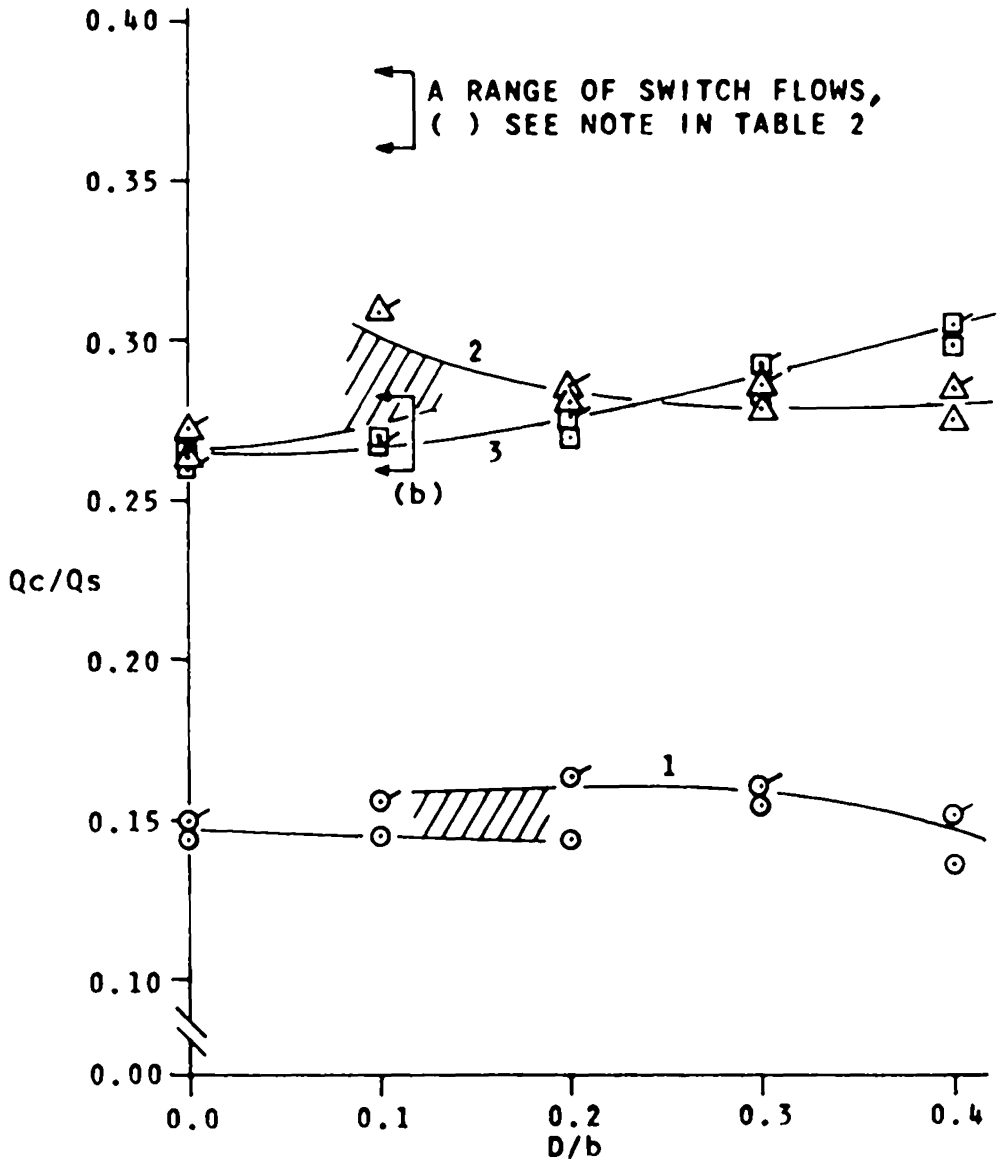


FIGURE 9. OFFSET EFFECTS ON SWITCH FLOW; 1 NOZZLE LOADING

LEGEND:

| REYNOLDS NO. | RIGHT SIDE | LEFT SIDE | CURVE LABEL |
|---|---|---|---|
| 1950 | ○ | ○ | 1 |
| 3900 | △ | △ | 2 |
| 5800 | □ | □ | 3 |

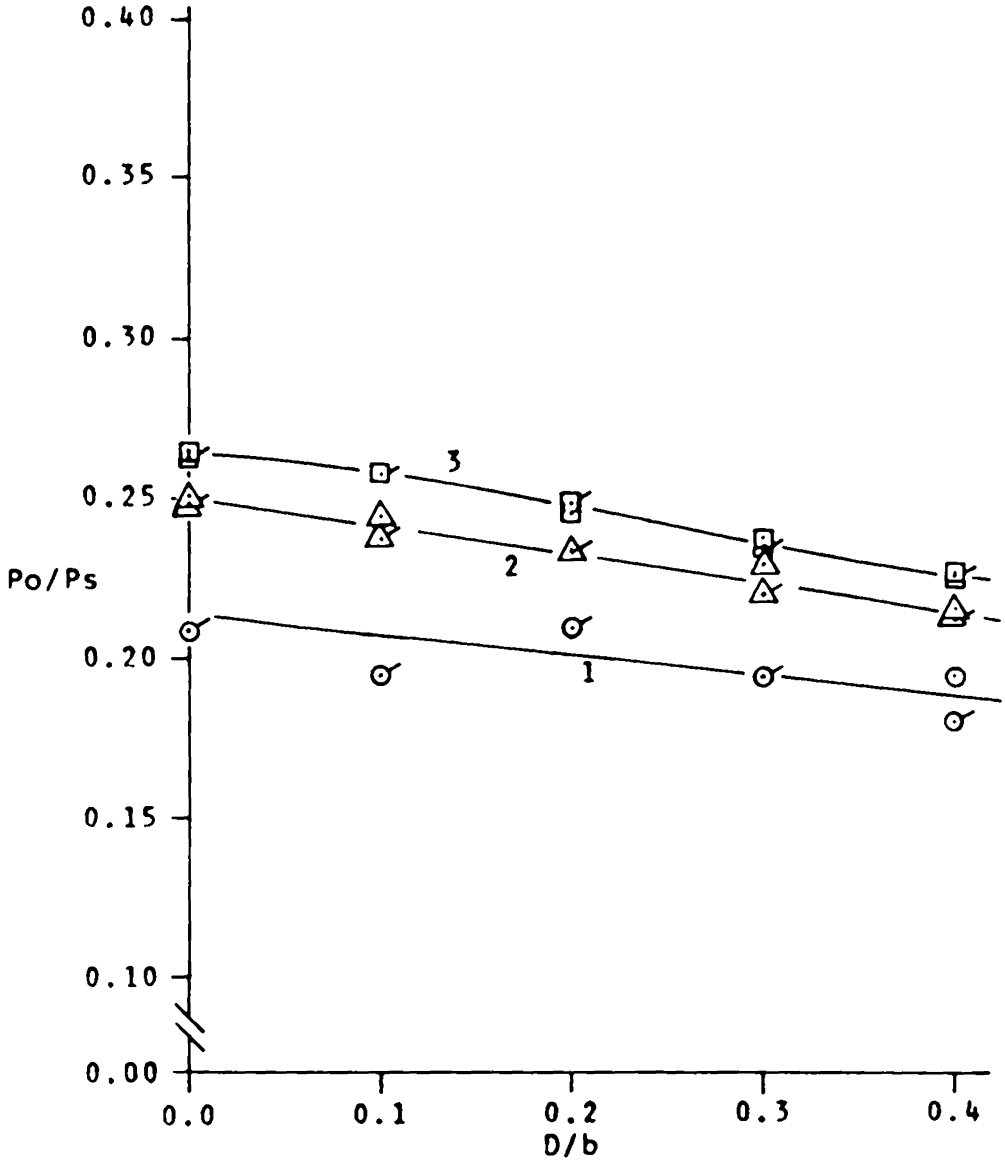


FIGURE 10. OFFSET EFFECTS ON RECOVERY PRESSURE; 1 NOZZLE LOADING

LEGEND:

| REYNOLDS NO. | RIGHT SIDE | LEFT SIDE | CURVE LABEL |
|---|---|---|---|
| 1950 | ○ | ○ | 1 |
| 3900 | △ | △ | 2 |
| 5800 | □ | □ | 3 |

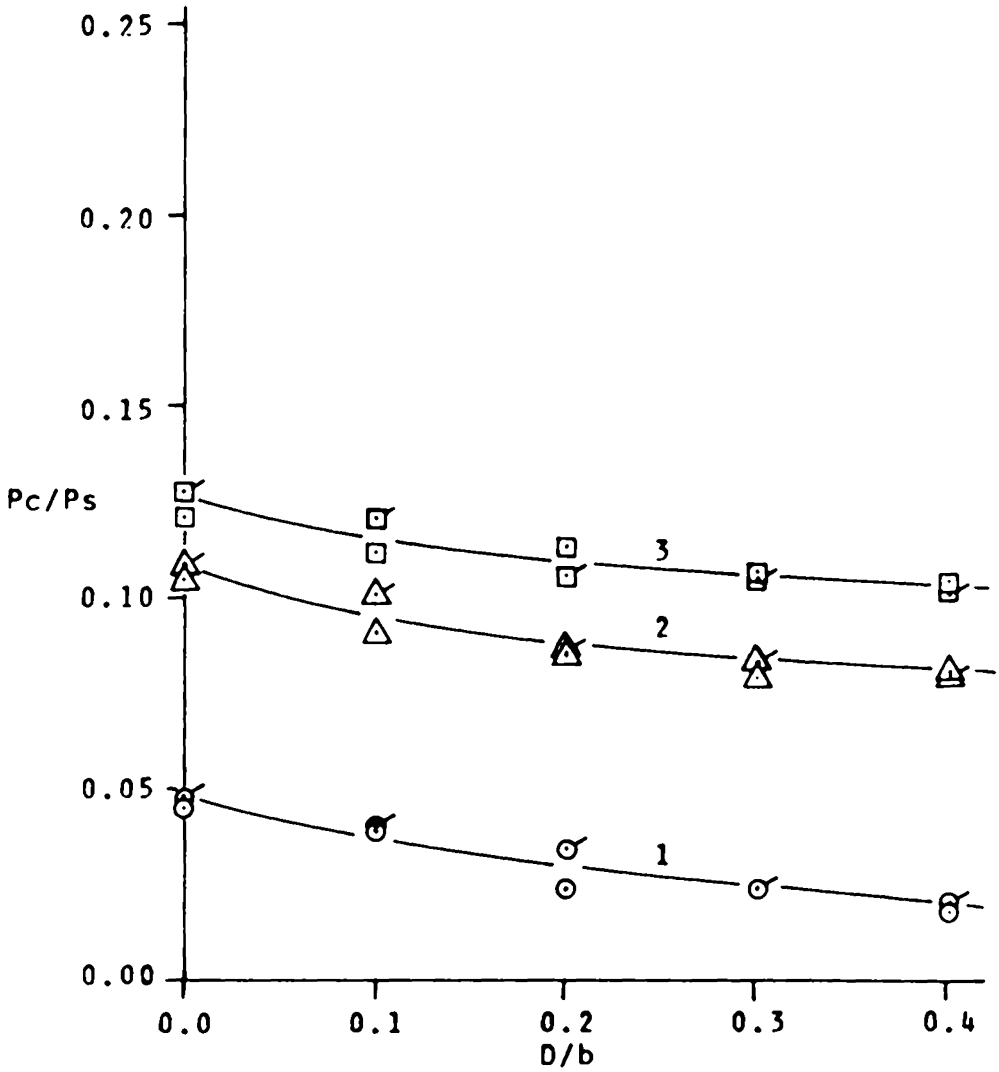


FIGURE 11. OFFSET EFFECTS ON SWITCH PRESSURE; BLOCKED OUTPUT

LEGEND:

| REYNOLDS NO. | RIGHT SIDE | LEFT SIDE | CURVE LABEL |
|---|---|---|---|
| 1950 | ○ | ○ | 1 |
| 3900 | △ | △ | 2 |
| 5800 | □ | □ | 3 |

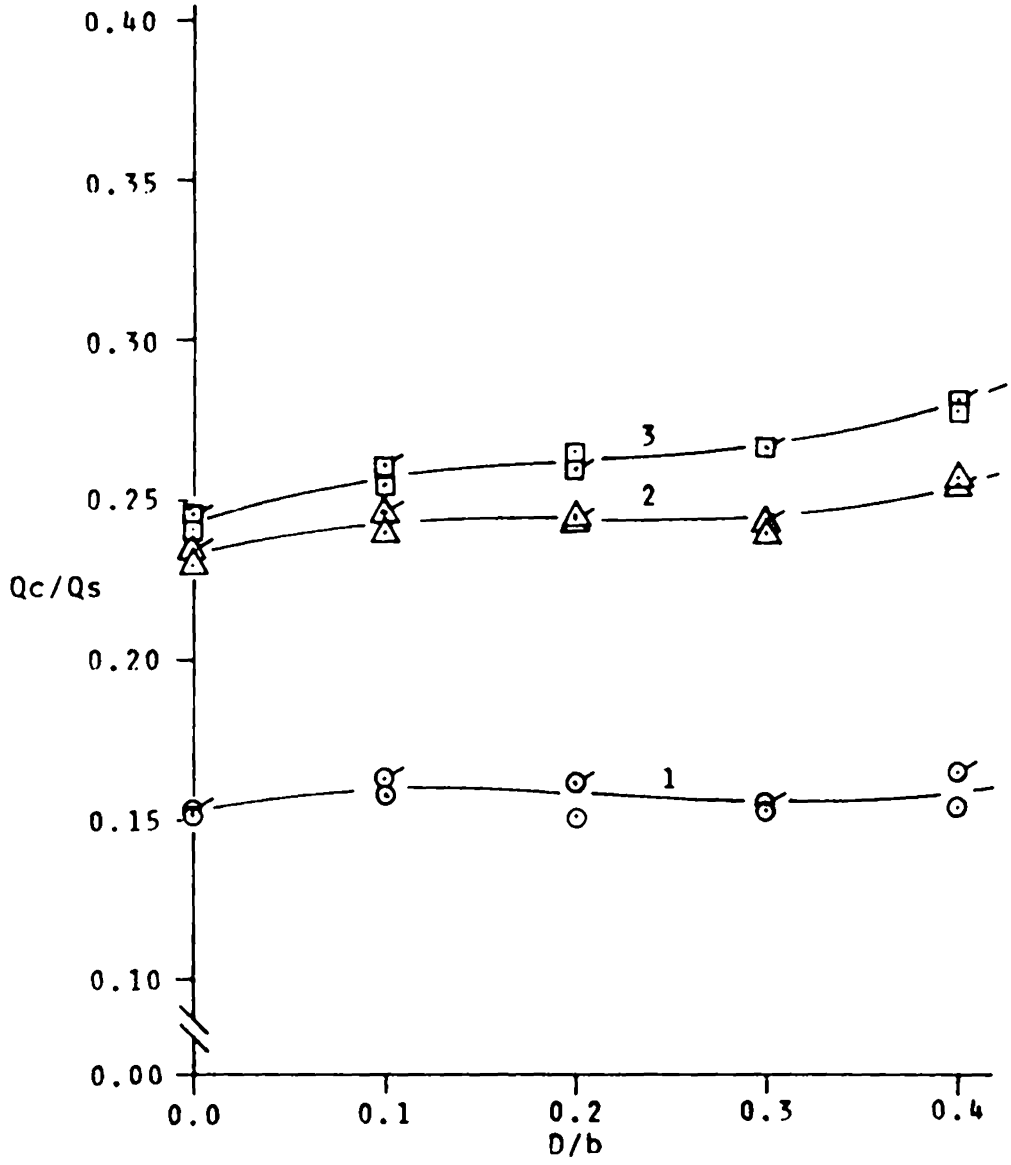


FIGURE 12. OFFSET EFFECTS ON SWITCH FLOW; BLOCKED OUTPUT

LEGEND:

| REYNOLDS NO. | RIGHT SIDE | LEFT SIDE | CURVE LABEL |
|---|---|---|---|
| 1950 | ○ | ○ | 1 |
| 3900 | △ | △ | 2 |
| 5800 | □ | □ | 3 |

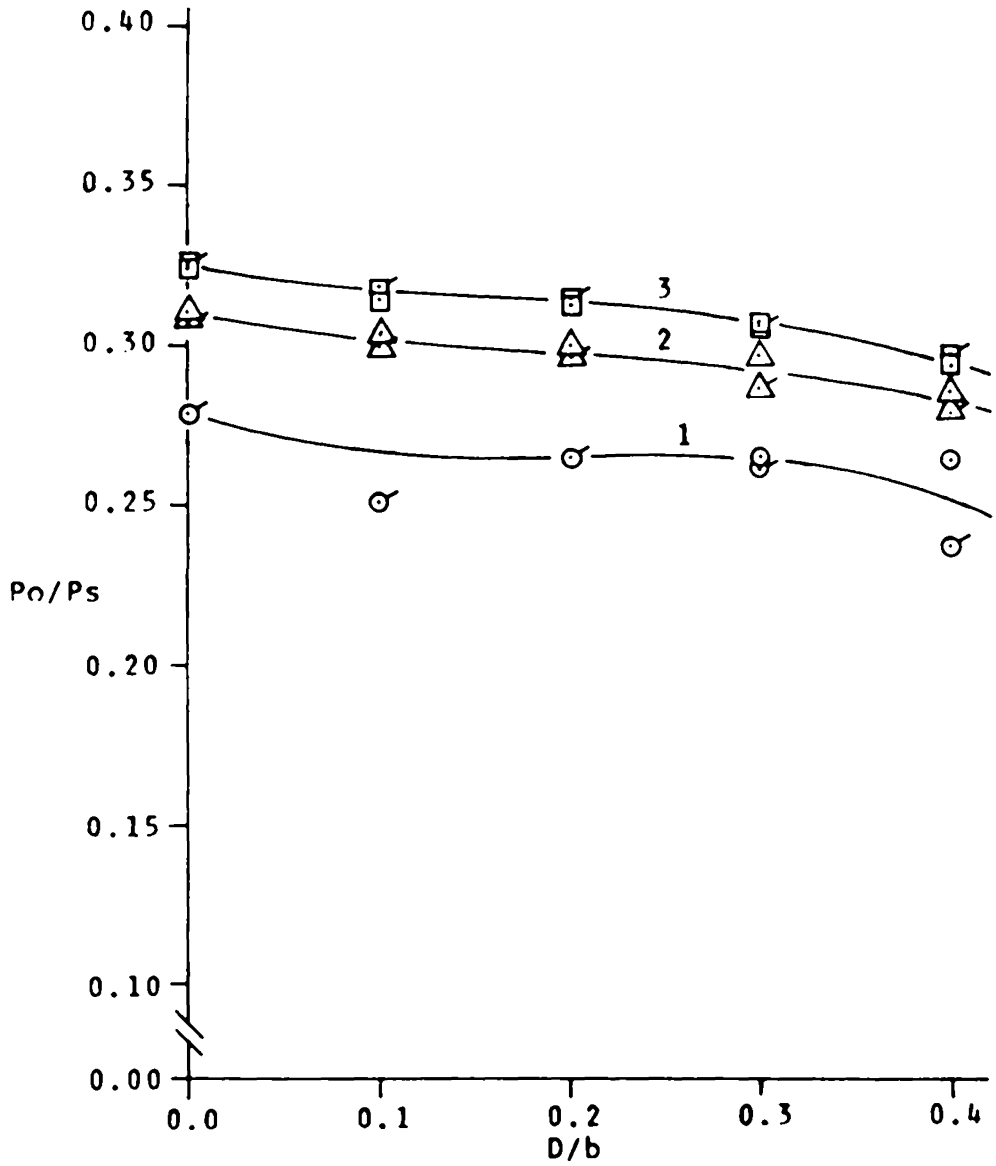


FIGURE 13. OFFSET EFFECTS ON RECOVERY PRESSURE; BLOCKED OUTPUT

| REYNOLDS NO. | RIGHT SIDE | LEFT SIDE | CURVE LABEL |
|---|---|---|---|
| 1950 | ○ | ○ | 1 |
| 3900 | △ | △ | 2 |
| 5800 | □ | □ | 3 |

Table 3. Wall Length Results

1 nozzle load:

| WL/b | $R_b$ | $Pc_r/Ps$ | $Pc_l/Ps$ | $Qc_r/Qs$ | $Qc_l/Qs$ | $Po_r/Ps$ | $Po_l/Ps$ |
|---|---|---|---|---|---|---|---|
| 8.81 | 1950 | .000 | .001 | .124 | .124 | .251 | .265 |
| | 2900 | .025 | .028 | .155 | .156 | .266 | .260 |
| | 3900 | .034 | .033 | .180 | .178 | .282 | .275 |
| | 4850 | .042 | .053 | .190 | .198 | .292 | .290 |
| | 5800 | .046 | .057 | .196 | .204 | .301 | .301 |
| 9.83 | 1950 | .008 | .019 | .132 | .138 | .223 | .237 |
| | 2900 | .064 | .071 | .214 | .227 | .248 | .235 |
| | 3900 | .073 | .079 | .223 | .236 | .262 | .258 |
| | 4850 | .092 | .096 | .248 | .254 | .270 | .270 |
| | 5800 | .104 | .099 | .254 | .254 | .279 | .279 |
| 10.86 | 1950 | .037 | .038 | .154 | .162 | .209 | .209 |
| | 2900 | .140 | note e | .280 | note e | .223 | .217 |
| | 3900 | .153 | .150 | .302 | .306 | .237 | .227 |
| | 4850 | .151 | .127 | .298 | .286 | .239 | .237 |
| | 5800 | .131 | .120 | .276 | .274 | .243 | .242 |
| 11.84 | 1950 | .058 | .060 | .179 | .185 | .181 | .181 |
| | 2900 | .228 | .228 | .353 | .355 | .198 | .198 |
| | 3900 | .209 | note f | .348 | note f | .209 | .202 |
| | 4850 | .161 | .140 | .305 | .294 | .210 | .207 |
| | 5800 | .139 | .131 | .288 | .285 | .214 | .212 |
| 12.84 | 1950 | .131 | .189 | .258 | .319 | .153 | .153 |
| | 2900 | .248 | .247 | .365 | .370 | .180 | .173 |
| | 3900 | .215 | .185 | .354 | .339 | .185 | .181 |
| | 4850 | .159 | .137 | .306 | .293 | .187 | .185 |
| | 5800 | .148 | .134 | .297 | .293 | .186 | .189 |

Notes on Table 3:

note e Strong indications of the coexistence of two switch points were noted.
$Pc_l/Ps$ 0.093 - 0.139 $Qc_l/Qs$ 0.254 - 0.289

note f Mild indications of the coexistence of two switch points were here.
$Pc_l/Ps$ 0.177 - 0.192 $Qc_l/Qs$ 0.327 - 0.338

Table 3. Continued

blocked output:

| WL/b | $R_b$ | $Pc_r/Ps$ | $Pc_l/Ps$ | $Qc_r/Qs$ | $Qc_l/Qs$ | $Po_r/Ps$ | $Po_l/Ps$ |
|---|---|---|---|---|---|---|---|
| 8.81 | 1950 | .000 | .000 | .119 | .119 | ---- | ---- |
| note g | 2900 | .004 | .006 | .130 | .130 | ---- | ---- |
| | 3900 | .004 | .009 | .152 | .152 | ---- | ---- |
| | 4850 | .005 | .012 | .154 | .159 | ---- | ---- |
| | 5800 | .004 | .011 | .155 | .161 | ---- | ---- |
| 9.83 | 1950 | .000 | .000 | .116 | .124 | .320 | .306 |
| | 2900 | .019 | .015 | .154 | .156 | .328 | .316 |
| | 3900 | .073 | note h | .223 | note h | .303 | .296 |
| | 4850 | .088 | note i | .243 | note i | .312 | .306 |
| | 5800 | .094 | .098 | .244 | .253 | .318 | .315 |
| 10.86 | 1950 | .040 | .035 | .160 | .158 | .279 | .265 |
| | 2900 | .077 | .072 | .218 | .220 | .285 | .279 |
| | 3900 | .107 | .098 | .255 | .254 | .296 | .293 |
| | 4850 | .129 | .114 | .275 | .272 | .297 | .299 |
| | 5800 | .123 | .108 | .268 | .264 | .304 | .305 |
| 11.84 | 1950 | .079 | .104 | .200 | .229 | .236 | .236 |
| | 2900 | .186 | .195 | .322 | .332 | .247 | .247 |
| | 3900 | .201 | .187 | .335 | .328 | .260 | .260 |
| | 4850 | .158 | .148 | .304 | .287 | .261 | .266 |
| | 5800 | .136 | .142 | .278 | .280 | .267 | .268 |
| 12.84 | 1950 | note j | .248 | note j | .374 | .195 | .195 |
| | 2900 | .252 | .253 | .373 | .383 | .223 | .217 |
| | 3900 | .220 | .188 | .356 | .336 | .227 | .223 |
| | 4850 | .162 | .140 | .302 | .288 | .228 | .230 |
| | 5800 | .152 | .128 | .298 | .285 | .232 | .234 |

Notes on Table 3:

note g With the outputs blocked and controls open to atmosphere the jet would not attach to either side and thus no recovery pressure data could be taken.

note h Positive identification of two distinct switch points was made.
$Pc_l/Ps$ 0.024 or 0.077 $Qc_l/Qs$ 0.150 or 0.231

note i Positive identification of two distinct switch points was made.
$Pc_l/Ps$ 0.030 or 0.096 $Qc_l/Qs$ 0.160 or 0.251

note j Positive identification of two distinct switch points was made.
$Pc_r/Ps$ 0.149 or 0.248 $Qc_r/Qs$ 0.282 or 0.370

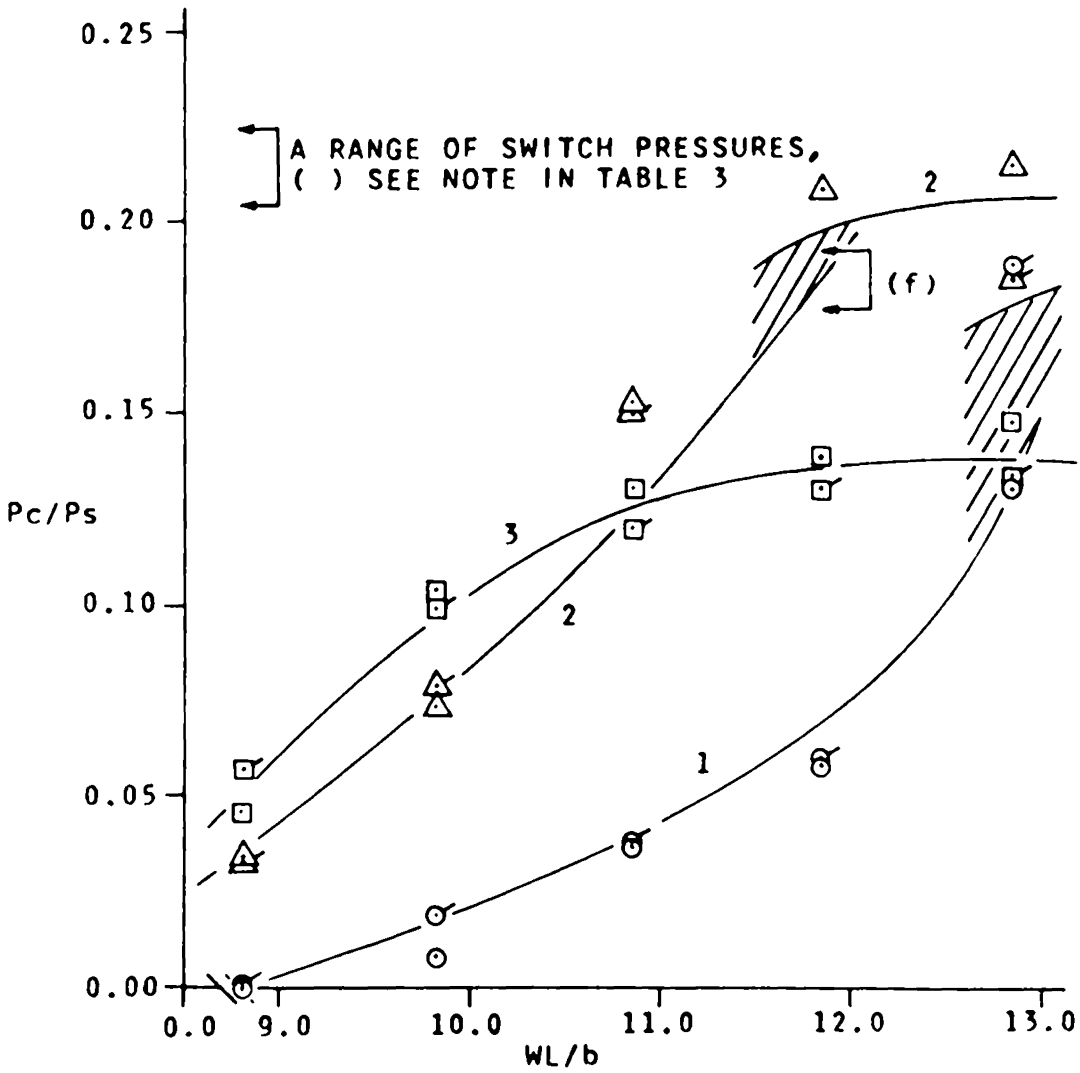


FIGURE 14. WALL LENGTH EFFECTS ON SWITCH PRESSURE; 1 NOZZLE LOADING

LEGEND:

| REYNOLDS NO. | RIGHT SIDE | LEFT SIDE | CURVE LABEL |
|---|---|---|---|
| 1950 | ○ | ○ | 1 |
| 3900 | △ | △ | 2 |
| 5800 | □ | □ | 3 |

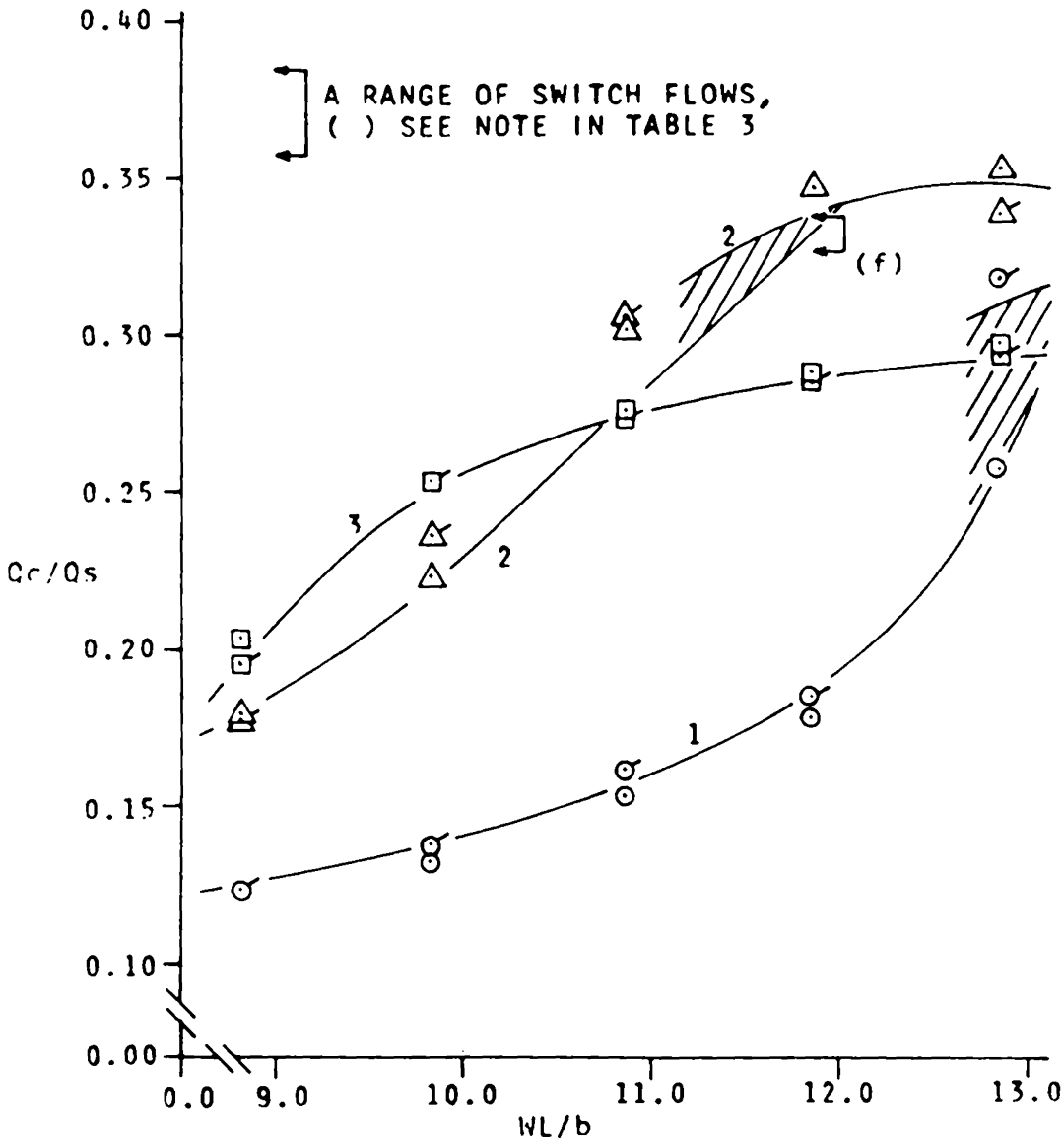


FIGURE 15. WALL LENGTH EFFECTS ON SWITCH FLOW; 1 NOZZLE LOADING

LEGEND:

| REYNOLDS NO. | RIGHT SIDE | LEFT SIDE | CURVE LABEL |
|---|---|---|---|
| 1950 | ○ | ○ | 1 |
| 3900 | △ | △ | 2 |
| 5800 | □ | □ | 3 |

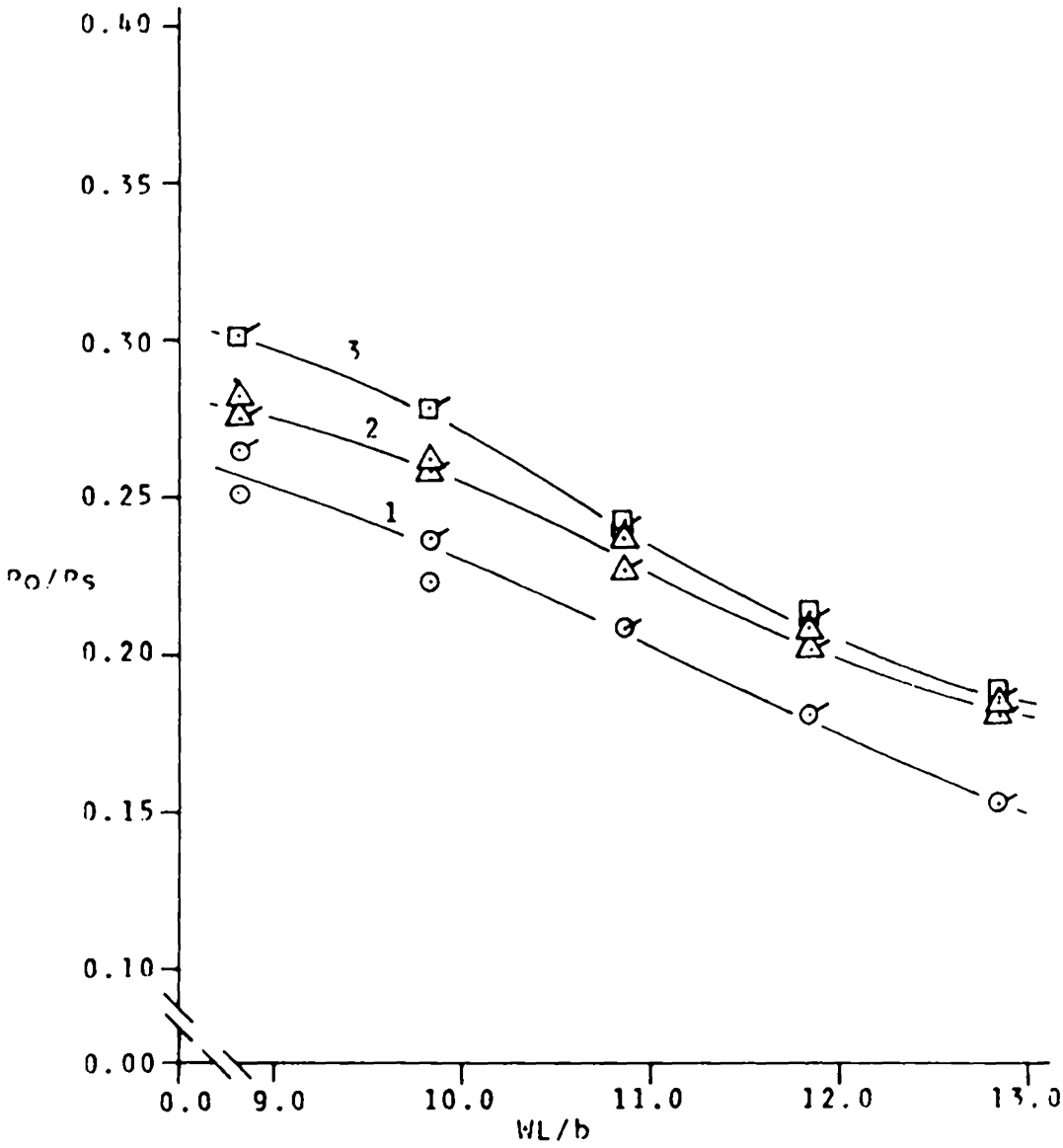


FIGURE 16. WALL LENGTH EFFECTS ON RECOVERY PRESSURE; 1 NOZZLE LOADING

LEGEND:

| REYNOLDS NO. | RIGHT SIDE | LEFT SIDE | CURVE LABEL |
|---|---|---|---|
| 1950 | ○ | ○ | 1 |
| 3900 | △ | △ | 2 |
| 5800 | □ | □ | 3 |

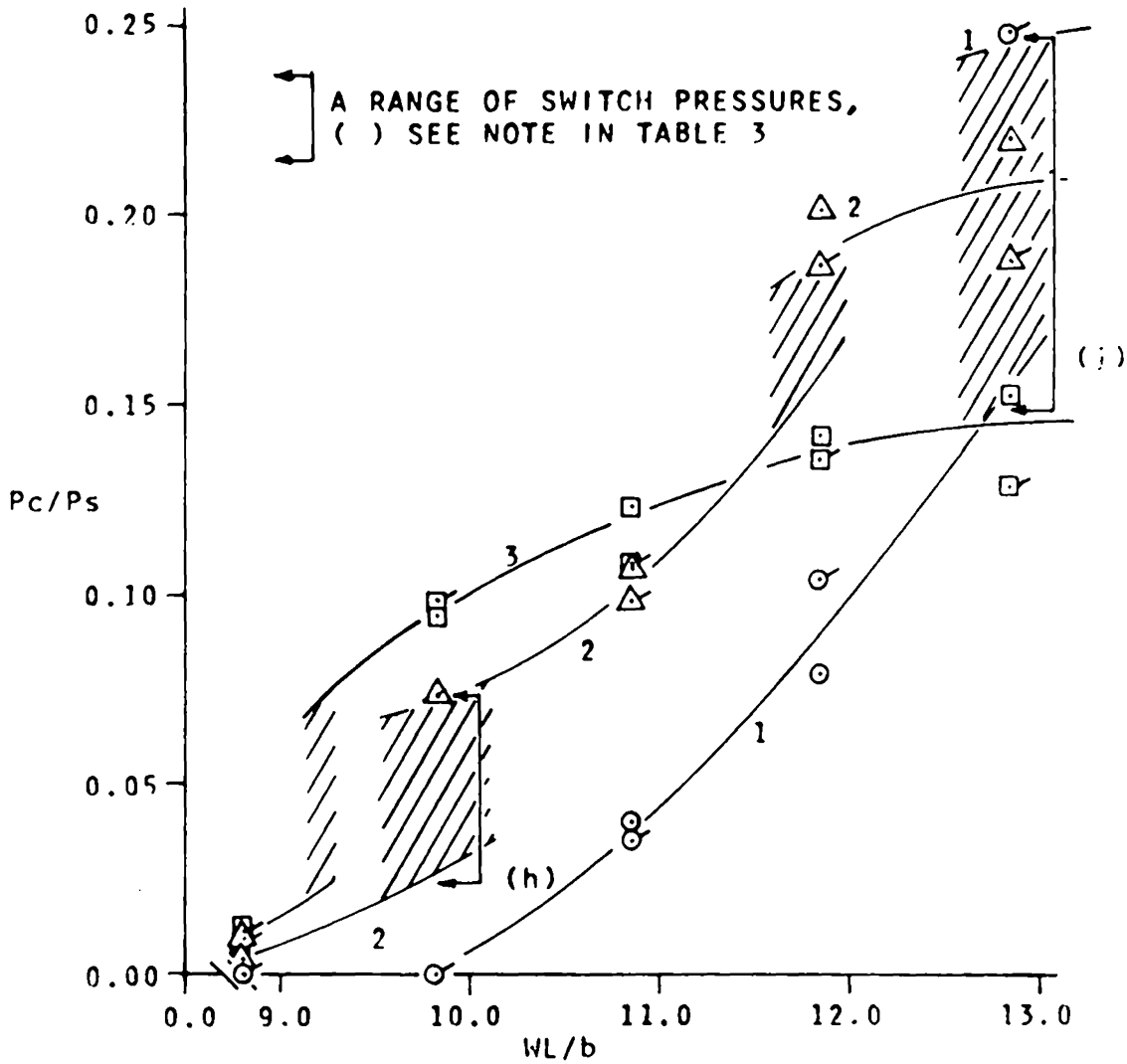


FIGURE 17. WALL LENGTH EFFECTS ON SWITCH PRESSURE; BLOCKED OUTPUT

LEGEND:

| REYNOLDS NO. | RIGHT SIDE | LEFT SIDE | CURVE LABEL |
|---|---|---|---|
| 1950 | ○ | ○ | 1 |
| 3900 | △ | △ | 2 |
| 5800 | □ | □ | 3 |

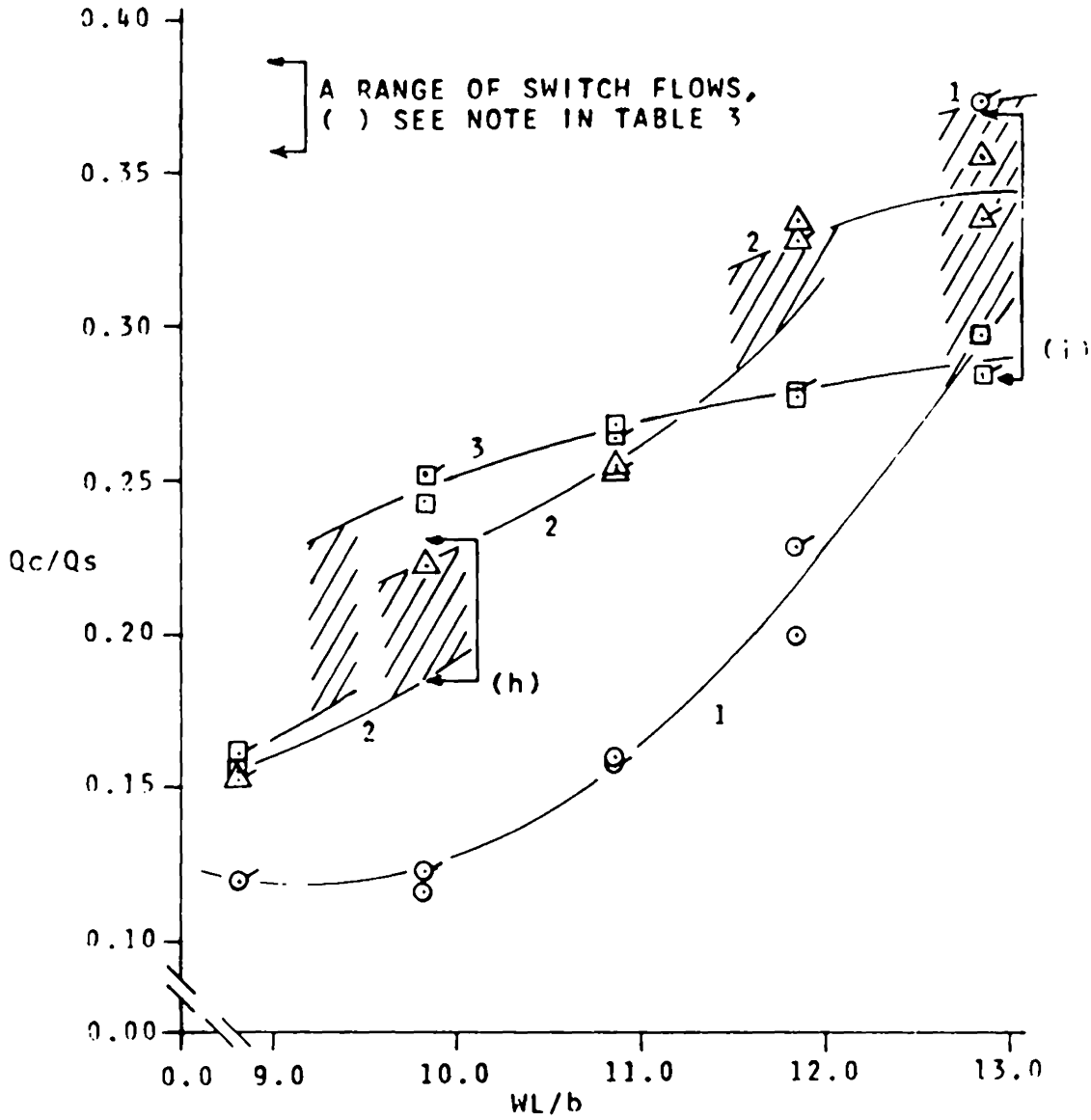


FIGURE 18. WALL LENGTH EFFECTS ON SWITCH FLOW; BLOCKED OUTPUT

LEGEND:

| REYNOLDS NO. | RIGHT SIDE | LEFT SIDE | CURVE LABEL |
|---|---|---|---|
| 1950 | ○ | ○ | 1 |
| 3900 | △ | △ | 2 |
| 5800 | □ | □ | 3 |

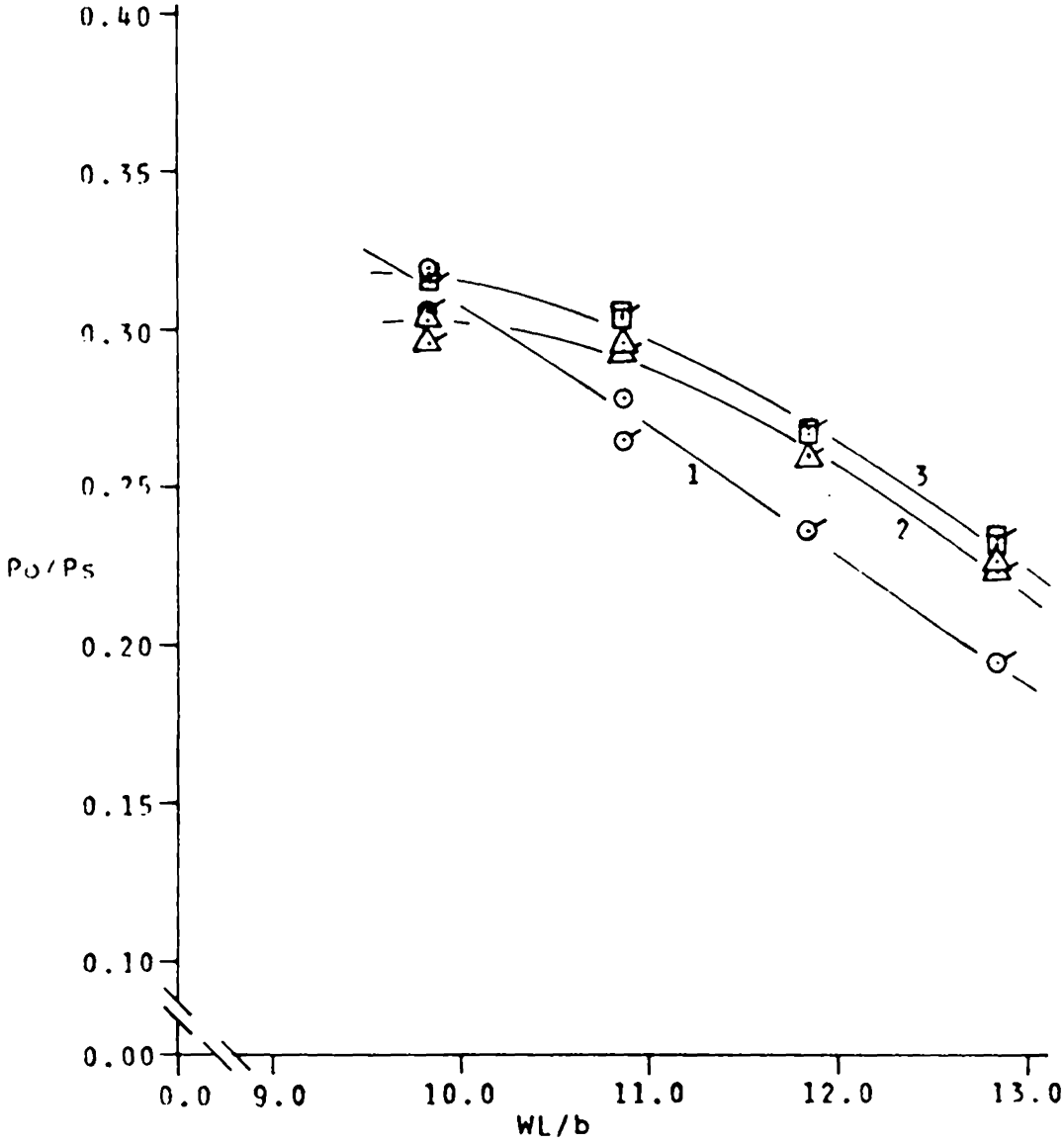


FIGURE 19. WALL LENGTH EFFECTS ON RECOVERY PRESSURE; BLOCKED OUTPUT

LEGEND:

| REYNOLDS NO. | RIGHT SIDE | LEFT SIDE | CURVE LABEL |
|---|---|---|---|
| 1950 | ○ | ○ | 1 |
| 3900 | △ | △ | 2 |
| 5800 | □ | □ | 3 |

Table 4. Control Width Results

1 nozzle load:

| CW/b | $R_b$ | $Pc_r/Ps$ | $Pc_l/Ps$ | $Qc_r/Qs$ | $Qc_l/Qs$ | $Po_r/Ps$ | $Po_l/Ps$ |
|---|---|---|---|---|---|---|---|
| 0.80 | 1950 | .037 | .042 | .133 | .144 | .209 | .209 |
| | 2900 | .224 | .259 | .301 | .327 | .217 | .217 |
| | 3900 | .238 | .211 | .315 | .305 | .241 | .237 |
| | 4850 | .205 | .168 | .290 | .272 | .243 | .243 |
| | 5800 | .173 | .170 | .265 | .280 | .246 | .251 |
| 0.90 | 1950 | .035 | .038 | .140 | .149 | .195 | .209 |
| | 2900 | .182 | .169 | .295 | .288 | .217 | .217 |
| | 3900 | .188 | .184 | .304 | .305 | .234 | .234 |
| | 4850 | .169 | .158 | .287 | .280 | .243 | .241 |
| | 5800 | .148 | .142 | .269 | .270 | .248 | .248 |
| 1.00 | 1950 | .038 | .039 | .153 | .161 | .209 | .209 |
| | 2900 | note k | note k | note k | note k | .223 | .217 |
| | 3900 | .150 | .145 | .294 | .294 | .241 | .237 |
| | 4850 | .151 | .141 | .294 | .289 | .248 | .243 |
| | 5800 | .130 | .120 | .273 | .270 | .253 | .251 |
| 1.10 | 1950 | .031 | .037 | .158 | .166 | .209 | .195 |
| note 1 | 2900 | .080 | .090 | .240 | .245 | .223 | .217 |
| | 3900 | .115 | .127 | .280 | .291 | .234 | .234 |
| | 4850 | .122 | .121 | .287 | .287 | .241 | .243 |
| | 5800 | .117 | .114 | .281 | .281 | .248 | .248 |
| 1.20 | 1950 | .028 | .029 | .160 | .168 | .195 | .195 |
| note 1 | 2900 | .067 | .071 | .231 | .237 | .223 | .223 |
| | 3900 | .094 | .103 | .270 | .280 | .241 | .237 |
| | 4850 | .116 | .115 | .296 | .295 | .243 | .245 |
| | 5800 | .110 | .104 | .287 | .283 | .249 | .251 |

Notes on Table 4:

note k Strong indications of the coexistence of two switch points were noted for either side of the device.

| | | | |
|---|---|---|---|
| $Pc_r/Ps$ | 0.093 - 0.140 | $Qc_r/Qs$ | 0.236 - 0.280 |
| $Pc_l/Ps$ | 0.086 - 0.125 | $Qc_l/Qs$ | 0.243 - 0.273 |

note 1 In general it was noted that for these wider control widths the switch was clean and sharp and further there was very little scatter in the data. Also noted was the decrease in precision required in dimensioning the device to achieve unbiased operation.

Table 4. Continued

blocked output:

| CW/b | $R_b$ | $Pc_r/Ps$ | $Pc_l/Ps$ | $Qc_r/Qs$ | $Qc_l/Qs$ | $Po_r/Ps$ | $Po_l/Ps$ |
|---|---|---|---|---|---|---|---|
| 0.80 | 1950 | .049 | .051 | .138 | .155 | .279 | .279 |
| | 2900 | .109 | .103 | .217 | .218 | .291 | .291 |
| | 3900 | .151 | .130 | .250 | .242 | .303 | .303 |
| | 4850 | .179 | .155 | .271 | .265 | .310 | .312 |
| | 5800 | .157 | .132 | .257 | .265 | .315 | .321 |
| 0.90 | 1950 | .040 | .046 | .146 | .144 | .265 | .265 |
| | 2900 | .092 | .081 | .220 | .215 | .285 | .279 |
| | 3900 | .126 | .111 | .242 | .236 | .296 | .296 |
| | 4850 | .149 | .136 | .269 | .263 | .303 | .306 |
| | 5800 | .133 | .129 | .257 | .257 | .308 | .311 |
| 1.00 | 1950 | .040 | .039 | .160 | .162 | .279 | .265 |
| | 2900 | .074 | .066 | .215 | .211 | .291 | .291 |
| | 3900 | .099 | .090 | .246 | .244 | .303 | .303 |
| | 4850 | .123 | .107 | .267 | .260 | .310 | .310 |
| | 5800 | .118 | .102 | .265 | .261 | .315 | .316 |
| 1.1 | 1950 | .029 | .029 | .160 | .160 | .265 | .279 |
| note 1 | 2900 | .058 | .058 | .213 | .212 | .291 | .285 |
| | 3900 | .084 | .081 | .246 | .246 | .300 | .296 |
| | 4850 | .100 | .097 | .266 | .265 | .306 | .310 |
| | 5800 | .100 | .096 | .263 | .261 | .310 | .315 |
| 1.2 | 1950 | .028 | .026 | .170 | .166 | .279 | .265 |
| note 1 | 2900 | .049 | .044 | .212 | .211 | .291 | .291 |
| | 3900 | .071 | .069 | .242 | .242 | .303 | .300 |
| | 4850 | .084 | .081 | .263 | .257 | .308 | .312 |
| | 5800 | .091 | .084 | .268 | .262 | .313 | .319 |

note 1 See previous page.

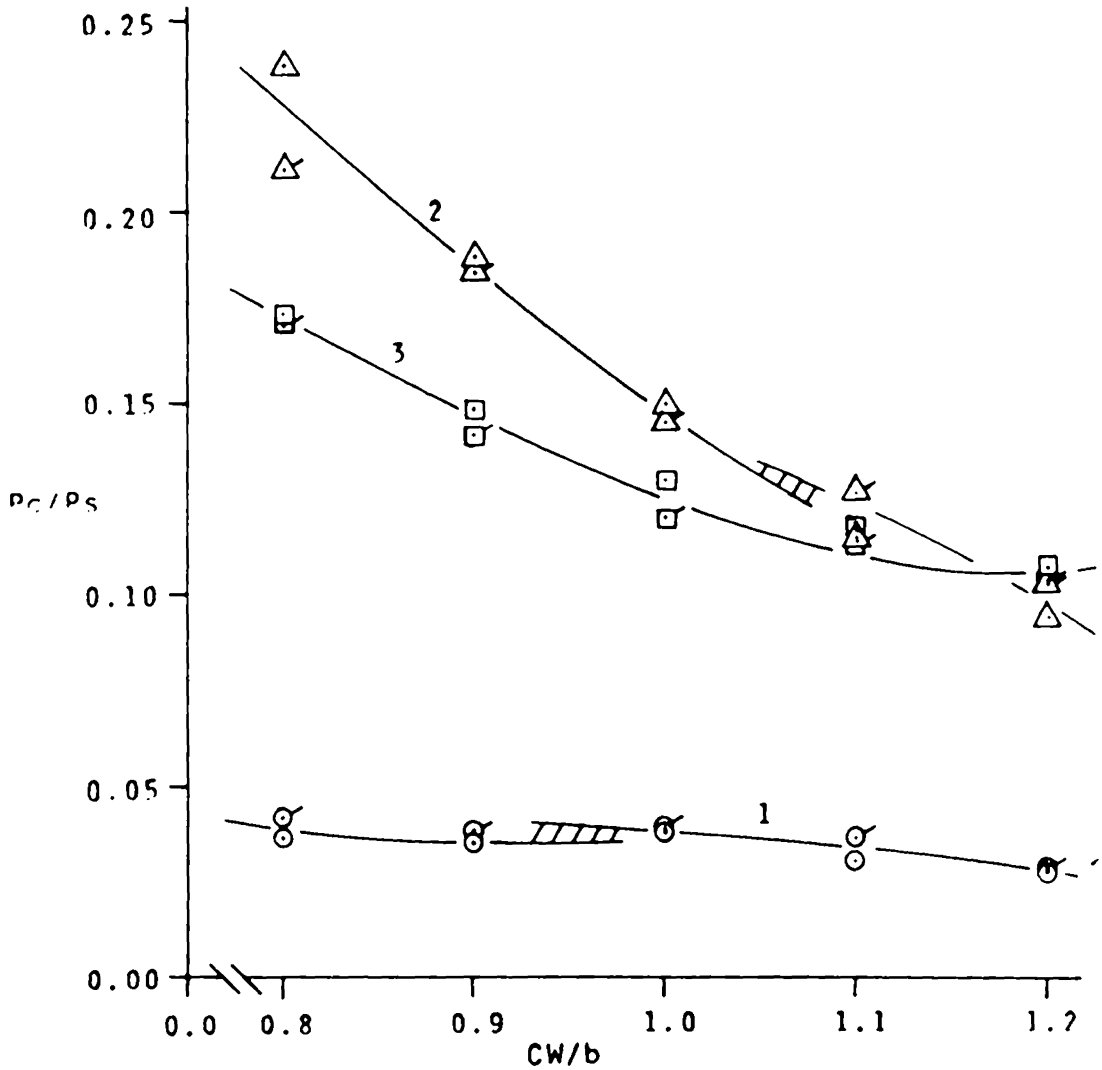


FIGURE 20. CONTROL WIDTH EFFECTS ON SWITCH PRESSURE; 1 NOZZLE LOADING

LEGEND:

| REYNOLDS NO. | RIGHT SIDE | LEFT SIDE | CURVE LABEL |
|---|---|---|---|
| 1950 | ○ | ○ | 1 |
| 3900 | △ | △ | 2 |
| 5800 | □ | □ | 3 |

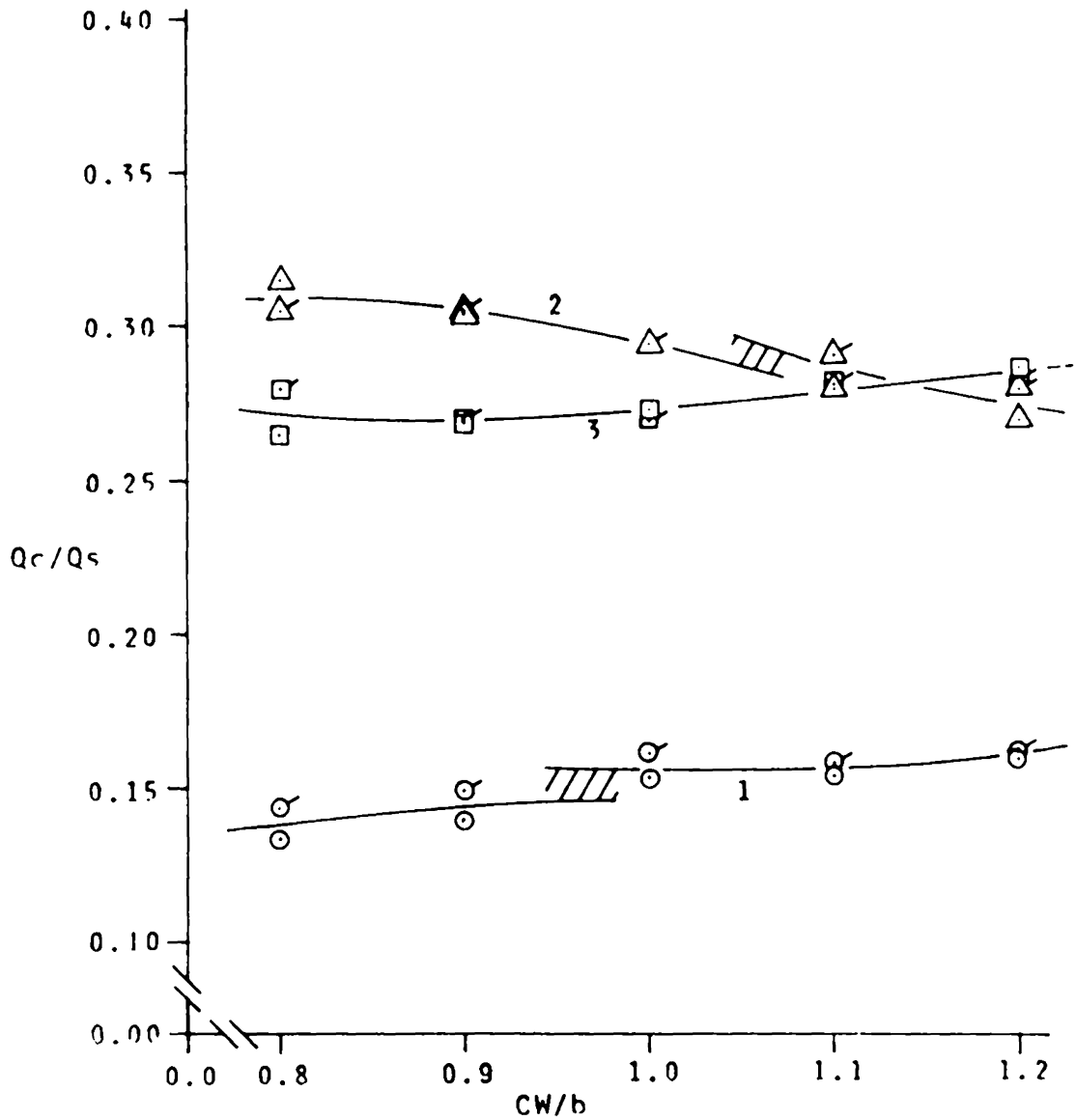


FIGURE 21. CONTROL WIDTH EFFECTS ON SWITCH FLOW; 1 NOZZLE LOADING

LEGEND:

| REYNOLDS NO. | RIGHT SIDE | LEFT SIDE | CURVE LABEL |
|---|---|---|---|
| 1950 | ○ | ○ | 1 |
| 3900 | △ | △ | 2 |
| 5800 | □ | □ | 3 |

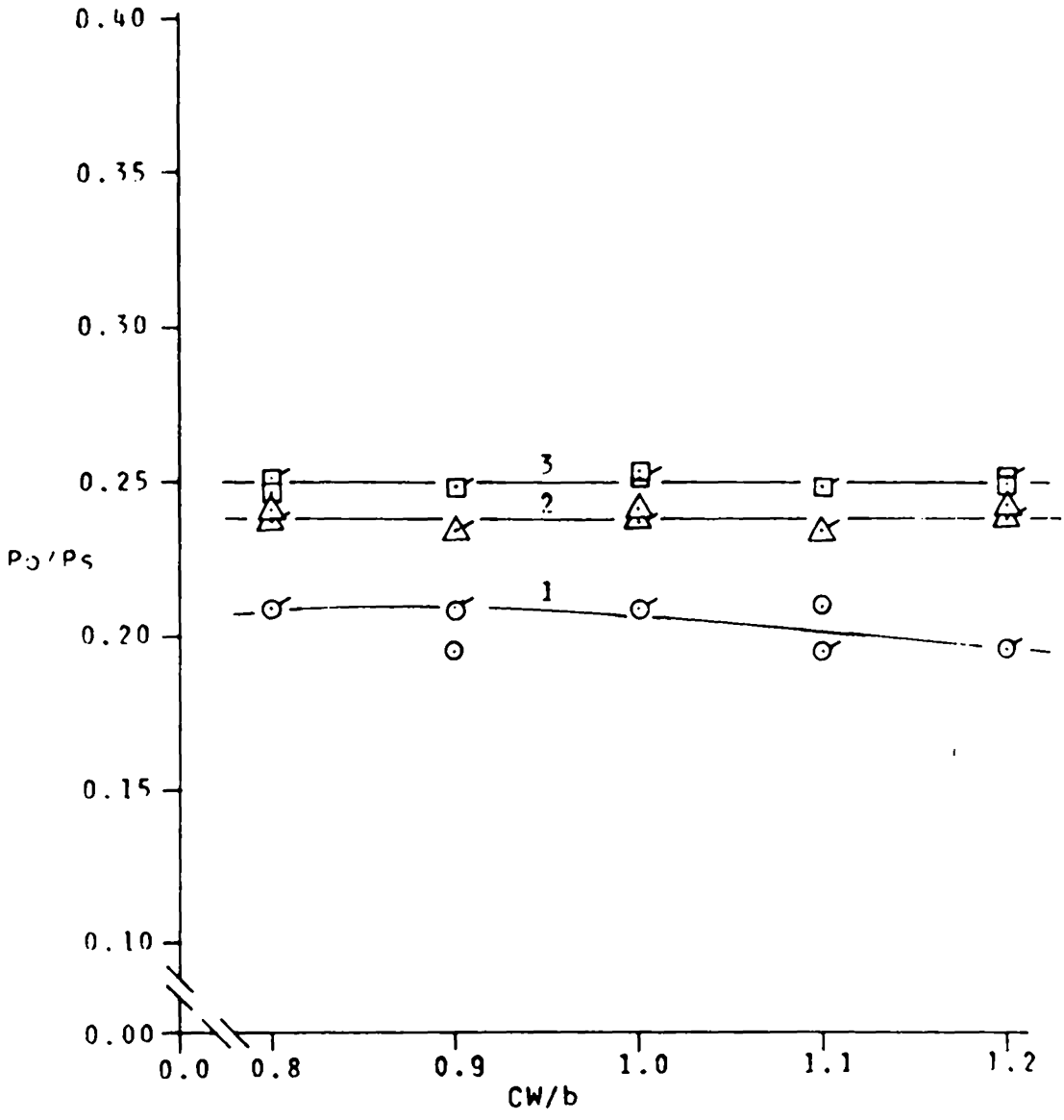


FIGURE 22. CONTROL WIDTH EFFECTS ON RECOVERY PRESSURE; 1 NOZZLE LOADING

LEGEND:

| REYNOLDS NO. | RIGHT SIDE | LEFT SIDE | CURVE LABEL |
|---|---|---|---|
| 1950 | ○ | ○ | 1 |
| 3900 | △ | △ | 2 |
| 5800 | □ | □ | 3 |

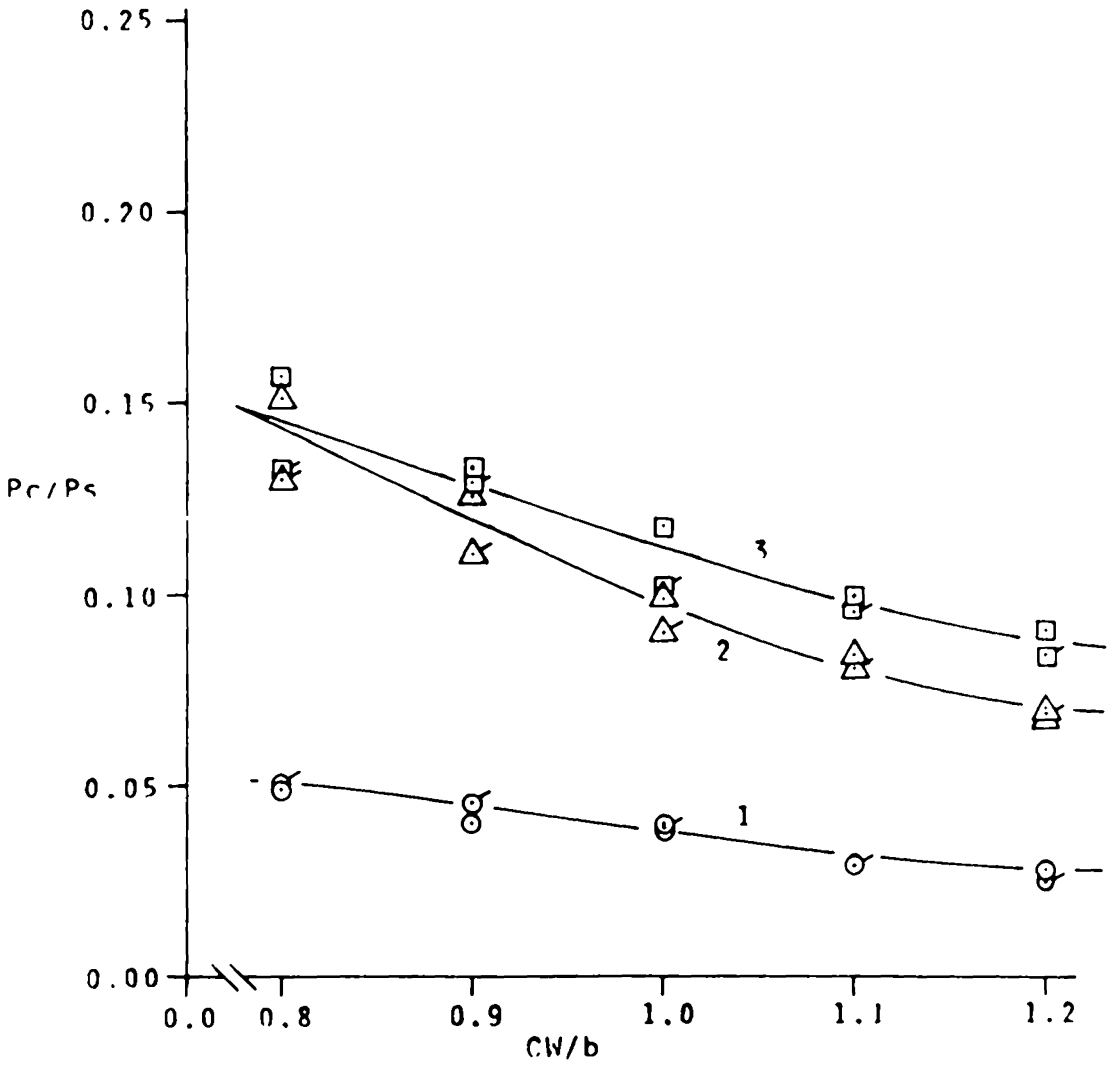


FIGURE 23. CONTROL WIDTH EFFECTS ON SWITCH PRESSURE; BLOCKED OUTPUT

LEGEND:

| REYNOLDS NO. | RIGHT SIDE | LEFT SIDE | CURVE LABEL |
|---|---|---|---|
| 1950 | ○ | ○ | 1 |
| 3900 | △ | △ | 2 |
| 5800 | □ | □ | 3 |

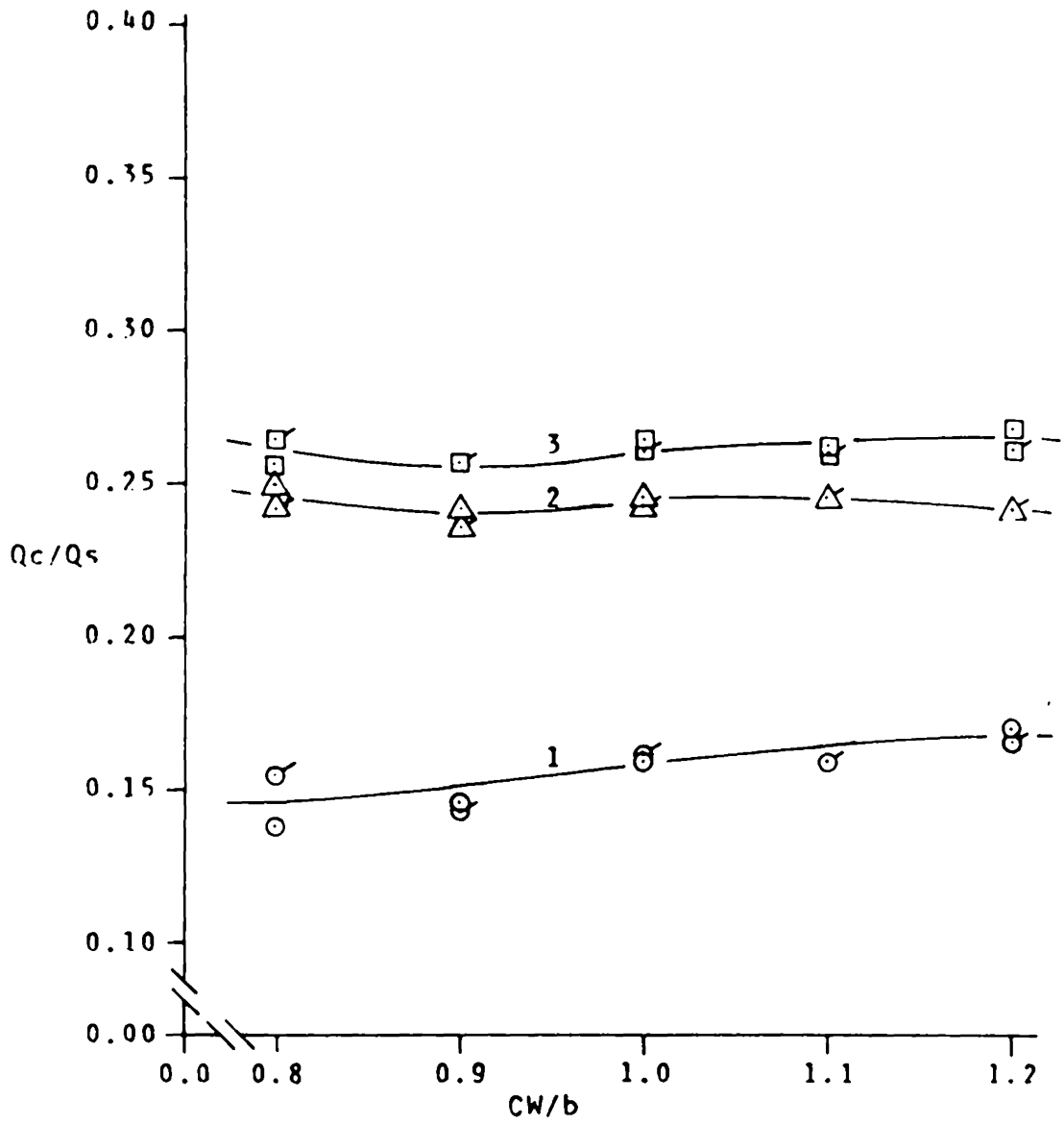


FIGURE 24. CONTROL WIDTH EFFECTS ON SWITCH FLOW; BLOCKED OUTPUT

LEGEND:

| REYNOLDS NO. | RIGHT SIDE | LEFT SIDE | CURVE LABEL |
|---|---|---|---|
| 1950 | ○ | ○ | 1 |
| 3900 | △ | △ | 2 |
| 5800 | □ | □ | 3 |

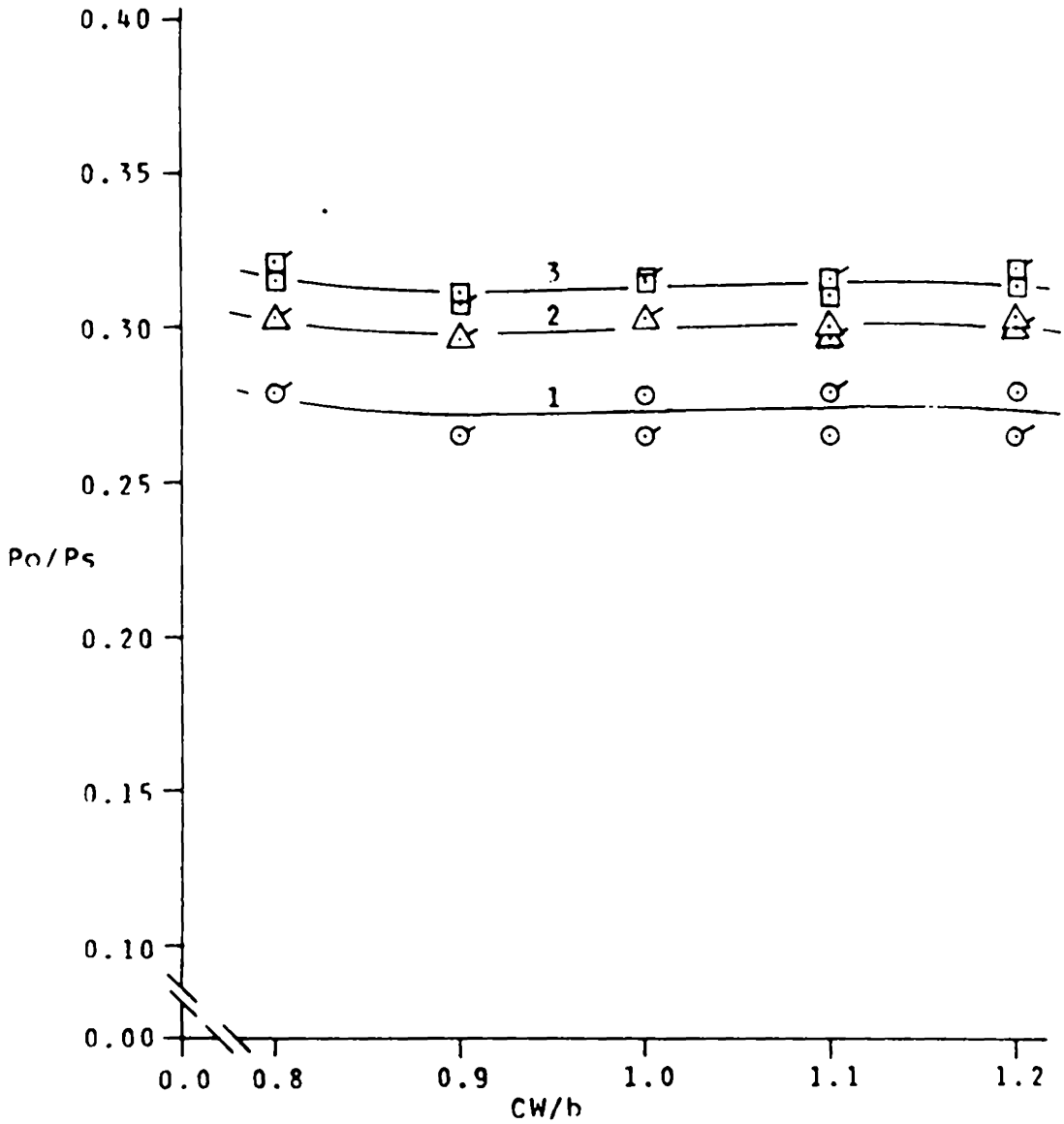


FIGURE 25. CONTROL WIDTH EFFECTS ON RECOVERY PRESSURE; BLOCKED OUTPUT

LEGEND:

| REYNOLDS NO. | RIGHT SIDE | LEFT SIDE | CURVE LABEL |
|---|---|---|---|
| 1950 | ○ | ⊙ | 1 |
| 3900 | △ | ⊿ | 2 |
| 5800 | □ | ⊡ | 3 |

Table 5. Power Nozzle Width Results

1 nozzle load:

| NW/b | $R_b$ | $Pc_r/Ps$ | $Pc_l/Ps$ | $Qc_r/Qs$ | $Qc_l/Qs$ | $Po_r/Ps$ | $Po_l/Ps$ |
|---|---|---|---|---|---|---|---|
| 0.8 | 1950 | .052 | .052 | .222 | .227 | .139 | .139 |
| | 2900 | .172 | .183 | .392 | .412 | .173 | .167 |
| | 3900 | .164 | .173 | .384 | .395 | .192 | .185 |
| | 4850 | .152 | .132 | .375 | .356 | .194 | .192 |
| | 5800 | .118 | .107 | .334 | .323 | .198 | .198 |
| 0.9 | 1950 | .045 | .048 | .184 | .190 | .181 | .181 |
| | 2900 | note m | .176 | note m | .351 | .198 | .192 |
| | 3900 | .167 | .168 | .348 | .352 | .213 | .209 |
| | 4850 | .151 | .132 | .337 | .320 | .219 | .219 |
| | 5800 | .121 | .114 | .299 | .297 | .223 | .226 |
| 1.0 | 1950 | .040 | .041 | .166 | .173 | .209 | .209 |
| | 2900 | .130 | note n | .278 | note n | .223 | .217 |
| | 3900 | note o | .156 | note o | .303 | .241 | .234 |
| | 4850 | .155 | .134 | .301 | .285 | .245 | .241 |
| | 5800 | .130 | .124 | .275 | .276 | .253 | .249 |
| 1.1 | 1950 | .022 | .025 | .138 | .143 | .237 | .237 |
| | 2900 | .103 | .111 | .230 | .236 | .242 | .242 |
| | 3900 | .115 | note p | .239 | note p | .268 | .262 |
| | 4850 | .139 | .136 | .255 | .256 | .274 | .299 |
| | 5800 | .135 | .130 | .255 | .257 | .282 | .279 |
| 1.2 | 1950 | .013 | .019 | .122 | .126 | .265 | .265 |
| | 2900 | .068 | .080 | .186 | .194 | .266 | .260 |
| | 3900 | .087 | .095 | .196 | .199 | .293 | .289 |
| | 4850 | .106 | .119 | .211 | .218 | .303 | .303 |
| | 5800 | .121 | .135 | .227 | .236 | .311 | .311 |

Notes on Table 5:

note m Strong indications of the coexistence of two switch points were noted.
$Pc_r/Ps$ 0.130 - 0.170 $Qc_r/Qs$ 0.311 - 0.339

note n Very strong indications of the coexistence of two switch points were noted.
$Pc_l/Ps$ 0.090 - 0.158 $Qc_l/Qs$ 0.242 - 0.304

note o Indications of the coexistence of two switch points were noted.
$Pc_r/Ps$ 0.122 - 0.150 $Qc_r/Qs$ 0.273 - 0.298

note p Mild indications of the coexistence of two switch points were noted.
$Pc_l/Ps$ 0.111 - 0.126 $Qc_l/Qs$ 0.237 - 0.250

Table 5. Continued

blocked output:

| NW/b | $R_b$ | $Pc_r/Ps$ | $Pc_l/Ps$ | $Qc_r/Qs$ | $Qc_l/Qs$ | $Po_r/Ps$ | $Po_l/Ps$ |
|---|---|---|---|---|---|---|---|
| 0.8 | 1950 | .058 | .055 | .227 | .227 | .209 | .195 |
| | 2900 | .113 | .116 | .320 | .328 | .223 | .217 |
| | 3900 | .132 | .137 | .350 | .359 | .237 | .234 |
| | 4850 | .146 | .126 | .367 | .351 | .239 | .239 |
| | 5800 | .117 | .104 | .325 | .316 | .246 | .245 |
| 0.9 | 1950 | .051 | .043 | .201 | .192 | .251 | .237 |
| | 2900 | .094 | .095 | .267 | .273 | .260 | .254 |
| | 3900 | .121 | .123 | .300 | .307 | .268 | .265 |
| | 4850 | .144 | .130 | .331 | .318 | .272 | .274 |
| | 5800 | .120 | .112 | .299 | .294 | .277 | .279 |
| 1.0 | 1950 | .031 | .031 | .158 | .160 | .265 | .265 |
| | 2900 | .073 | .069 | .223 | .218 | .291 | .285 |
| | 3900 | .101 | .100 | .250 | .252 | .300 | .300 |
| | 4850 | .121 | .116 | .272 | .273 | .308 | .306 |
| | 5800 | .118 | .110 | .264 | .262 | .311 | .332 |
| 1.1 | 1950 | .027 | .024 | .134 | .133 | .306 | .306 |
| note q | 2900 | .054 | .051 | .183 | .183 | .316 | .316 |
| | 3900 | .073 | .069 | .207 | .205 | .338 | .335 |
| | 4850 | .092 | .082 | .220 | .215 | .344 | .346 |
| | 5800 | .097 | .089 | .209 | .206 | .352 | .353 |
| 1.2 | 1950 | .009 | .015 | .112 | .111 | .348 | .334 |
| note r | 2900 | .028 | .029 | .150 | .149 | .347 | .341 |
| | 3900 | .049 | .042 | .168 | .165 | .373 | .370 |
| | 4850 | .056 | .055 | .179 | .176 | .404 | .386 |
| | 5800 | .058 | .059 | .178 | .179 | .389 | .394 |

Notes on Table 5:

note q For the right side at $R_b$=1950, the switching was such that the jet would detach and oscillate before finally attaching to the opposite wall.

note r For both sides at $R_b$=1950 and the right side at $R_b$=2900, the switch was such that the jet would detach and oscillate before attaching to the opposite wall.

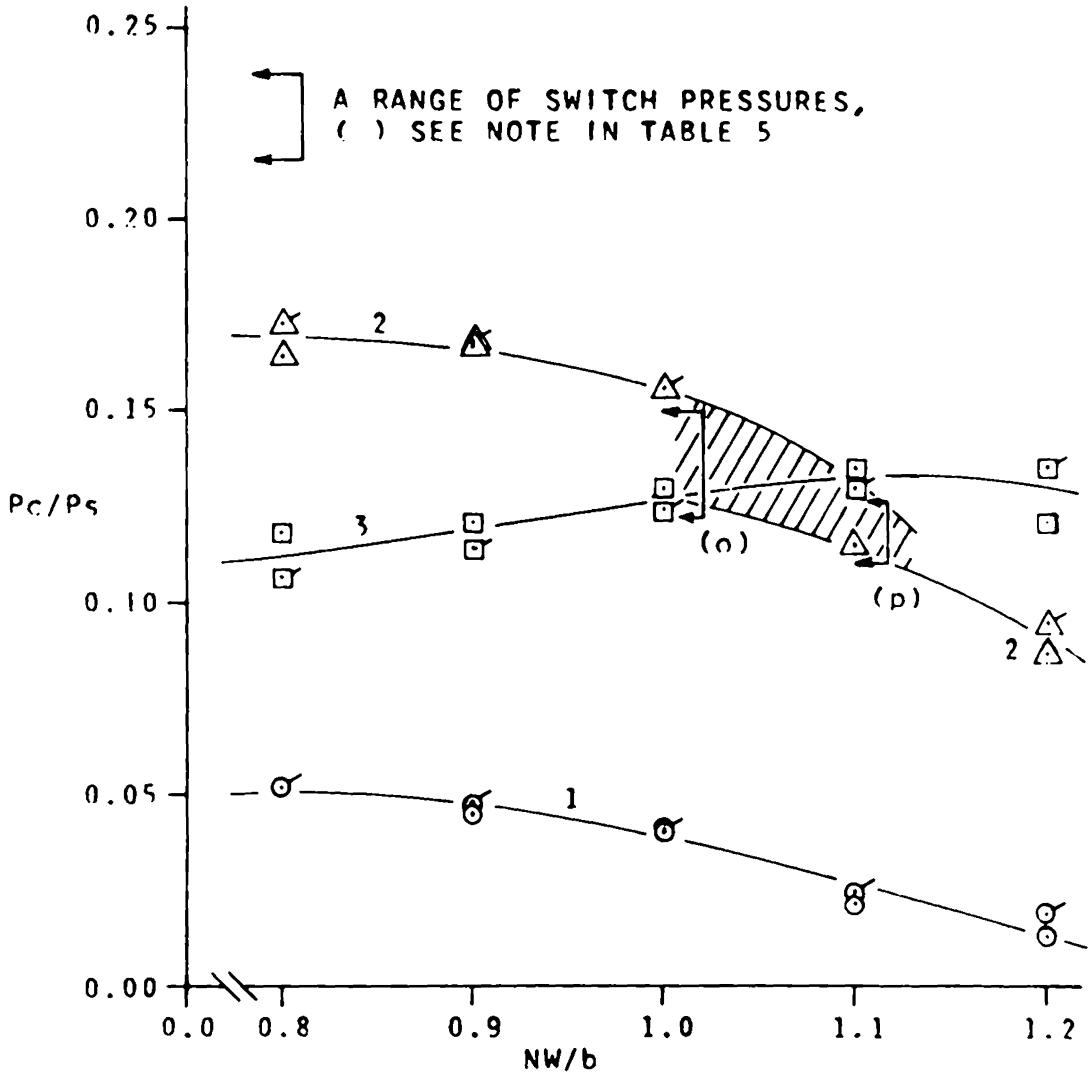


FIGURE 26. POWER NOZZLE WIDTH EFFECTS ON SWITCH PRESSURE; 1 NOZZLE LOADING

LEGEND:

| REYNOLDS NO. | RIGHT SIDE | LEFT SIDE | CURVE LABEL |
|---|---|---|---|
| 1950 | ○ | ○ | 1 |
| 3900 | △ | △ | 2 |
| 5800 | □ | □ | 3 |

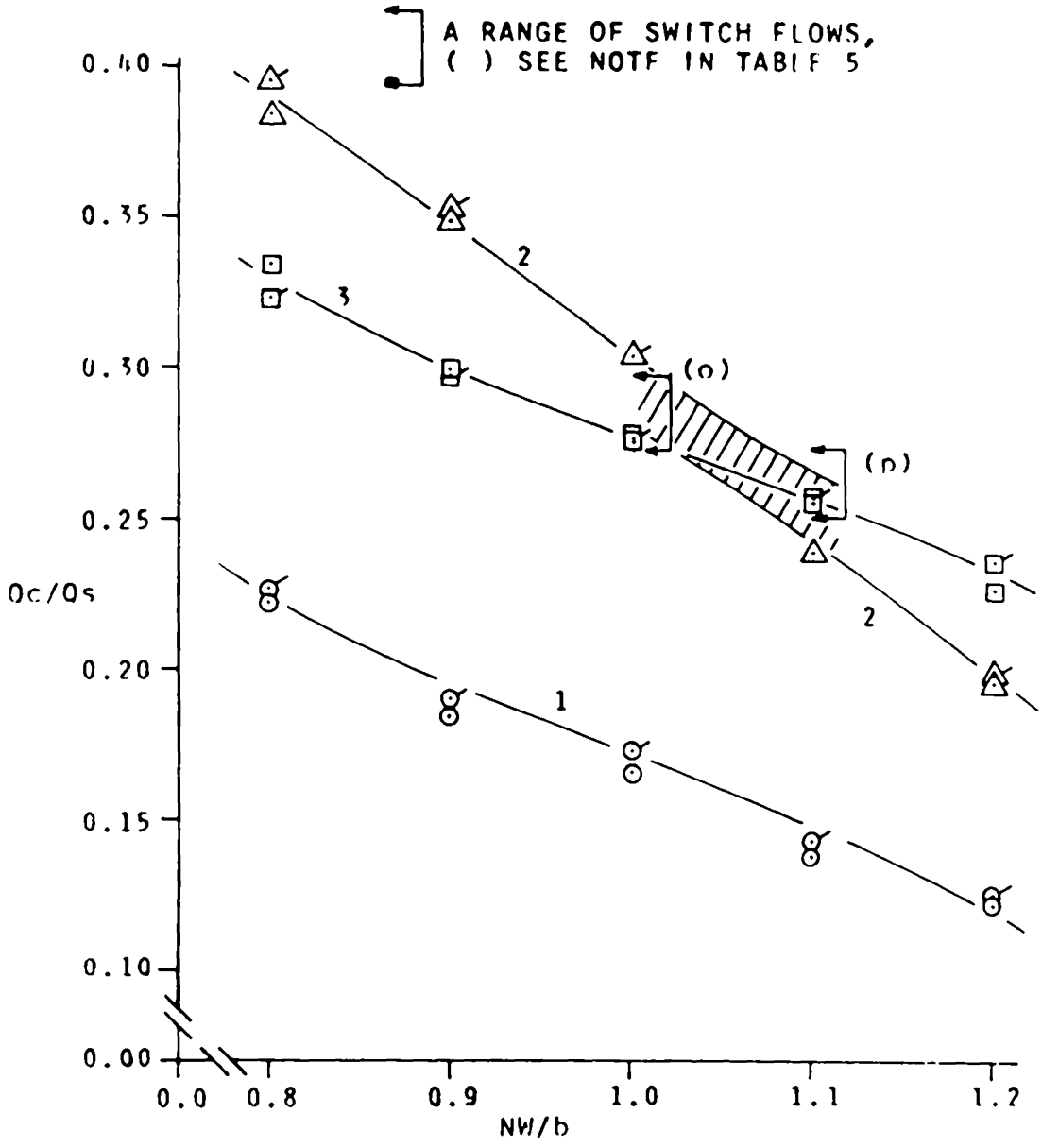


FIGURE 27. POWER NOZZLE WIDTH EFFECTS ON SWITCH FLOW; 1 NOZZLE LOADING

LEGEND:

| REYNOLDS NO. | RIGHT SIDE | LEFT SIDE | CURVE LABEL |
|---|---|---|---|
| 1950 | ○ | ○ | 1 |
| 3900 | △ | △ | 2 |
| 5800 | □ | □ | 3 |

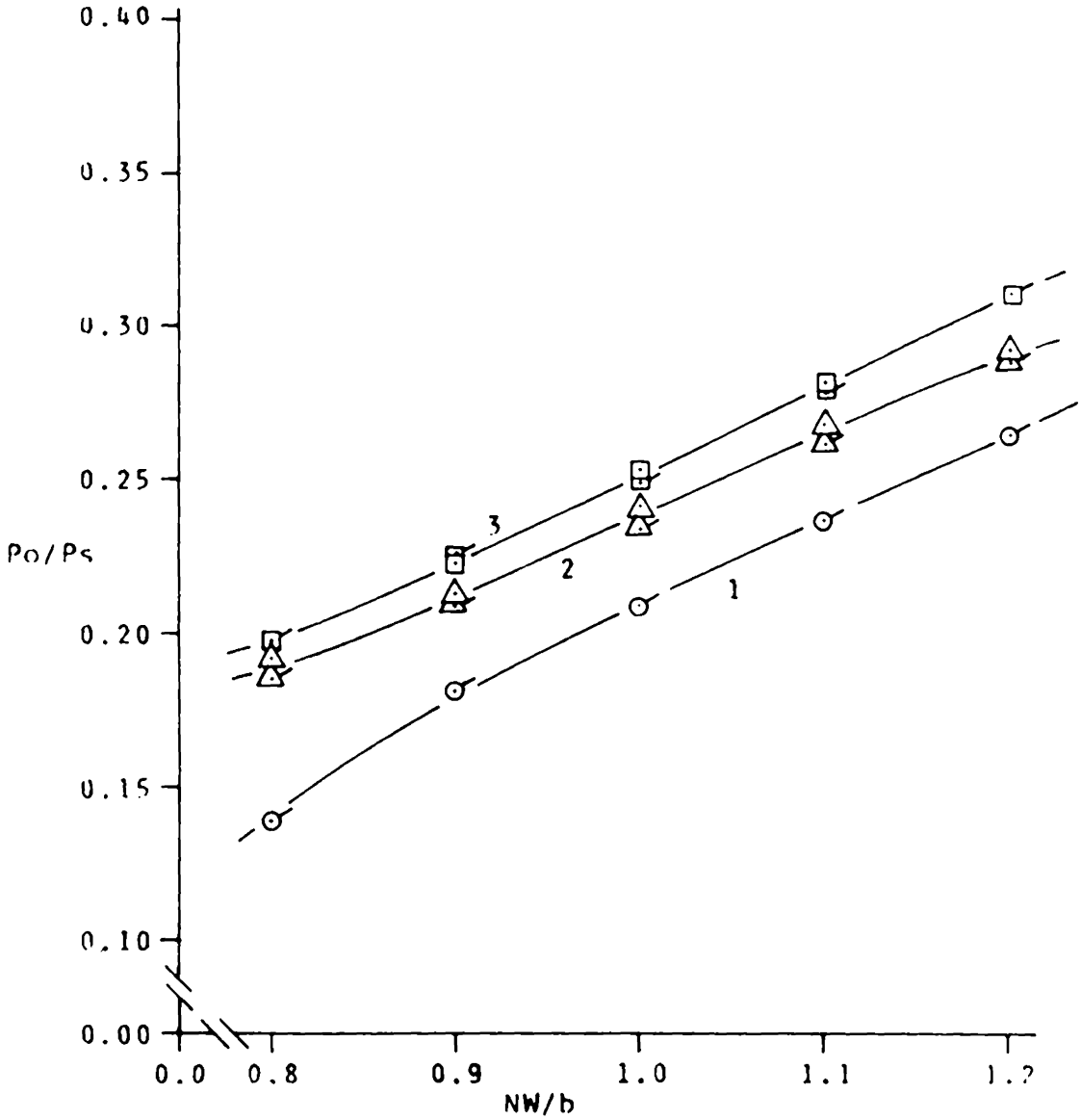


FIGURE 28. POWER NOZZLE WIDTH EFFECTS ON RECOVERY PRESSURE; 1 NOZZLE LOADING

LEGEND:

| REYNOLDS NO. | RIGHT SIDE | LEFT SIDE | CURVE LABEL |
|---|---|---|---|
| 1950 | ○ | ○ | 1 |
| 3900 | △ | △ | 2 |
| 5800 | □ | □ | 3 |

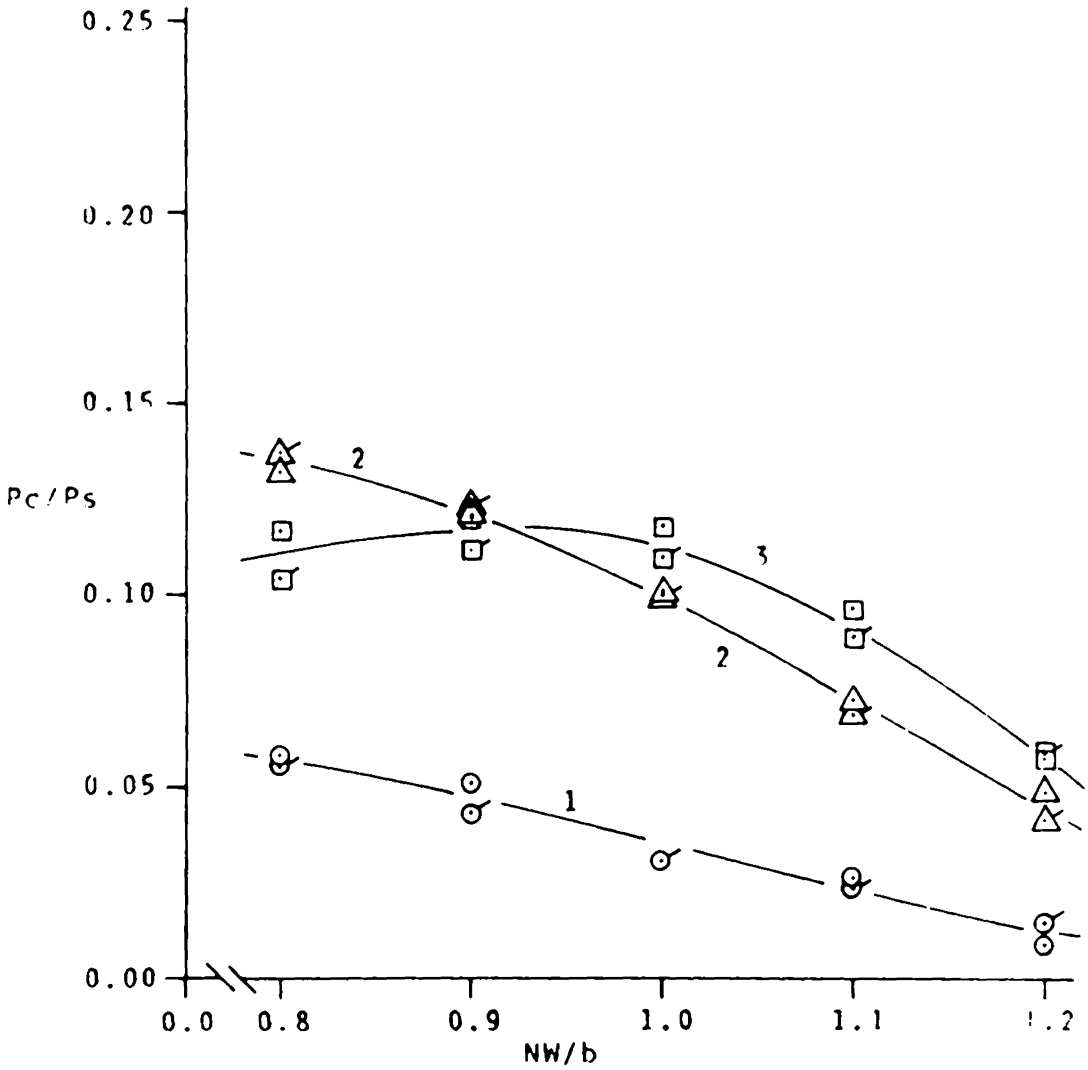


FIGURE 29. POWER NOZZLE WIDTH EFFECTS ON SWITCH PRESSURE; BLOCKED OUTPUT

LEGEND:

| REYNOLDS NO. | RIGHT SIDE | LEFT SIDE | CURVE LABEL |
|---|---|---|---|
| 1950 | ○ | ○ | 1 |
| 3900 | △ | △ | 2 |
| 5800 | □ | □ | 3 |

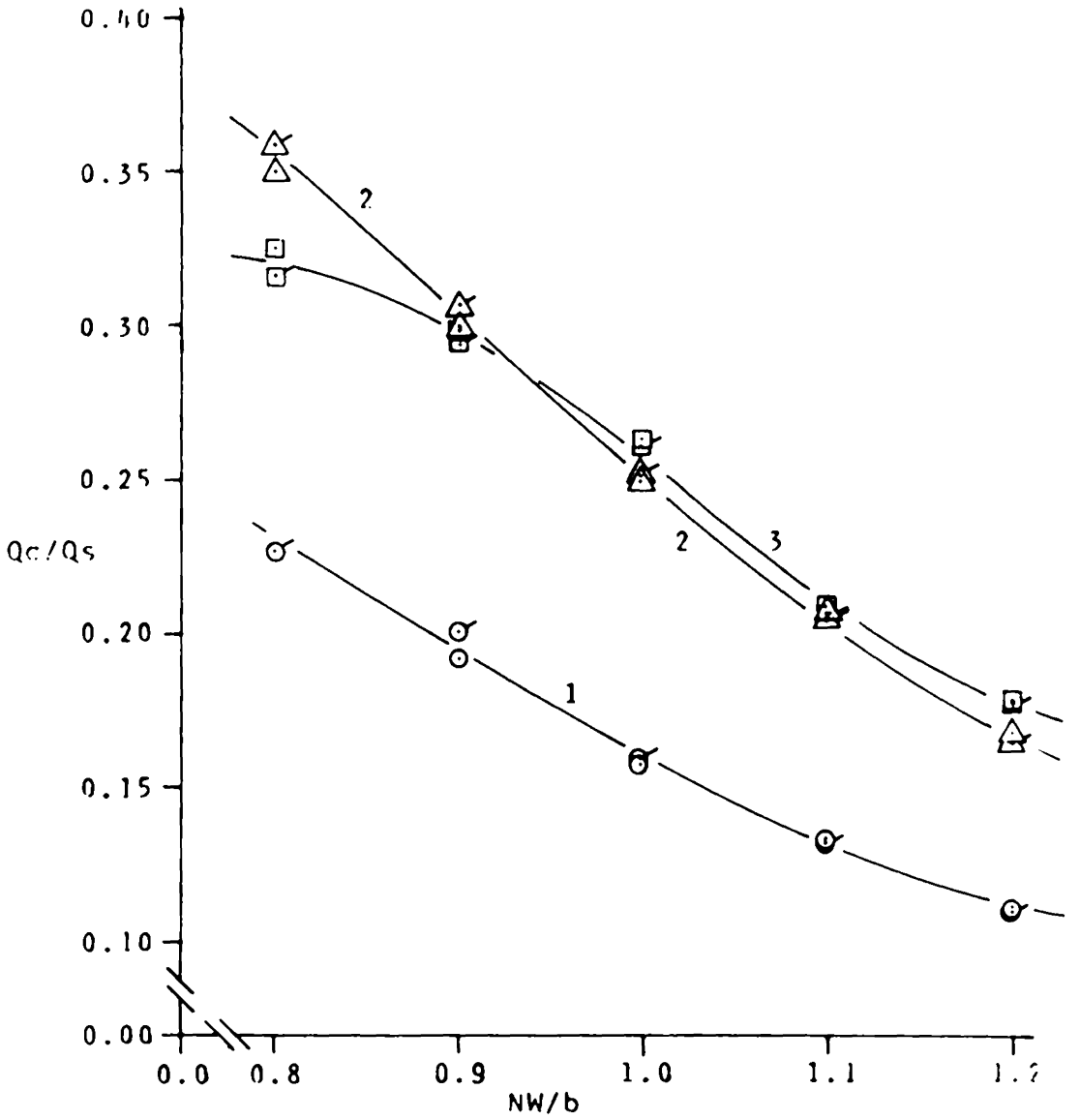


FIGURE 30. POWER NOZZLE WIDTH EFFECTS ON SWITCH FLOW; BLOCKED OUTPUT

LEGEND:

| REYNOLDS NO. | RIGHT SIDE | LEFT SIDE | CURVE LABEL |
|---|---|---|---|
| 1950 | ○ | ○ | 1 |
| 3900 | △ | △ | 2 |
| 5800 | □ | □ | 3 |

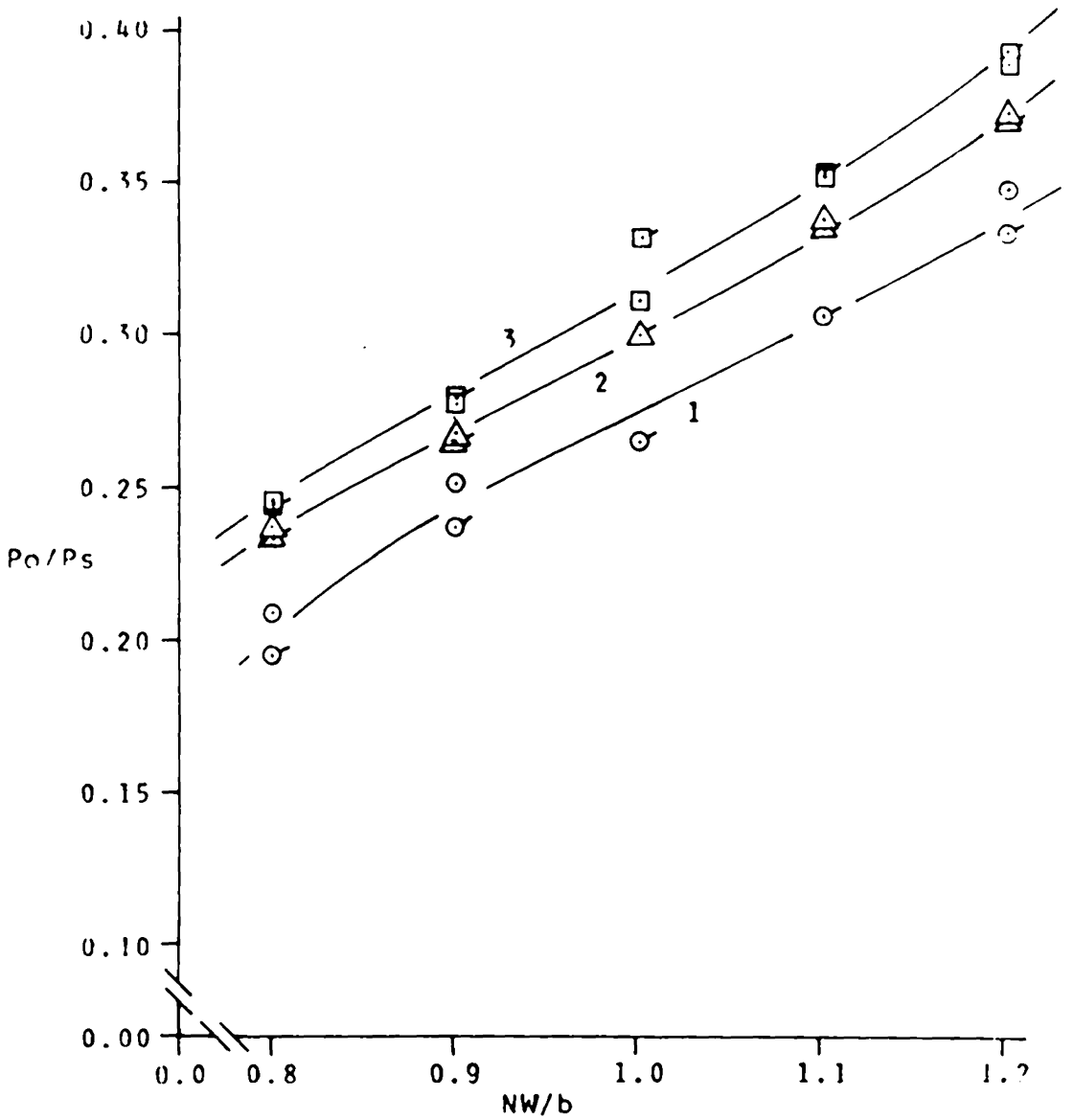


FIGURE 31. POWER NOZZLE WIDTH EFFECTS ON RECOVERY PRESSURE; BLOCKED OUTPUT

LEGEND:

| REYNOLDS NO. | RIGHT SIDE | LEFT SIDE | CURVE LABEL |
|---|---|---|---|
| 1950 | ○ | ○ | 1 |
| 3900 | △ | △ | 2 |
| 5800 | □ | □ | 3 |

Table 6. Wall Flat Results

1 nozzle load:

| WF/b | $R_b$ | $Pc_r/Ps$ | $Pc_l/Ps$ | $Qc_r/Qs$ | $Qc_l/Qs$ | $Po_r/Ps$ | $Po_l/Ps$ |
|---|---|---|---|---|---|---|---|
| 0.0 | 1950 | .070 | .071 | .137 | .138 | .181 | .181 |
| | 2900 | .218 | .221 | .263 | .274 | .217 | .211 |
| | 3900 | .205 | .211 | .255 | .261 | .230 | .233 |
| | 4850 | note s | note s | note s | note s | .237 | .232 |
| | 5800 | .200 | .195 | .239 | .241 | .242 | .237 |
| 1.55 | 1950 | .040 | .041 | .166 | .173 | .209 | .209 |
| | 2900 | .130 | note n | .278 | note n | .223 | .217 |
| | 3900 | note o | .156 | note o | .303 | .241 | .234 |
| | 4850 | .155 | .134 | .301 | .285 | .245 | .241 |
| | 5800 | .130 | .124 | .275 | .276 | .253 | .249 |
| 2.52 | 1950 | .031 | .038 | .171 | .177 | .209 | .209 |
| | 2900 | .093 | .100 | .255 | .261 | .223 | .217 |
| | 3900 | .105 | .125 | .275 | .292 | .237 | .234 |
| | 4850 | .120 | .114 | .292 | .287 | .241 | .243 |
| | 5800 | .112 | .115 | .281 | .293 | .246 | .249 |

blocked output:

| WF/b | $R_b$ | $Pc_r/Ps$ | $Pc_l/Ps$ | $Qc_r/Qs$ | $Qc_l/Qs$ | $Po_r/Ps$ | $Po_l/Ps$ |
|---|---|---|---|---|---|---|---|
| 0.0 | 1950 | .081 | .079 | .138 | .137 | .265 | .251 |
| | 2900 | .205 | .206 | .247 | .253 | .279 | .279 |
| | 3900 | .206 | .203 | .251 | .251 | .286 | .286 |
| | 4850 | .198 | note t | .238 | note t | .295 | .290 |
| | 5800 | .183 | .186 | .225 | .231 | .297 | .297 |

Notes on Table 6:

note s Mild indications of the existence of the coexistence of two switch points were noted.

$Pc_r/Ps$ 0.198 - 0.212 $Qc_r/Qs$ 0.245 - 0.253

$Pc_l/Ps$ 0.200 - 0.212 $Qc_l/Qs$ 0.250 - 0.259

note n See Table 5, page 49

note o See Table 5, page 49

note t Mild indications of the coexistence of two switch points were noted.

$Pc_l/Ps$ 0.182 - 0.200 $Qc_l/Qs$ 0.236 - 0.250

Table 6. Continued

| WF/b | $R_b$ | $Pc_r/Ps$ | $Pc_l/Ps$ | $Qc_r/Qs$ | $Qc_l/Qs$ | $Po_r/Ps$ | $Po_l/Ps$ |
|---|---|---|---|---|---|---|---|
| 1.55 | 1950 | .031 | .031 | .158 | .160 | .265 | .265 |
| | 2900 | .073 | .069 | .223 | .218 | .291 | .285 |
| | 3900 | .101 | .100 | .250 | .252 | .300 | .300 |
| | 4850 | .121 | .116 | .272 | .273 | .308 | .306 |
| | 5800 | .118 | .110 | .264 | .262 | .311 | .332 |
| 2.52 | 1950 | .033 | .037 | .172 | .172 | .265 | .265 |
| note u | 2900 | .055 | .053 | .214 | .212 | .285 | .285 |
| | 3900 | .079 | .077 | .246 | .246 | .300 | .300 |
| | 4850 | .094 | .092 | .261 | .262 | .308 | .308 |
| | 5800 | .097 | .085 | .263 | .267 | .311 | .313 |

Notes on Table 6:

note u For the right side at $R_b$=1950, the switch is such that the jet detaches from the wall and oscillates before attaching to the opposite wall.

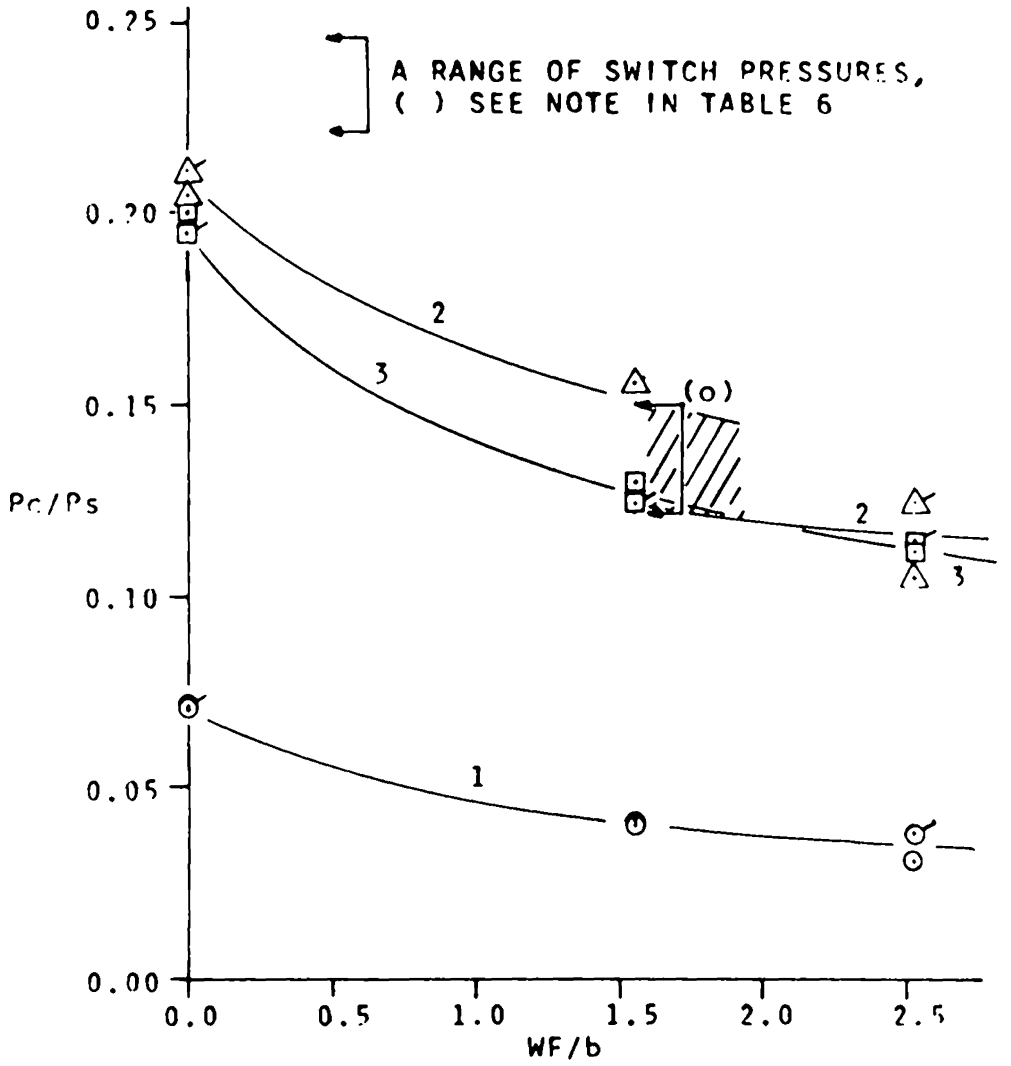


FIGURE 32. WALL FLAT EFFECTS ON SWITCH PRESSURE; 1 NOZZLE LOADING

LEGEND:

| REYNOLDS NO. | RIGHT SIDE | LEFT SIDE | CURVE LABEL |
|---|---|---|---|
| 1950 | ○ | ○ | 1 |
| 3900 | △ | △ | 2 |
| 5800 | □ | □ | 3 |

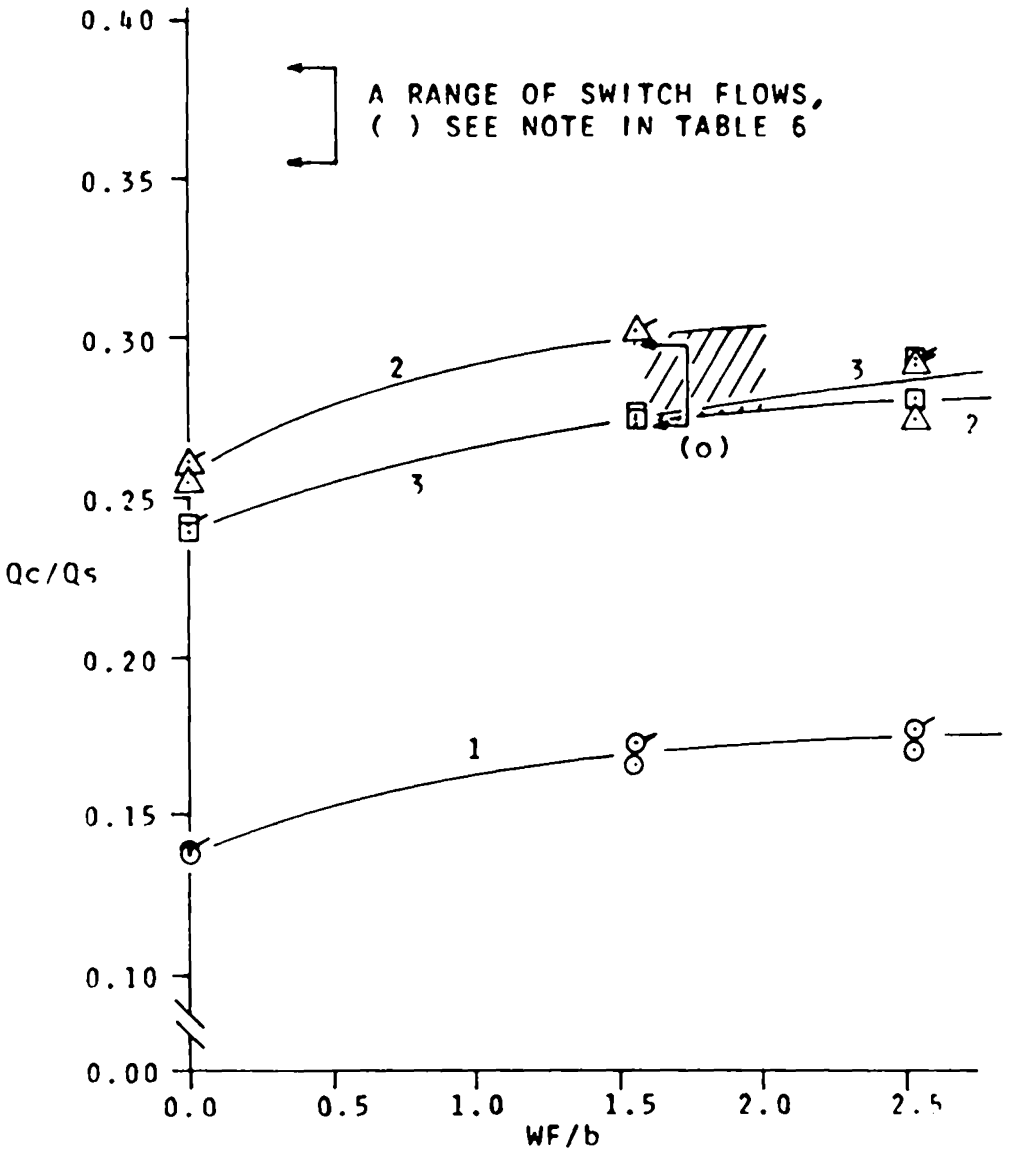


FIGURE 33. WALL FLAT EFFECTS ON SWITCH FLOW; 1 NOZZLE LOADING

LEGEND:

| REYNOLDS NO. | RIGHT SIDE | LEFT SIDE | CURVE LABEL |
|---|---|---|---|
| 1950 | ○ | ○ | 1 |
| 3900 | △ | △ | 2 |
| 5800 | □ | □ | 3 |

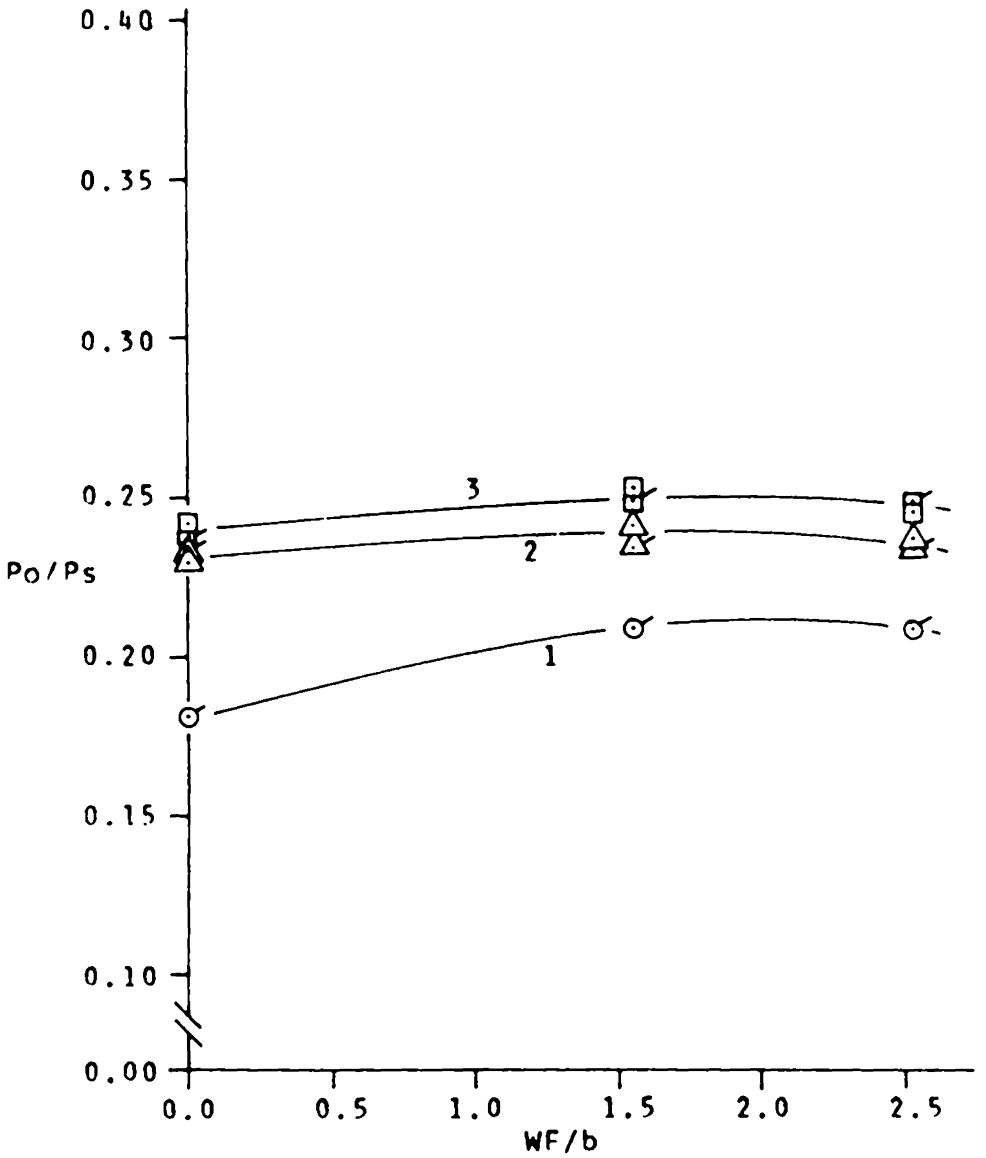


FIGURE 34. WALL FLAT EFFECTS ON RECOVERY PRESSURE; 1 NOZZLE LOADING

LEGEND:

| REYNOLDS NO. | RIGHT SIDE | LEFT SIDE | CURVE LABEL |
|---|---|---|---|
| 1950 | ○ | ○ | 1 |
| 3900 | △ | △ | 2 |
| 5800 | □ | □ | 3 |

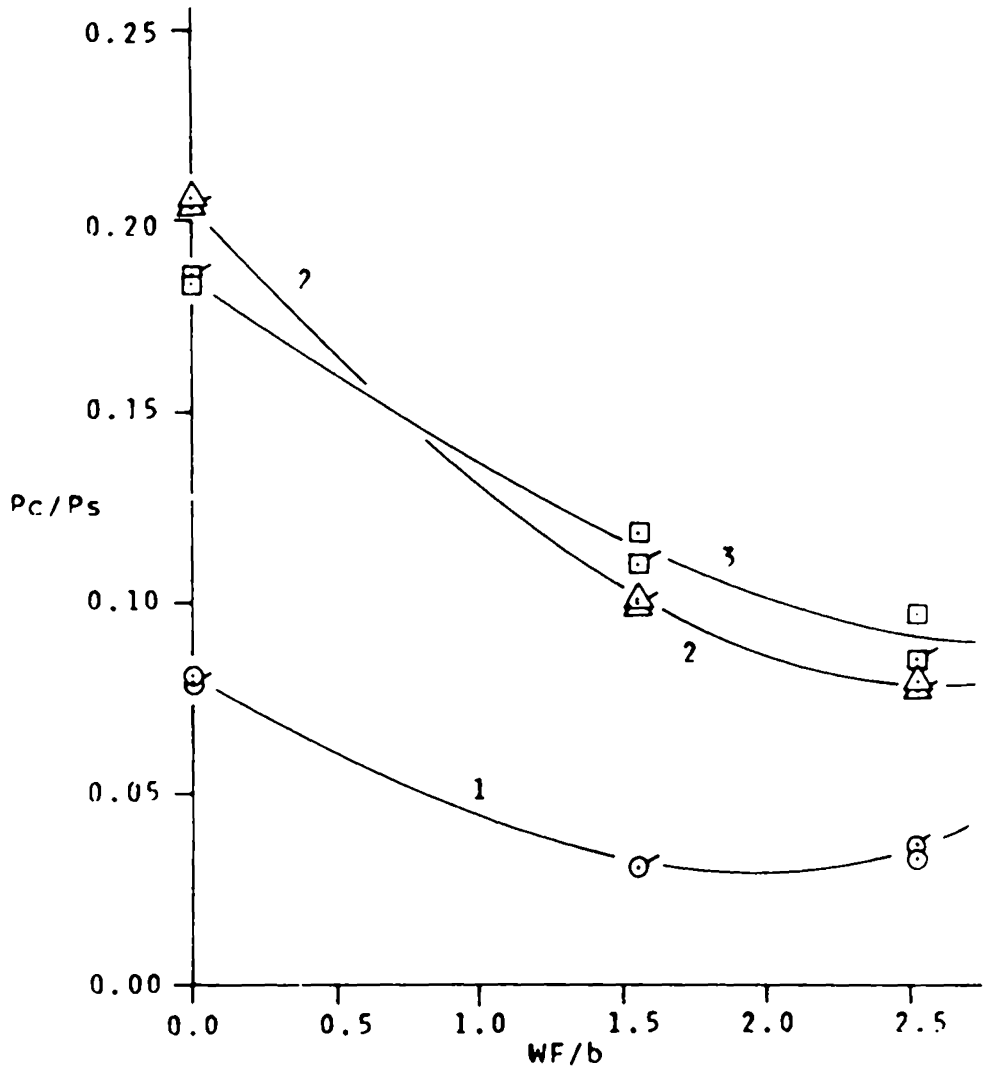


FIGURE 35. WALL FLAT EFFECTS ON SWITCH PRESSURE; BLOCKED OUTPUT

LEGEND:

| REYNOLDS NO. | RIGHT SIDE | LEFT SIDE | CURVE LABEL |
|---|---|---|---|
| 1950 | ○ | ○ | 1 |
| 3900 | △ | △ | 2 |
| 5800 | □ | □ | 3 |

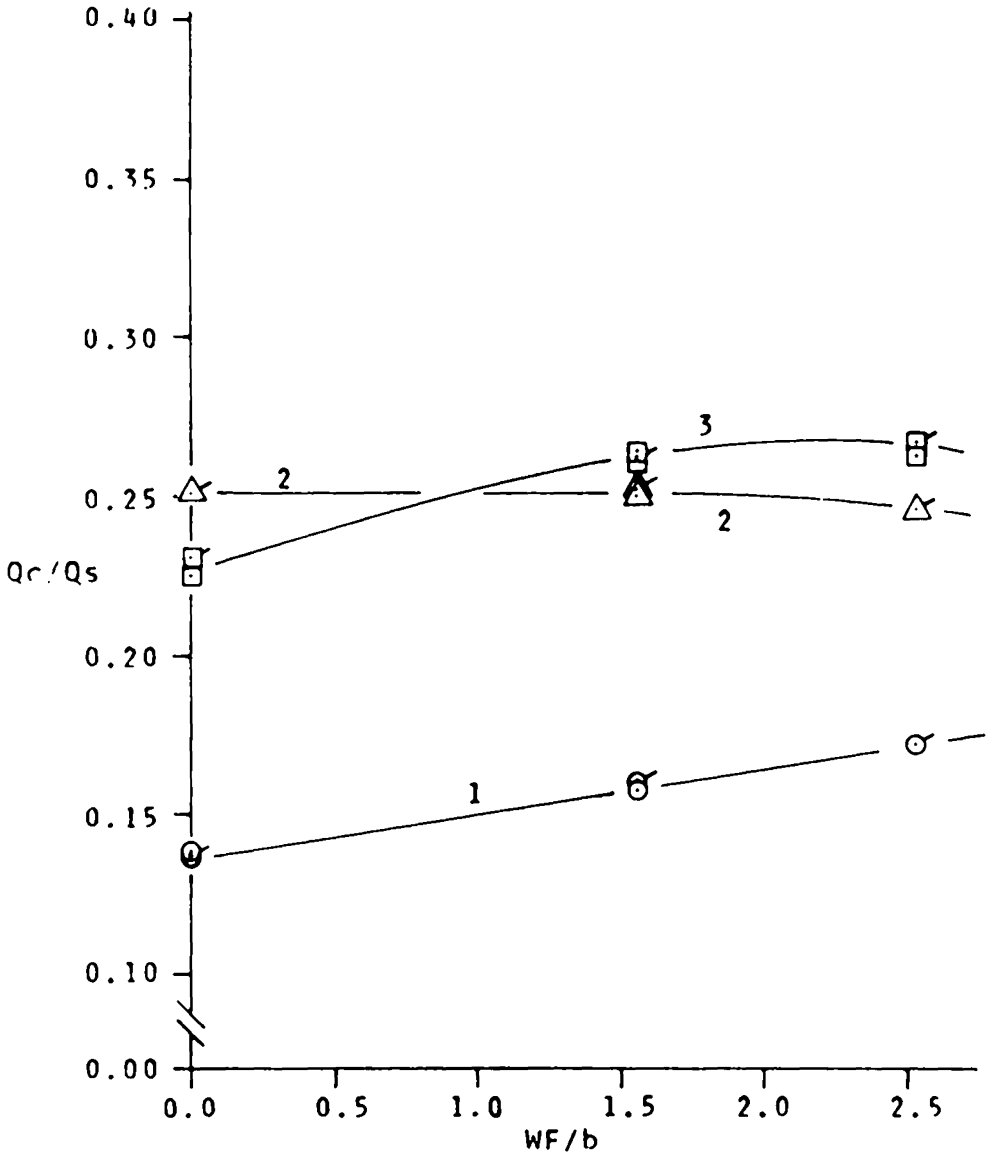


FIGURE 36. WALL FLAT EFFECTS ON SWITCH FLOW; BLOCKED OUTPUT

LEGEND:

| REYNOLDS NO. | RIGHT SIDE | LEFT SIDE | CURVE LABEL |
|---|---|---|---|
| 1950 | ○ | ○ | 1 |
| 3900 | △ | △ | 2 |
| 5800 | □ | □ | 3 |

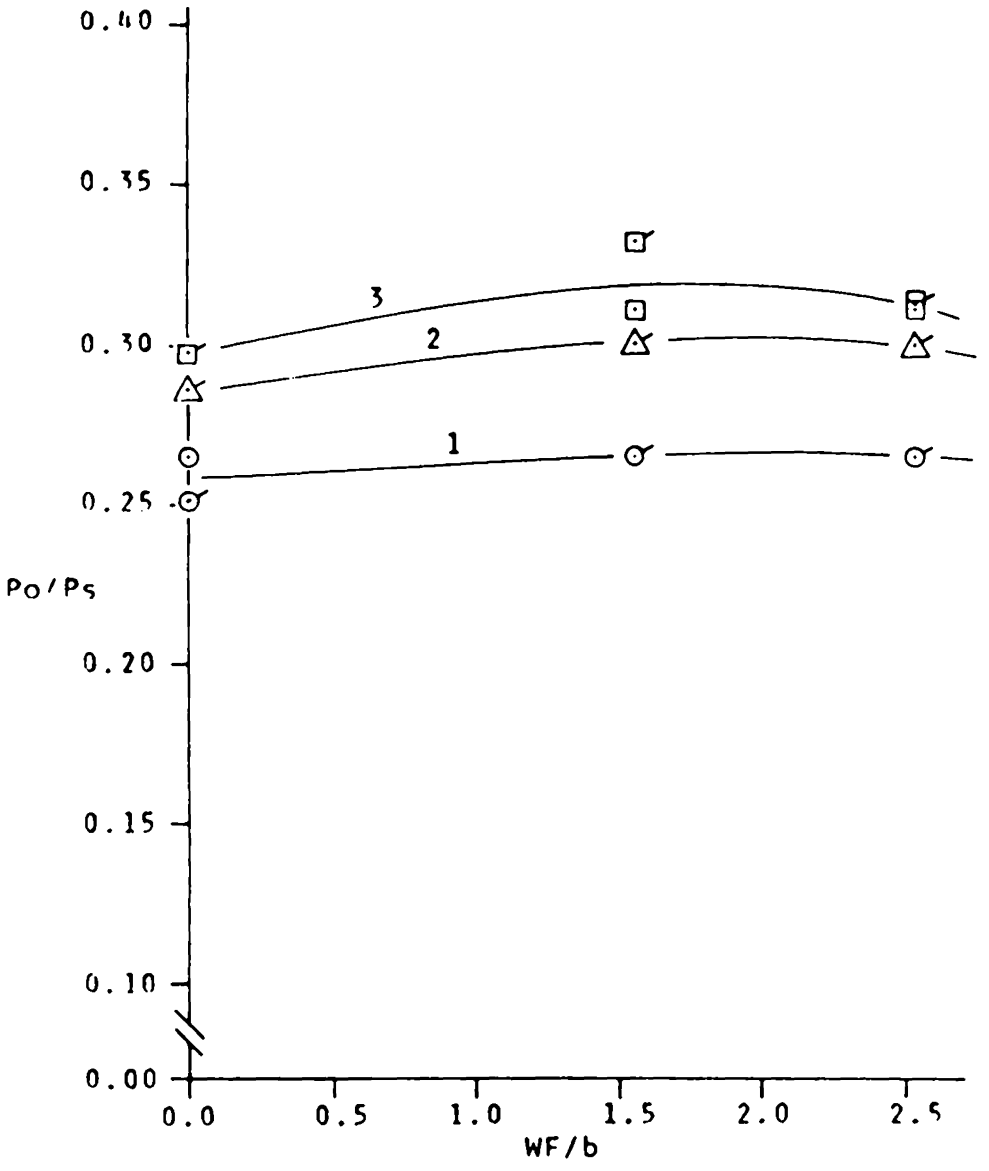


FIGURE 37. WALL FLAT EFFECTS ON RECOVERY PRESSURE; BLOCKED OUTPUT

LEGEND:

| REYNOLDS NO. | RIGHT SIDE | LEFT SIDE | CURVE LABEL |
|---|---|---|---|
| 1950 | ○ | ○ | 1 |
| 3900 | △ | △ | 2 |
| 5800 | □ | □ | 3 |

Table 7. Power Nozzle Shape Results

1 nozzle load:

| LN/b | $R_b$ | $Pc_r/Ps$ | $Pc_l/Ps$ | $Qc_r/Qs$ | $Qc_l/Qs$ | $Po_r/Ps$ | $Po_l/Ps$ |
|---|---|---|---|---|---|---|---|
| 27.0 | 1950 | .040 | .041 | .166 | .173 | .209 | .209 |
| | 2900 | .130 | note n | .278 | note n | .223 | .217 |
| | 3900 | note o | .156 | note o | .303 | .241 | .234 |
| | 4850 | .155 | .134 | .301 | .285 | .245 | .241 |
| | 5800 | .130 | .124 | .275 | .276 | .253 | .249 |
| 15.0 | 1950 | .075 | .084 | .205 | .212 | .223 | .223 |
| note v | 2900 | .131 | .159 | .277 | .291 | .242 | .242 |
| | 3900 | .159 | .183 | .304 | .313 | .255 | .250 |
| | 4850 | .143 | .157 | .286 | .290 | .263 | .263 |
| | 5800 | .123 | .147 | .277 | .283 | .270 | .271 |
| 10.0 | 1950 | .089 | .063 | .211 | .189 | .237 | .237 |
| note v | 2900 | .148 | .067 | .270 | .255 | .254 | .260 |
| | 3900 | .170 | .154 | .294 | .283 | .268 | .272 |
| | 4850 | .157 | .147 | .277 | .272 | .277 | .283 |
| | 5800 | .123 | .123 | .270 | .258 | .284 | .294 |

blocked output:

| LN/b | $R_b$ | $Pc_r/Ps$ | $Pc_l/Ps$ | $Qc_r/Qs$ | $Qc_l/Qs$ | $Po_r/Ps$ | $Po_l/Ps$ |
|---|---|---|---|---|---|---|---|
| 2.70 | 1950 | .031 | .031 | .158 | .160 | .265 | .265 |
| | 2900 | .073 | .069 | .223 | .218 | .291 | .285 |
| | 3900 | .101 | .100 | .250 | .252 | .300 | .300 |
| | 4850 | .121 | .116 | .272 | .273 | .308 | .306 |
| | 5800 | .118 | .110 | .264 | .262 | .311 | .332 |

Notes on Table 7:

note n See Table 5, page 49

note o See Table 5, page 49

note v For these shorter power nozzle shapes it was found that dimensioning of the model to achieve unbiased operation was next to impossible.

Table 7. Continued

| LN/b | $R_b$ | $Pc_r/Ps$ | $Pc_l/Ps$ | $Qc_r/Qs$ | $Qc_l/Qs$ | $Po_r/Ps$ | $Po_l/Ps$ |
|---|---|---|---|---|---|---|---|
| 15.0 | 1950 | .051 | .049 | .202 | .198 | .292 | .292 |
| note v | 2900 | .086 | .094 | .238 | .240 | .304 | .297 |
| | 3900 | .107 | .115 | .260 | .260 | .317 | .314 |
| | 4850 | .119 | .125 | .265 | .265 | .324 | .328 |
| | 5800 | .101 | .124 | .281 | .263 | .332 | .335 |
| 10.0 | 1950 | .051 | .032 | .176 | .164 | .306 | .306 |
| note v | 2900 | .102 | .065 | .187 | .172 | .316 | .322 |
| | 3900 | .123 | .086 | .257 | .237 | .328 | .335 |
| | 4850 | .131 | .091 | .255 | .231 | .339 | .346 |
| | 5800 | .112 | .098 | .251 | .235 | .344 | .356 |

Notes on Table 7:

note v See note on previous page.

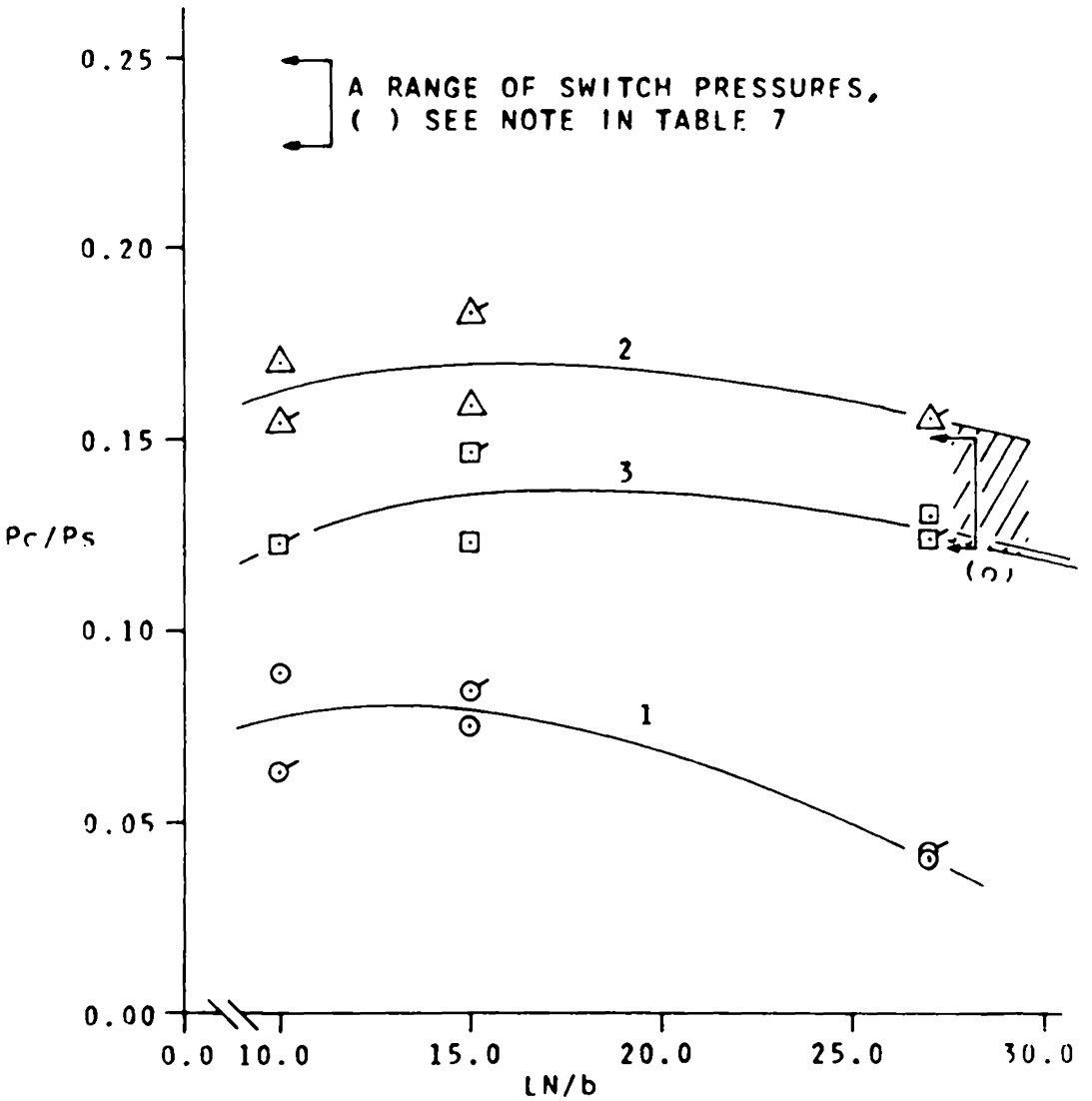


FIGURE 38. POWER NOZZLE SHAPE EFFECTS ON SWITCH PRESSURE; 1 NOZZLE LOADING

LEGEND:

| REYNOLDS NO. | RIGHT SIDE | LEFT SIDE | CURVE LABEL |
|---|---|---|---|
| 1950 | ○ | ○ | 1 |
| 3900 | △ | △ | 2 |
| 5800 | □ | □ | 3 |

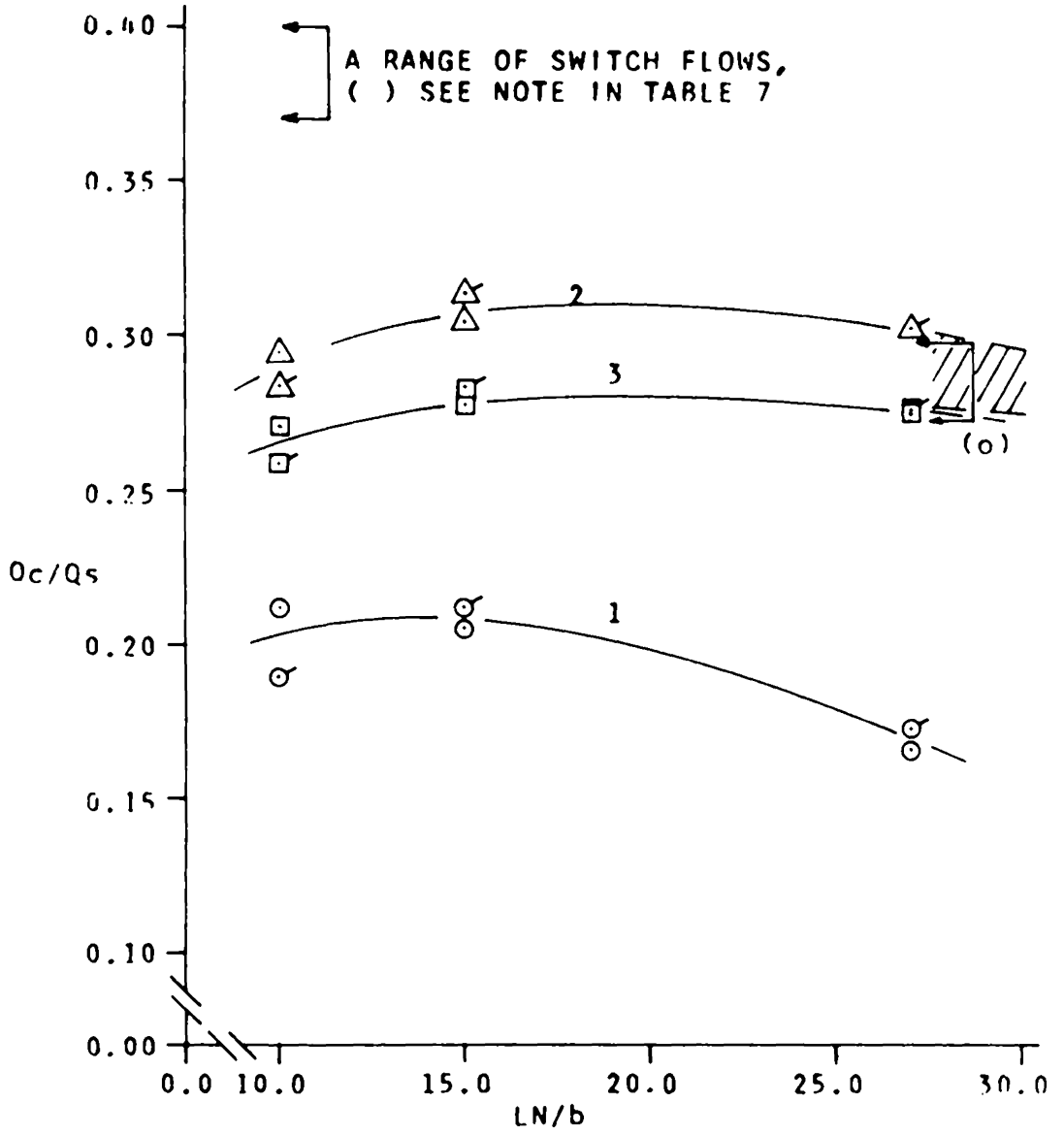


FIGURE 39. POWER NOZZLE SHAPE EFFECTS ON SWITCH FLOW; 1 NOZZLE LOADING

LEGEND:

| REYNOLDS NO. | RIGHT SIDE | LEFT SIDE | CURVE LABEL |
|---|---|---|---|
| 1950 | ○ | ○ | 1 |
| 3900 | △ | △ | 2 |
| 5800 | □ | □ | 3 |

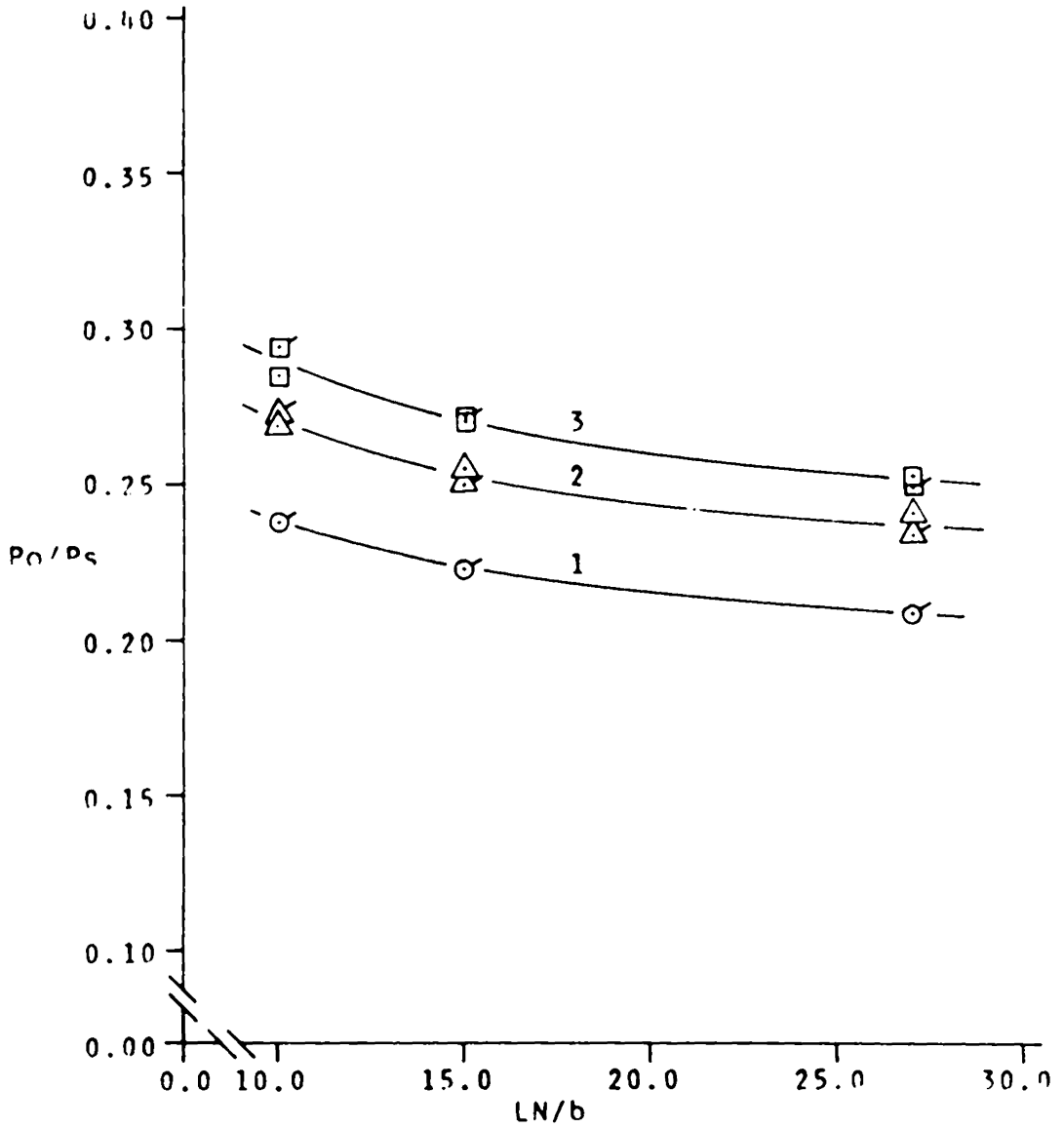


FIGURE 40. POWER NOZZLE SHAPE EFFECTS ON RECOVERY PRESSURE; 1 NOZZLE LOADING

LEGEND:

| REYNOLDS NO. | RIGHT SIDE | LEFT SIDE | CURVE LABEL |
|---|---|---|---|
| 1950 | ○ | ○ | 1 |
| 3900 | △ | △ | 2 |
| 5800 | □ | □ | 3 |

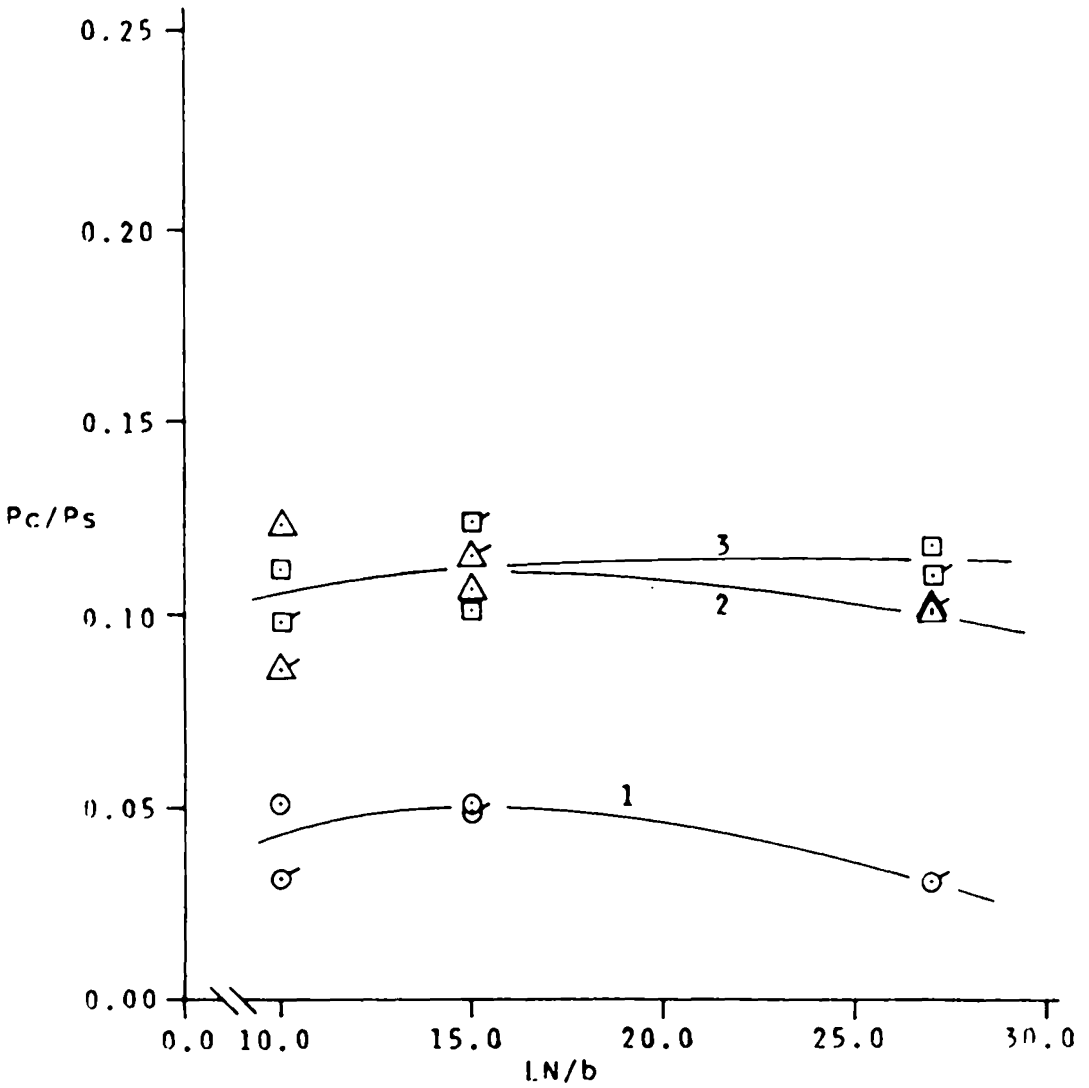


FIGURE 41. POWER NOZZLE SHAPE EFFECTS ON SWITCH PRESSURE; BLOCKED OUTPUT

LEGEND:

| REYNOLDS NO. | RIGHT SIDE | LEFT SIDE | CURVE LABEL |
|---|---|---|---|
| 1950 | ○ | ○ | 1 |
| 3900 | △ | △ | 2 |
| 5800 | □ | □ | 3 |

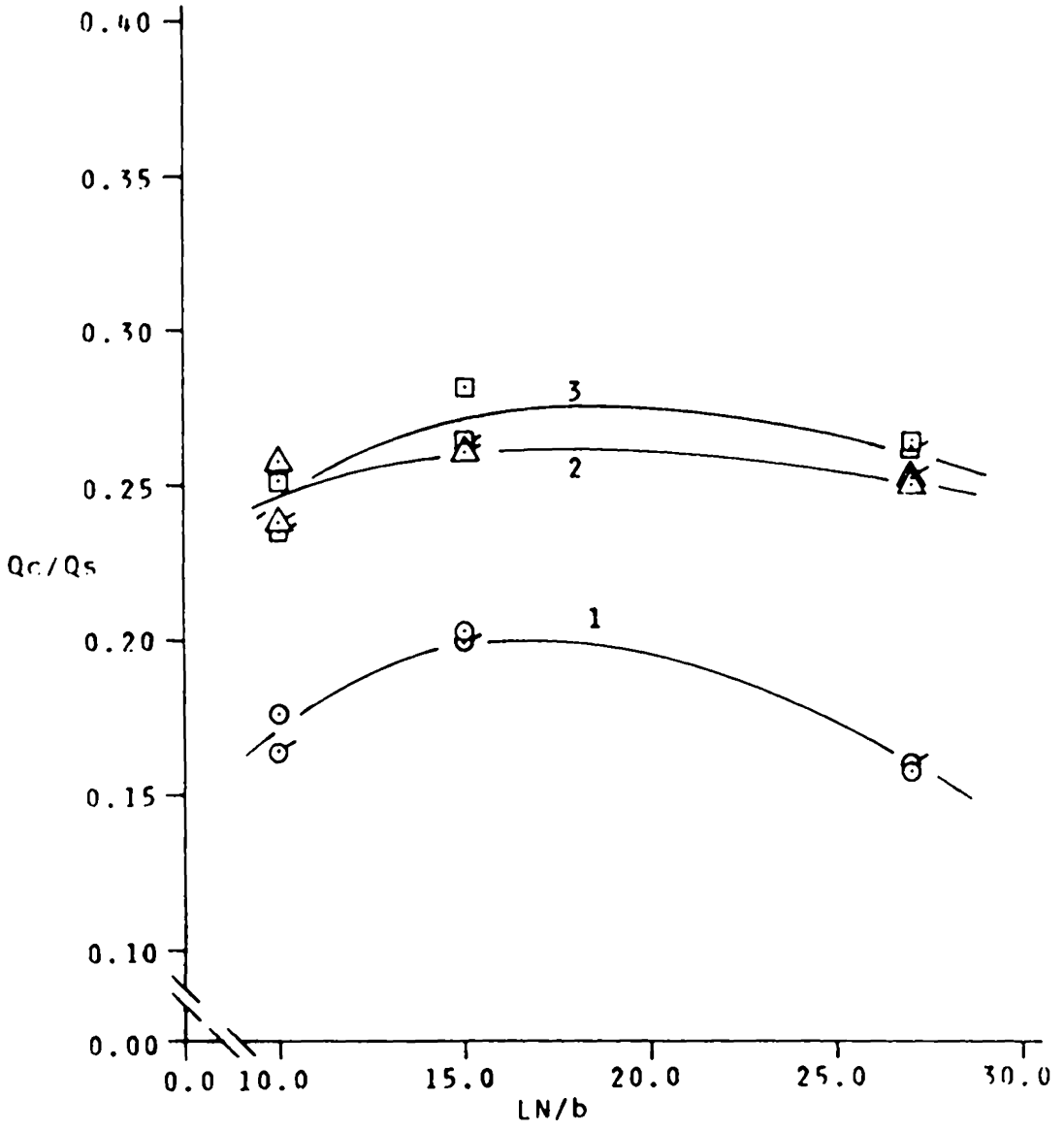


FIGURE 42. POWER NOZZLE SHAPE EFFECTS ON SWITCH FLOW; BLOCKED OUTPUT

LEGEND:

| REYNOLDS NO. | RIGHT SIDE | LEFT SIDE | CURVE LABEL |
|---|---|---|---|
| 1950 | ○ | ○ | 1 |
| 3900 | △ | △ | 2 |
| 5800 | □ | □ | 3 |

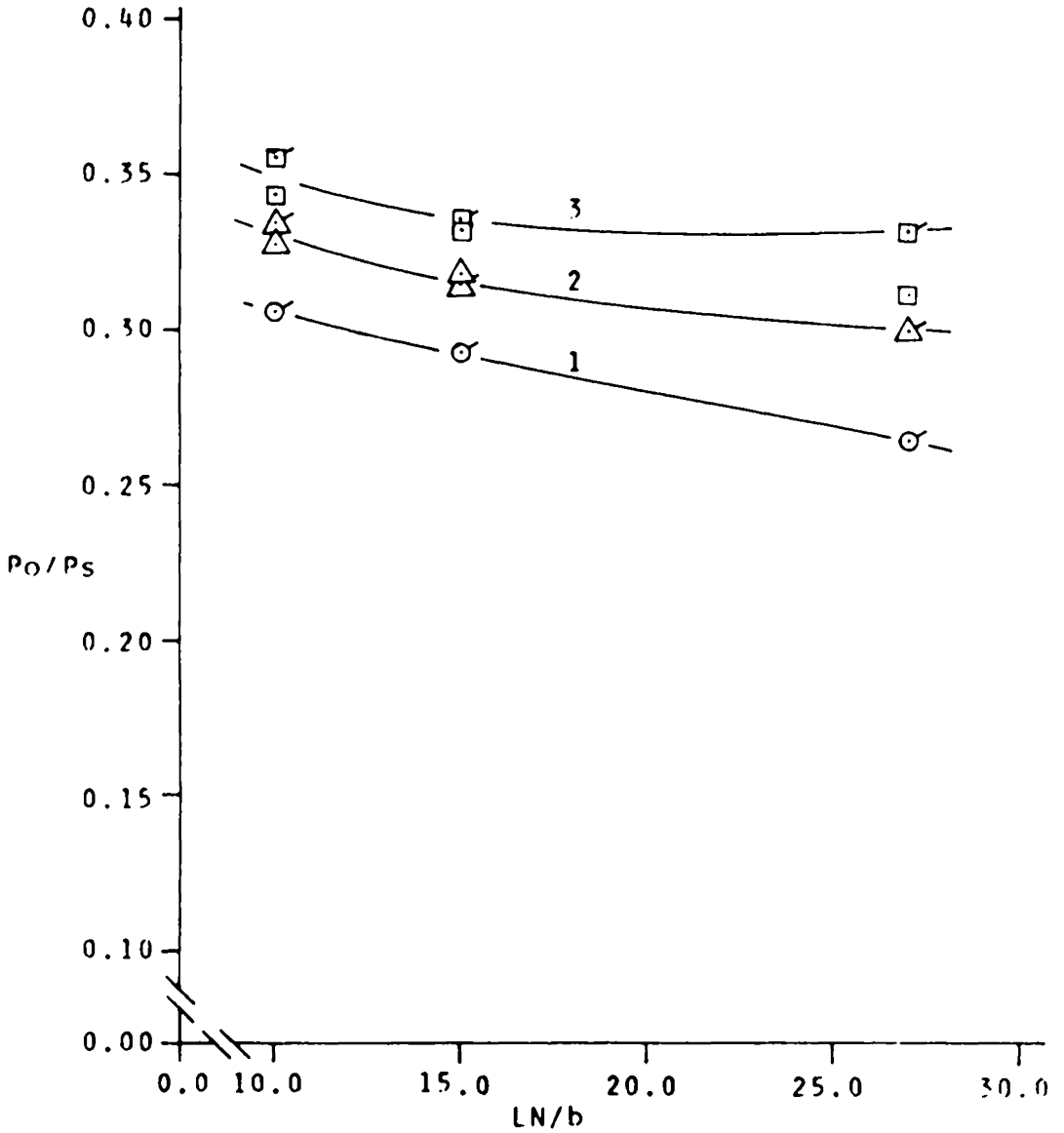


FIGURE 43. POWER NOZZLE SHAPE EFFECTS ON RECOVERY PRESSURE; BLOCKED OUTPUT

LEGEND:

| REYNOLDS NO. | RIGHT SIDE | LEFT SIDE | CURVE LABEL |
|---|---|---|---|
| 1950 | ○ | ○ | 1 |
| 3900 | △ | △ | 2 |
| 5800 | □ | □ | 3 |

## DISCUSSION OF RESULTS

This section is primarily an explanation of the manner in which the curves of the figures of the previous section were fitted to the data. Once this has been done, the curves are self explaining and show the characteristics of the particular dimension parameter.

The first step in the explanation of the curves is to establish the coexistence of at least two switch points for a particular geometric configuration at particluar operating conditions. It is known that there are different switching modes. (These were described in the Introduction.) It is also known that the geometry and operating conditions determine what mode the device is in; so, there must be a transition from one mode to another taking place at certain geometric and operating conditions. It is plausible that this transition is neither smooth nor at the same level. (The switch pressure and/or flow might be different values for the different switch modes.) It is also plausible that the modes are not only at different levels but that they overlap, thus giving the flip-flop a choice of switching in either mode. This is exactly what was found when the wall length parameter was studied. (See notes h, i, j of Table 3.) In these positive identifications of two coexistent switch points, the behavior was such that once the pressure on the control passed the lower of the two switch points, switching would not occur until the higher point was reached. The next logical question to ask is, does this overlapping of switch points at different levels occur in milder form? The answer to this question is yes as evidenced by the observations made during the operation of the model. The notes that are placed in the tables concerning the coexistence of two switch points were,

in all cases, made for the following reason. At these locations, very slight differences in the mechanics of performing the switch would consistently cause the flip-flop to switch at a high or a low value. In general, a control signal that was absent of noise (very steady increase in the control pressure) would consistently cause a high switch. A rise in control pressure that was the least bit unsteady (as noted by watching the movement of the pen of the x - y recorder) would cause a consistently low switch. A change from the smooth to unsteady operation when the control pressure was between the high and low values would cause the switch to occur at that point. To explain this, the coexistence of two switch points is needed. Once the pressure on the control rises above the lower switch point, it can continue to rise to the higher switch point or at any time revert back to the lower point to perform the switch.

There is more evidence that supports this hypothesis of two switch points. For example, it is seen from Table 2 that the notes of this unusual switching behavior cluster around the middle of the Reynolds number range as well as around the nominally dimensioned device. Movement to high or low Reynolds numbers, or high or low offsets causes the observation of unusual behavior to disappear. This indicates that the device is in a transition from one switch mode to another. Scanning the data from the retested nominal device in Tables 2 through 5 reveals that large amounts of scatter occur in the switch pressures and flows for operating conditions near those where the notes of unusual switching behavior were made; yet, there is repeatable data away from these operating conditions. There is still more evidence supporting the hypothesis but the above is sufficient to establish the coexistence of different

level switch points.

Having established the existence of two, different level, overlapping switch points (hereafter called mode-changes) it was a very simple process to fit curves to the data. For data that were far away from known or suspected mode-changes, smooth and regular curves were fitted to the data with surprising similarity noted between the curves for different Reynolds numbers. To fit curves to data near known or suspected mode-changes, a little extrapolation of the mode-change to other Reynolds numbers and geometries nearby, and a search for curve shape similarities was needed. To explain this process, it is convenient to consider a specific example. Consider the offset data presented in Fig. 8. The curve labeled 2 is for $R_b$=3900 and shown in that curve, by way of a shaded area, is a known mode-change at $D/b \cong 0.1$. It was then noted (from Table 2) that a mode-change existed at the same offset for $R_b$=2900. The extrapolation process was to simply say that this mode-change probably extends into the curve for $R_b$=1950. This curve (labeled 1) in Fig. 8 was then constructed noting that similar shaped curves (similar to that of other Reynolds numbers) fit the data points if a small mode-change was placed at $D/b \cong 0.15$.

It was this process (exercised with caution) of curve fitting that was used in all of the figures presented, with exception of the recovery pressure data where the mode-change does not have an influence.

Having completed the tables and figures, this investigation has been essentially completed. The characteristics of the dimensional parameters are displayed in these curves; and, a quick examination of the figures reveals these characteristics. It is entirely too cumbersome to attempt

a detailed explanation of the characteristics of each dimensional parameter because of the influence of operating conditions (Reynolds number and output load) on these curves and mode-changes; so, for the remainder of this section the dimensional characteristics will be discussed in general terms pointing out some of the more significant features of the curves. Any specific details the reader might want on trends, characteristics, or location of mode-changes are quickly obtained by examining the figures and tables.

There are only a few significant things to be pointed out in the offset data. Note in Fig. 8 and 9 versus Fig. 11 and 12, the significant general drop in the switch pressure and flow due to the blockage of the outputs. For both output loadings, as a general rule, the switch pressure slowly drops and the switch flow rises for increases in offset. Another interesting item is that blocked outputs not only change the shapes of the curves but also remove the mode-change. Note that in the recovery pressure results (Fig. 10 and 13), there is a downward trend of the data for increasing offset for both load conditions. Note also that there is a slight change in shape of the curves for the blocked outputs.

The wall length data (Fig. 14 through 19) is one of the more dramatic dimensional parameters. The first thing seen in Fig. 14, 15, 17, and 18 is the severe influence of Reynolds numbers on the switch pressure and flow curves. It appears that the higher Reynolds number not only changes the level and shape of the curves but moves the mode-change from the higher to lower wall lengths. Another significant item concerning both the switch pressures and flows is the large slopes of the curves at the

low Reynolds numbers. When considering the influences of output loading (Fig. 14 and 15 versus 17 and 18), it is noted that the blocked outputs, besides changing shapes and levels, also increase the severity of the mode-changes as well as adding a second mode-change in the curves labeled 2 and 3. Concerning the recovery pressure, Fig. 16 and 19, the general decrease in recovery pressure for increasing wall length is noted. Also noted is the change in shapes of the curves for blocked outputs.

The best behaved data taken in this investigation were that for control width (Fig. 20 through 25). Noting first the switch flows for both 1 nozzle load and blocked output (Fig. 21 and 24 respectively), although blocked output and Reynolds numbers change the levels of the curves, each flow rate curve is essentially unaffected by changes in the control width. The same is also true for recovery pressure. (See Fig. 22 and 25.) Concerning switch pressures, the general trend of decreasing switch pressures for increasing width is noted (see Fig. 20 and 23) for both output loadings and most of the Reynolds numbers. Concerning the mode-changes, it is noted that they disappear for blocked outputs as well as for movement to high or low control widths as well as for high or low Reynolds numbers. As a final item to point out, it is noted (see note 1 in Table 4) that the higher control widths promoted, in general, very clean and consistent switches and that the device is less sensitive to biasing.

The first thing to note concerning the nozzle width data (Fig. 26 through 31) is that the switch pressure for 1 nozzle load (Fig. 26) is not dramatically influenced by changes in the nozzle width; yet, for blocked outputs (Fig. 29) there is a general downward trend in the switch pressure for increasing nozzle width. Concerning flow rates (Fig. 27 and 30),

the strong influence of Reynolds numbers and loading is again noted; but contrary to the switch pressure, it is noted the general steep decrease in flow rates for increasing nozzle width. When examining recovery pressure (Fig. 28 and 31), a steep increase in recovery pressure for increasing nozzle width is noted. In examining the existence of mode-changes, it is seen that blocked output removes the mode-change seen in the 1 nozzle load case. Other ways of removing the mode-change are either to go to a high or a low Reynolds number, or high or low nozzle widths.

When considering the effects of wall flat (Fig. 32 through 37), very few specific things can be said about this parameter because of the lack of data for it. For the few data points that have been plotted, there are some general items to point out. Concerning the switch pressures (Fig. 32 and 35), it is noted the general downward trend to switch pressures with increasing wall flat in both loading conditions. The influence of loading condition is depicted by the larger slopes of the curves as well as their change in shapes and levels that is seen for the case of blocked outputs. Concerning the switch flow rates (Fig. 33 and 36), it should be noted that Reynolds number and loading have dramatic influences; but given operating conditions of Reynolds numbers and load, the flow rates are essentially unaffected by changes in the wall flat. As in most of the other dimensional parameters, the blocked outputs remove the mode-change from the nominal dimension. The mode-change is also removed by movement to high or low wall flats. Concerning the recovery pressures (Fig. 34 and 37), it is pointed out that, other than the now normal influences of Reynolds number and output

loadings, the recovery pressures are essentially unaffected by changes in the wall flat.

The last dimensional parameter to be investigated was the power nozzle shape (Fig. 38 through 43). Due to the lack of data on this parameter, not too many specific remarks can be made about it. With the points that were taken, some surprising general effects can be noted concerning this parameter. Concerning switch pressures and flows (Fig. 38, 39, 41, and 42) for both output loads, a slight rise and then fall of switch pressures and flows are noted for increasing lengths of the power nozzle. Although this shape is preserved throughout the curves, the influence of Reynolds number and output load on the level of the curves is noted. The unexpected behavior of this parameter is the downward trend in the recovery pressures (Fig. 40 and 43) for increasing power nozzle contraction lengths. The most important observation concerning the power nozzle shape data is that made in note v of Table 7 which points out the extreme sensitivity (for unknown reasons) to biasing for the shorter power nozzles.

To conclude this section it is pointed out that only some general remarks concerning the effects of the dimensional parameters have been discussed. Many specific remarks can be made concerning the effects of a dimensional parameter provided operating conditions (Reynolds number and output loading) are first specified. This is due to the overshadowing influences of Reynolds number and output loading on the shape and position of the curves as well as locations and magnitudes of mode-changes. The center of this investigation has been the generation of the six tables and the hypothesis used in generating figures from this

data. With this being done the user can extract any specific information desired.

## SUMMARY AND CONCLUSIONS

The purpose of this investigation was to study how the performance (switch pressure, switch flow, and recovery pressure) was affected by small dimensional changes in the six dimensional parameters of offset, wall length, control width, power nozzle width, wall flat, and power nozzle shape of the bistable fluid amplifier. The investigation studied small dimensional changes from a typical, commercially available device and was conducted simulating the actual device's operating conditions. The ultimate goal in mind was to provide data on these dimensional parameters that would be useful to the designer and manufacturer in refining the current design and production process of flip-flops. This object was produced in the form of six tables (one for each dimensional parameter) and a hypothesis and process which can be used to generate figures and characteristics for the particular needs of the user. In this investigation, thirty-six figures of typical cases from the tables were generated to point out just some of the significant features of the dimensional parameters.

The most significant contribution made in this investigation was the formation of and evidence supporting a hypothesis which can be used to explain some unusual behaviors in the flip-flop; but, more specifically, it was used to fit smooth and regular curves to the data. The hypothesis was simply that there are conditions under which there coexists two, different level, overlapping switch points. The locations of these overlapping switch points were called mode-changes because they are believed to be caused by the transition from one switching mode to another. These mode-changes were then used to explain behaviors such as

scatter in experimental data at certain geometries and operating conditions.

The next contributions made by this investigation were simply the generation of the tables of experimental data and the use of the hypothesis to fit smooth and well-behaved curves to the data in the tables. This process was illustrated in the generation of the thirty-six figures presented so that the user could extract any specific information desired concerning the dimensional parameters, or generate more figures.

The primary conclusion to be made from this investigation is the overshadowing influence of operating conditions (Reynolds numbers and output loading) on the characteristics of all dimensional parameters. This point is dramatically illustrated in the results presented for the wall length parameter. The location, size, and number of mode-changes are dramatically changed by Reynolds number and output loading. Also observed in the wall length data are dramatic changes in the shapes and overall level of the curves. Because of this influence, the operating conditions of Reynolds number and output loading must be specified before discussing the characteristics of a dimensional parameter in detail.

In general, the wall length parameter has the most severe influence on the performance of the flip-flop. It is severe in the sense that several large mode-changes occur for this parameter as well as the most severe changes in the curves for different operating conditions. The best behaved parameter is that of control width. The mode-change that is located in the middle of the operating range of the nominally dimensioned device can be removed by changes in any of the parameters, but increases in control width remove this mode-change and promote a

very clean and consistent switching process.

To conclude this investigation, it is pointed out the need for more data on wall flat and power nozzle shape. Further, it is pointed out that caution must be used if a shorter power nozzle is going to be employed. For unknown reasons the flip-flop became very sensitive to biasing for the shorter power nozzles.

## REFERENCES


1. Foster, K. and Parker, G. Fluidics, John Wiley & Sons Ltd., London, 1970.

2. Kirshner, J. M. (Ed.) Fluid Amplifiers, McGraw Hill Book Co., 1966, pp. 192-203.

3. Borque, C. and Newman, B. G. "Reattachment of a Two-Dimensional Incompressible Jet to an Adjacent Flat Plate," Aero-Quarterly, Vol. II, August 1960.

4. Levin, S. G., and Manion, F. M., "Jet Attachment Distance as a Function of Adjacent Wall Offset and Angle," H. D. L. Report TR-1087, December 1962.

5. Sher, N. C., "Jet Attachment and Switching in Bistable Fluid Amplifiers," ASME Paper 64-FE-19, May 1964.

6. Borque, C., "Reattachment of a Two-Dimensional Jet to an Adjacent Flat Plate," Advances in Fluidics, ASME 1967.

7. McRee, D. I., and Moses, H. L., "The Effect of Aspect Ratio and Offset on Nozzle Flow and Jet Reattachment," pp. 142-161, Advances in Fluidics, ASME 1967.

8. McRee, D. I., and Edwards, B. G., "Three-Dimensional Turbulent Jet Reattachment," ASME Paper 70-WA/Flcs-5, 1970.

9. Cone, J. C., "An Experimental Investigation of the Effects of Inlet Geometry on the Performance of a Bistable Fluid Amplifier," M. S. Thesis, Dept. of Mechanical Engineering, VPI & SU, August 1972.

10. Nurmohamed, A. R., "Effects of the Inlet and Nozzle Geometrics on the Performance of a Fluidic Power Nozzle," M. S. Thesis, Dept. of Mechanical Engineering, VPI & SU, September 1973.

11. Wagner, W. B., and Owczarek, J. A., "An Experimental Study of Flow Fields in Bistable Fluid Amplifiers," ASME Paper 72-WA/Flcs-9, 1972.

12. Moses, H. L., and Comparin, R. A., "Flow and Pressure Recovery in Wall Attachment Fluid Amplifiers," ASME Paper 70-WA/Flcs-9, 1970.

13. Moses, H. L., and McRee, D. I., "Switching in Digital Fluid Amplifiers," ASME Paper 69-Flcs-31, 1969.

14. Goto, J. M., and Drzewiecki, T. M., "An Analytical Model for the Response of Flueric Wall Attachment Amplifiers," Harry Diamond Laboratories, HDL-TR-1598, 1972

15. Moses, H. L., and Comparin, R. A., "The Effect of Geometric and Fluid Parameters on Static Performance of Wall-Attachment-Type Fluid Amplifiers," to be published in the Proceedings of the H. D. L. Fluidics State-of-the Art Symposium, October 1974

**The vita has been removed from the scanned document**

# THE EFFECTS OF SMALL DIMENSIONAL VARIATIONS ON THE PERFORMANCE OF A TYPICAL BISTABLE FLUID AMPLIFIER

by

Charles S. Aldrich

(ABSTRACT)

Small dimensional changes in six parameters were experimentally studied for their effects on the performance of the bistable fluid amplifier. These dimensional parameters were offset, wall length, control width, power nozzle width, wall flat, and power nozzle shape. The investigation was conducted on a ten times actual size model of a typical, commercially available amplifier. Data were taken for operating conditions of 1 nozzle load and blocked outputs over a range of Reynolds numbers (based on the nominal nozzle width) of 2000 to 6000.

Evidence in support of the hypothesis of the coexistence of two, different level, overlapping switch points was presented. The hypothesis was used to explain unusual behavior and to fit smooth and regular curves to the experimental data obtained.

The center of the investigation was the six tables of data generated and the method used to obtain figures of the specific dimensional characteristics desired by the user. It was found that the overwhelming influence of operating conditions (Reynolds number and output loading) prevented specific discussion of dimension characteristics without having the user's specific needs or operating conditions specified.

From a broad or general look at the dimensional characteristics, it was found that wall length had the most severe characteristics. It was also found that the wider control width promoted a clean and well-behaved

switch absent of two coexistent switch points. For reasons unknown, it was found that the shorter power nozzle shapes made the device extremely sensitive to biasing.